Effects of HIV and different Antiretroviral therapy regimens on brain morphometry in HIV-infected children at age 7

By

Emmanuel .C. Nwosu

(Student Number: EMMNWO001)

SUBMITTED TO THE UNIVERSITY OF CAPE TOWN

In fulfilment of the requirements for the degree MSc (Med) in Biomedical Engineering

Faculty of Health Sciences

UNIVERSITY OF CAPE TOWN

Date of submission: **July, 2015**

Supervisor: **Prof. Ernesta .M. Meintjes**

Co-supervisor: **Dr. Frances .C. Robertson**

Department of Human Biology

University of Cape Town

DECLARATION

I, **EMMANUEL .C. NWOSU**, hereby declare that the work on which this thesis/dissertation is based is my original work (except where acknowledgements indicate otherwise) and that neither the whole work nor any part of it has been, is being, or is to be submitted for another degree in this or any other university. I authorise the University to reproduce for the purpose of research either the whole or any portion of the contents in any manner whatsoever.

Signature: signature removed Date: 20th July, 2015

Acknowledgements

Thanks to Ernesta Meintjes and Frances Robertson for supervising the work. They provided the context, expert ideas, advice, support and numerous resources required for the completion of this project. Thanks to Babara Laughton, Mark Cotton and Els Dobbels of Children's Infectious Diseases Clinical Research Unit, Department of Pediatrics and Child Health, Stellenbosch University that facilitated the participants used in this work. Thanks to staff of Cape Town Universities Brain Imaging Centre (CUBIC) that provided MRI scan and other imaging resources for this study. FreeSurfer neuroimaging tool was used in MRI structural analysis, a product of the Athinuola .A. Martinos centre for biomedical imaging, MGH, U.S.A. Thanks to Kenneth Mbugua for generously providing initial guidance on FreeSurfer and other resources. Thanks to Kenneth Otwombe for providing the clinical data for this study.

Thanks to the following members of our research group; Ali Alhamud, Martha Holmes, Paul Taylor, Lindie du Plessis, Jia Fan, Muhammad Saleh, Keri Wood, Jadi Toich, Steven Randall, Stephen Jermy, Mwape Mofya and others for the various support they offered while the work was in progress.

I am grateful to my family (my Mum and sisters) for their prayers, support and understanding. I am grateful to Sinesipho Jojo for all the moral support and prayers.

Finally, am most grateful to God for his unlimited guidance and provision in my life.

Abstract

By 2013, more than 300, 000 children were living with HIV-infection in South Africa. The World Health Organization (WHO) recommended early aggressive antiretroviral therapy (ART) initiation to manage HIV in children, based on studies that reported this protocol as effective in reducing mortality and HIV progression.

Early ART initiation in HIV-infected children generated new concern about the long-term effects on neurodevelopment. There is still much to understand about the outcome of HIV and early ART on children's brain structure and neurocognitive skills. This study therefore investigated the effects of HIV and early ART on brain morphometry in 7-year old children using magnetic resonance imaging (MRI).

Participants were 99 Xhosa children (56 HIV-infected children 43 uninfected controls, 50 boys, mean age = 7.21 ± 0.14 years) from the neuroimaging follow-on study of the Children with HIV Early Antiretroviral (CHER) trial. T1-weighted structural MRI data were acquired on a 3T Allegra (Siemens, Erlangen, Germany) within 6 months of their 7th birthday. In the CHER trial, HIV-infected infants were randomized at 7 weeks of age into three arms, two of which received immediate ART for either 40 or 96 weeks. The third arm received ART when clinically or immunologically indicated by WHO 2006 criteria. At age 7 years, all children were stable on ART. Scans were performed in accordance with protocols approved by the human research ethics committees of Stellenbosch and Cape Town Universities; all parents provided written informed consent and children provided oral assent. MRI scans were analysed with FreeSurfer's automated processing stream (http://freesurfer.net/) to generate measures of cortical thickness, local gyrification index (LGI), and regional (corpus callosum, bilateral caudate, hippocampus, putamen, thalamus, and lateral ventricle) and global brain volumes. Vertex-wise and region of interest (ROI) comparisons were performed between and within HIV-infected and uninfected children. Relationships between morphometric and clinical data were investigated.

Our results showed no significant difference in cortical thickness between HIV-infected and uninfected children. Uninfected children had greater gyrification than HIV-infected children in a left medial parietal region while HIV-infected children had smaller volumes of the bilateral putamen (p=0.001) and right hippocampus (p=0.01), and smaller total white (p=0.001) and gray (p=0.02) matter volumes. There was no effect of duration of ART in HIV-infected children except in the left hippocampus where longer (96 weeks) duration was associated with greater volume.

There was no significant relationship between cortical thickness at age 7 and immunological status at enrollment, but regional (caudal middle frontal, pars orbitalis, lateral occipital and superior parietal

regions) gyrification showed a relationship with immune system parameters (CD4 count, CD4 percentage and CD4/CD8 ratio) respectively. A healthier immune system at enrollment - CD4 percentage and CD4/CD8 ratio – was associated with reduced volume in the caudate nucleus, while longer cumulative duration on ART was associated with increased volume of the bilateral thalamus at age 7.

There was no difference in brain volume or cortical thickness measures between HIV-exposed but uninfected (HEU) children and HIV-unexposed uninfected (HUU), but HEU children had greater gyrification in the left precuneus region which may be abnormal due to HIV/ART exposure *in utero*.

In conclusion, LGI and subcortical volumes were affected in HIV-infected children but their cortical thickness was not affected. This may likely have effects on neurodevelopmental skills and cortical folding development.

Table of Contents

List of Figures

List of Tables

List of Abbreviations

A

ADC – AIDS dementia complex

ANI – Asymptotic neurocognitive impairment

ANCOVA – Analysis of covariance

ANOVA – Analysis of variance

ART – Antiretroviral therapy

ARV – Antiretroviral drugs

AZT – Zidovudine

B

BBB – Blood brain barriers

BCR – Bi-caudate ratio

C

CD4 – Cluster of differentiation 4 (a glycoprotein on surface of immune cells)

CD8 – Cluster of differentiation 8 (a glycoprotein associated with T-cell receptor as co-receptor)

CHER – Children with HIV Early Anti-retroviral Therapy

CNS – Central nervous system

CSF – celebrospinal fluid

CT – Computerized Tomography

D

ddl – Dideoxyinosine

D4T – Stavudine

E

EEG – Electroencephalography

F

FLASH – Fast low angle shot

fMRI – functional MRI

H

HAART – Highly active antiretroviral therapy

HAD – HIV associated dementia

HAND – HIV-associated neurocognitive disorder

HIV – Human immunodeficiency virus

I

IQ – Intelligence quotient

L

LGI – Local gyrification index

M

MEG – Magnetoencephalography

MEMPRAGE - Multiecho magnetisation prepared rapid gradient echo

MND – Mild neurocognitive disorder

MPRAGE - Magnetisation prepared rapid gradient echo

MRI – Magnetic resonance imaging

MTCT – Mother to child transmission

NMR – Nuclear magnetic resonance

N

NRTI – Nucleoside reverse transcriptase inhibitor

P

PHE – Progressive HIV encephalopathy

PI – Protease inhibitors

PML – Progressive multiple leukoencephalopathy

Q

QDEC – Query, design, estimate, contrast

R

ROI – Region of interest

S

SA – South Africa

SNR – Signal – to – noise ratio

SSA – Sub-saharan Africa

T

TE – Echo time

TR – Repetition time

U

UNAIDS - Joint United Nations Programme on HIV/AIDS

V

VBR – Ventricular brain ratio

W

WHO – World health organisation

3TC – Lamivudine

Glossary

Calcification – a neurological disorder that is characterised by deposition of calcium on brain regions that controls motor activities of the body.

CD4 count – An absolute count of helper T-Helper cells (a type of lymphocyte or white blood cell) per cubic millimetre of blood to determine health of immune system. It fluctuates under conditions like ill-health, time of the day, etc.

CD4 percentage – total number (percentage) of blood lymphocytes that are CD4 cell which also represent the state of health of the immune system. It is a more consistent measure of body immune system

CD8 count – An absolute count of T-lymphocyte (CD8 cell) per cubic millimetre of blood. CD8 cells help in fighting neoplastic cell. It is often linked with inflammation due to microglial/macrophage activation in the brain

CD4/CD8 ratio – this compares the ratio of the two major blood lymphocyte, usually used to check for reduction of body immune system (CD4 cell) in comparison to CD8 cell. It is a complementary measure of health of immune system.

Cerebral Haemorrhage – bleeding within brain tissues instead of outside which is caused by rupture of blood vessel or vessel networks that supplies the affected brain tissue. This is usually preceded by formation of blood clot (aneurysm) on blood vessels.

Choroid plexus – a plexus that projects from the lateral ventricle where cerebrospinal fluid (CSF) is produced usually among the first tissues attacked by the HIV

Cortical thickness – measure of thickness of layers of the cerebral cortex in human brain, either locally or by taking average global thickness. Cortical thickening usually positively correlates with cognitive ability.

Dementia – group of symptoms that affects mental abilities like memory loss, impaired judgement or language skills, etc, which can interfere with performing daily activity. It has been linked with Alzheimer disease, old age (at least 60 years) and with adult HIV infection

Endothelial cells – thin layer of cells that lines the interior of the blood vessel which filters biochemical substance that crosses through the vessel, is usually attacked by the HIV

Encephalopathy – a condition of brain malfunction or damage that leads to slowing down, damaging or complete halting of developmental processes, functions or structures controlled by the affected brain region(s). It is often linked with brain viral infections especially HIV infection.

FreeSurfer – neuroimaging software tool used in this study to perform morphometric analyses of T1 MRI scan of study participants' brain. It is designed and developed at the Martinos centre for biomedical and computational neuroimaging analyses

Freeview – recent GUI and visualization tool developed for FreeSurfer, similar in functionality to tkmedit, tksurfer. It differs from tkmedit in that it can load multiple volumes at once and can be used to visualize high resolution (100um) data as well as tractography splines.

Gyrification – the process that involves changing of brain morphology to generate the gyral and sulcal regions on cerebral cortex, it is also a measure of numeric value of gyral convolution in brain imaging analyses.

Gyrus – convolutions on both brain hemispheres due to infolding of the cerebral cortex, they are surrounded by grooves known as sulci. (Plural: gyri)

Intracranial volume – in context of FreeSurfer reconstruction algorithm, it is all the volume within the cranium including the brain, meninges and CSF

In utero – function(s), process (es) or action (s) that occur in the womb or before birth

Isixhosa – a language spoken by a group of tribe that lives at the south-eastern part of South Africa, in South Africa Republic. Children used in this study are born by mothers from IsiXhosa tribe.

Lymphocytes – immune cells that fight bacteria, toxins and neoplasmic cells and acts as the human body's defence mechanism against foreign and harmful organisms and substances. Among them are the CD4 and CD8 cells

Microcephaly – condition of drastic reduction in brain volume or non-attainment of normal brain size usually due to neuronal atrophy associated with viral infections especially in HIV infection.

Morphometry – measurement of structural landmark, dimension and external shape of the whole organism, tissue, organ of a living organism.

Myelination – the process of growth of electric insulating, myelin sheath around neurones of the nervous system, especially long neurones to improve fast transmission of signal across neurones.

Neuroimaging – the part of medical imaging that is associated with investigation of the nervous system of the body and its peripherals.

Neuronal atrophy – a terminology that translates to neuronal cell death and usually relates to decrement in size and loss of connection in neuronal tissue due to loss of cytoplasmic protein. It is observed in cases like microcephaly in pediatric HIV infection.

Neurone – the basic unit of the nervous system that processes and transmits information through the nervous system as chemical or electrical excitations.

Neurotoxins – biochemical substances that are toxic to neurones, nervous system or its peripheral components.

QDEC – GUI platform of FreeSurfer used for inter-subject averaging and comparison of morphometric data generated from FreeSurfer's reconstruction stream and to draw statistical inference based on vertex wise comparison of groups of subjects.

Radio frequency – band of pulse frequencies within the range of 10^4 and 10^{12} HZ, usually applied in MRI scan

Spin – quantum characteristic of elementary particles which is visualized in the rotation of these particles on their axes and responsible for measurable angular momentum and magnetic moment

Structural MRI – The modality in MRI scan that involves imaging and investigation of changes in anatomical structures of the body, in this case the brain.

Sub-cortical – regions of the brain inferior to cerebral cortex

Sulcal enlargement – it is a brain structural disorder in which deep, narrow grooves of sulci and fissures begin to widen and become shallow. This disorder is associated with ventriculomegaly and has been observed as a structural defect in HIV infection.

Sulcus – deep, narrow groove that separates adjacent convolutions of the brain (plural: sulci)

TKMEDIT – a program used for visual inspection and editing voxels of 2D slice of sub-cortical segmented brain MRI scan during reconstruction process in FreeSurfer.

TKSURFER – a program interface also used for inspecting voxels of 3D cortical brain MRI scan during reconstruction process in FreeSurfer.

Voxel – the basic unit of measurement for 3-dimensional, spatial or graphical or pictorial entity. It is a combination of “volume” and “pixel” – unit of measurement of 2-Dimensional pictorial entity.

Viral load – measure of amount of viral substance in a host, environment or bloodstream, used often to quantify the amount of HIV viruses in infected subjects.

Ventriculomegaly – abnormal dilation of the lateral ventricles of the brain in which the ventricular atrium diameter is up to or more than 10mm. It is associated with hydrocephalus and advanced pediatric HIV infection.

1. Introduction

1.1 Background

By 2011 it was estimated that 2.3 million children were infected with HIV globally, while approximately 1500 new cases of vertical transmission were recorded each day in the same year (Phelps and Rakhmanina, 2011). According to the UNAID global report of 2012, the number of new HIV infections around the globe had decreased by at least 20% since 2005. The Caribbean recorded the highest reduction of 42%, followed by sub-Saharan Africa (SSA), with a decrease of 25%. Despite a drop of 32% in the number of deaths due to HIV-related conditions between 2005 and 2011, SSA continues to have the highest percentage of people living with HIV, namely 69% of about 34 million at the end of 2011. These patients may not be at risk of death because of the aggressive anti-retroviral therapy (ART) regimen being provided by the health care system, but concern has shifted to the effect of HIV infection and ART in the long term (Van Rie et al., 2007; Phelps and Rakhmanina, 2011).

Statistics show that each year 15% of new infections are in children in the developing world (Phelps and Rakhmanina, 2011), including South Africa. The introduction of the highly active anti-retroviral therapy (HAART) combination has changed HIV infection from an acute condition with a high mortality rate, to a chronic condition where the chance of long term survival has increased over the years (Van Rie et al., 2007; Banks, 1999). However, there is concern over the number of children living with HIV infection and its effect on their development. There are approximately 360 000 HIV-infected children in South Africa (UNAIDS report 2013).

Mother-to-child transmission (MTCT) is the dominant mode of HIV infection in children, especially in sub-Saharan Africa (SSA) (Sharland et al., 2005; Le Doare, 2012), and has the greatest risk for irreversible damage to neurological processes, with evidence of developmental delay (Le Doare, 2012). MTCTs can occur *in utero*, during labor and delivery or during breast feeding (Sharland et al., 2005; Le Doare, 2012) and these modes of transmission account for the greatest percentage of MTCT. Most cases of MTCT occur within low income and uneducated populations, where there is a corresponding increased risk of devastating neurological and developmental deficit before the initiation of ART (Prendergast et al., 2007; UNAID, 2012).

In 2005 it was estimated that 50 000 HIV-infected children were born yearly in South Africa, compared to around 25 per year and 190 per year in the UK and USA, respectively (Sharland et al., 2005). Policies have been adopted to manage pediatric cases in low and middle income countries, but cases of vertical transmission have yet to be wiped out completely. While 90% of children infected with HIV live in the developing world (especially Africa), very few studies on its neurological manifestations have been conducted outside Europe and the USA (Van Rie et al., 2007).

Pediatric infection is of concern because of severe associated conditions, such as progressive HIV encephalopathy (PHE) in children less than 3 years old (Epstein et al., 1986) and HIV-related effects on developmental milestones and reduction in global brain volume (microcephaly). HIV affects children's neurological, psychomotor and behavioral maturity into adulthood (Wachsler-Felder et al., 2002). Studies suggest that developmental and behavioral effects of HIV in children are more severe with decreased age of infection (Wachsler-Felder et al., 2002; Rausch et al., 2001). Despite improving immune systems, the effects of anti-retroviral therapy (ART) on developmental and neurological processes in HIV-infected children are poorly understood. Experience in children on ART reveals high rates of arrested HIV-related encephalopathy but also high rates of residual behavioral problems, neurologic, cognitive and scholastic impairments, and risk for relapse of progressive HIV encephalopathy (Van Rie et al., 2007). This means that effects of HIV are still seen, as these developmental and neurological adverse conditions are not completely treated even with HAART initiation.

Reduced brain volume (microcephaly) due to neuronal atrophy and impaired brain growth (encephalopathy) are common in HIV-infected children (Ances et al., 2012; Ellis, 2010; Chiriboga et al., 2005). These structural deficits are associated with neurodevelopmental effects including gradual loss of voluntary motor and executive function skills (Epstein et al., 1986; Ances et al., 2012); severe cases of learning difficulty, impaired cognition and general Intelligent Quotient (IQ) deficit (Chiriboga et al., 2005; Ellis, 2010); as well as cases of withdrawal syndrome, and emotional and social defects (Epstein et al., 1986; Ances et al., 2012).

The Children with HIV Early Anti-retroviral Therapy (CHER) clinical trial (Violari et al. 2008) examined outcomes of early initiation of ART in infants with HIV infection, and showed that early HIV diagnosis and

early ART (between 6-12 weeks of age) reduced early infant mortality by 76% and HIV progression by 75% (Violari et al., 2008). Infants were recruited from two sites, namely the Perinatal HIV Research Unit at Chris Hani Baragwanath Hospital in Soweto, and the Children's Infectious Diseases Clinical Research Unit at Tygerberg Children's Hospital in Cape Town. ART was initiated at a mean age of 7.2 weeks which was more effective in reducing child mortality and pediatric HIV progression, compared to standard ART initiation in children at symptomatic stage or at a threshold CD4 percentage less than 25% (WHO, 2013) (Violari et al., 2008). The World Health Organization (WHO) Consolidated Guidelines on the use of Antiretroviral (ARV) drugs (June 2013) now also supports early initiation of ART in children below age 5, regardless of CD4 percentage or clinical stage (WHO, 2013). Implementation of these guidelines has raised concerns over the long-term effects of ART initiation at an early age, especially on the central nervous system (CNS) and neurodevelopment (WHO, 2013; Violari et al., 2008). While early ART is generally accepted as being effective in reducing infant mortality and preventing further HIV progression, no study has investigated the impact of this early treatment on the brain throughout development (WHO, 2013; Violari et al., 2008). In order to avoid possible side effects that may be associated with lifelong treatment, proper investigation and understanding of the effects of ART is needed, including the potential long-term toxicity of anti-retroviral therapy, adherence issues, and possible risk of viral resistance to antiretroviral therapy (Violari et al., 2008).

Very few studies have used neuroimaging to investigate brain-related complications in children with HIV infection. The few existing studies have further been limited by small samples sizes, wide age ranges, and have largely been performed in the developed world where treatment strategies are highly heterogeneous, making it difficult to draw conclusions and interpret findings.

The HIV infected children at the Cape Town site of the CHER study, together with 43 uninfected control children from the same community who were recruited as part of an interlinking vaccine trial, have been followed since birth using comprehensive clinical and neurodevelopmental testing up to 5 years of age. Detailed clinical records, laboratory results, compliance information, and behavioral outcomes are available from birth for all these children. As part of an on-going NIH-funded study, these children are being followed for a further four years with neurocognitive assessment and neuroimaging at 5, 7 and 9 years in order to assess the long-term effects of HIV and ARV treatment regimens on brain development. The present study aims to investigate differences in brain structure and associations of structural

alterations with clinical measures (CD4 parameters at enrollment, age at ART initiation, and cumulative duration on ART) in children in this cohort within 6 months of their 7th birthday.

1.2 Problem definition

As the study of HIV advances in different fields, HIV infection has progressed from an acute to a chronic condition and presently infected patients can lead a near normal life with ART (Phelps and Rakhmanina, 2011; McCoig et al., 2002). A major research focus is determining the best time to commence ART, either to reverse or to prevent the detrimental effects of HIV infection on development. It is still debated when best to commence treatment to avoid adverse drug effects of ARTs and at the same time inhibit the debilitating effect of HIV on delicate tissues and organs (Gavin et al., 2009; Avison et al., 2002).

Newer ARVs can cross the blood-brain barrier (BBB) and sustain high concentrations, keeping viral load in the brain at minimum as long as the recommended treatment regimen is maintained (Van Rie et al., 2007; Banks, 1999). Yet there have been reports of adverse effects of HAART on the brain, for example aneurysm and cerebrovascular hemorrhage (Ellis, 2010; McCoig et al., 2002; Mitchell, 2001). There is a need to investigate the effects of high concentrations of antiretroviral (ARV) drugs on brain structures and processes, especially in developing children.

Further, with the emergence of aggressive HAART for HIV infected mothers to prevent Mother -to -Child transmission (MTCT) (Sharland et al., 2005; Le Doare, 2012), a new generation of children is being born to infected mothers who are not infected, but have been exposed to ARV *in utero*. Little is known about the effect of *in utero* exposure to ARV on these children's brain tissues.

The goal of Africa and especially South Africa to raise a generation that is AIDS-free increases the need to investigate the effects of ART/HIV infection as well as *in utero* ART exposure on the developing brain in children that have been exposed to these aggressive treatment plans. As well as investigating the effect of HIV/ART on brain structure in children, this study also investigates the effect of timing of HAART initiation, duration of uninterrupted treatment, and cumulative period on ART on brain structure in 7 year old children. We were also particularly interested in the effect of immune status at enrollment on structural brain development. In addition, some of the children in this study were born to infected mothers but are not infected (Exposed-Uninfected), allowing us to investigate the effects of *in utero* ARV exposure on brain structure in these children.

1.3 Study objectives

The objectives of this study were:

- To use FreeSurfer software (FREESURFER, 2012; Fischl et al, 2012) to perform automated morphometric analyses of high-resolution structural MRI data acquired in 56 HIV-infected children and 43 controls (n = 99) at age 7 to obtain data of cortical thickness, local gyrification index (LGI), regional and global brain volumes.
- To perform vertex-wise and ROI comparisons of brain morphometric measures between infected and uninfected children, as well as among different treatment arms, in order to determine the effects of HIV and early HAART on brain development.
- To investigate the relationship between neuroimaging outcomes and clinical measures (CD4 parameters at enrollment, cumulative period on ART, and age at ART initiation).

The rest of this chapter gives a concise review of background of the study, with emphasis on the manifestation of HIV in the brain and effects that have been found in previous studies. It also looks at the effect of HIV infection on children's brains in structural, psychomotor and functional domains and provides a literature review on the effects and side-effects of various ART regimens. The last sections of this chapter review studies that have used MRI to investigate structural and functional abnormalities and neurological conditions associated with HIV infection, as well as studies that have investigated morphometric measures, including cortical thickness, local gyrification and regional brain volume differences, in HIV-infected children and adults.

Chapter 2 briefly discusses the theoretical background and tools used in the study, especially structural MRI , FreeSurfer – as a neuroimaging toolkit – for assessing structural alterations associated with various pathophysiological conditions and effects of biochemical and synthetic drugs, clinical implication of changes in neuroimaging parameters (cortical thickness, LGI and brain volume) investigated in this study on HIV-infected participants and especially in children.

Chapter 3 introduces the participants and methods used in the study.

Chapter 4 presents results for both vertex-wise and region of interest (ROI) analyses performed in this study, including between-group differences as well as relationships between neuroimaging measures and

clinical continuous variables (CD4 count, CD4 percentage, CD4/CD8 ratio (all at enrollment), age at ART initiation and cumulative period on ART).

Chapter 5 provides a discussion and interpretation of the results, with reference to the literature reviewed in chapter 1 and theories described in chapter 2. It describes how the major findings of this study contribute to what is already known about the effect of HIV/ART on the brain in developing children. Finally the concluding section makes recommendations on trends that require further investigation, but which were beyond the scope of this study.

1.4 Background and literature review

1.4.1 HIV infection in the brain

Although studies have shown that the brain is a major reservoir for the HI virus (Van Rie et al., 2007; Banks, 1999), recently-developed anti-retroviral (ARV) drugs can cross the blood-brain-barrier (BBB) and sustain high concentrations that are not removed by the BBB flux mechanism, thus minimizing brain viral load as long as the recommended treatment regimen is maintained (Hanning et al., 2011; Ellis, 2010; McCoig et al., 2002). More recently, studies are shifting focus to the effects of ARV concentration on brain structure and function.

The BBB regulates bio-molecular transport through the blood-cerebrospinal fluid (CSF) interface in the brain and protects brain tissues from antibodies and neurotoxins (Banks, 1999). It is still unknown precisely how HIV penetrates the BBB, but it is speculated that the virus and viral products flowing in blood vessels stimulate endothelial cells (astrocytes and microglia) of the BBB to release neurotoxins (cytokines, nitric oxides and prostagladins) and viral gene products (tat and gp 120), which cause neuronal atrophy and allow the influx of free virus and viral products through the compromised BBB into the CSF and brain tissues (Banks, 1999; Steinbrink, 2013). Another theory proposes that brain infection results from two major processes: trafficking of infected cells of monocyte-macrophage lineage across the BBB or “Trojan Horse” effects during principal infection of activated CD4 + lymphocytes, and infiltration of infected cells through the choroid plexus (Avison et al., 2002; Ellis, 2010). There is general acceptance that HIV enters the CNS within days to weeks after infection and that viral load increases with disease progression (Van Rie et al., 2007; Paul et al., 2002; Persidsky et al., 1999; Banks, 1999). On entering the CNS, HIV neurotoxins and mediator hosts (monocyte-macrophages cells) destroy the neuronal connections (dendrite-synapse) and damage the complex networks of the CNS, leading to HIV-associated

neurocognitive disorders (HAND)(Ellis, 2010; Lindsey et al., 2007; Chriboga et al., 2005). These pathophysiologic processes are observed in brain tissues that are most susceptible to high viral load, including the caudate nucleus, hippocampus, lateral ventricle, putamen, thalamus, corpus callosum, deep white matter and basal ganglia, and affect global gray matter and total brain volume (Paul et al., 2002; Holt et al., 2012).

Because ARVs enter the CNS with influx transporters and are continuously removed by the BBB efflux mechanism, accumulating a significant quantity in the CNS presents a major challenge to the management of HIV (Bank, 1999). An inadequate ARV concentration prevents viral load suppression, resulting in increased replication of the virus so that the brain becomes a major reservoir for HIV and a point for re-infection (Persidsky, 2006; Bank, 1999). An increased research focus on ARVs that can penetrate the BBB has resulted in the development of a number of ARVs that are believed to penetrate the BBB and reach a high enough concentration to keep the viral load at a minimum (Chriboga et al., 2005; McCoig et al., 2002). However, the effect of this high concentration of ARVs on brain tissues is not yet known.

1.4.2 The effect of HIV infection on the adult brain

Epidemiologic and neurological data suggest that it is difficult to detect significant early-stage effects of HIV on brain structure; this is because structural brain alterations manifest with viral replication and progression (Prendergast et al., 2007; Spudich et al., 2012). However, other studies state that neurological complications are among the earliest manifestation of viral infection (Du, 2012; Spudich, 2012). They all agree that neurological complications manifest in one of the following forms:

- Deterioration of neuropsychological performance and emotional instability (Paul et al., 2002; Spudich et al., 2012)
- Psychomotor effect and loss of executive functions (Rausch et al, 2001; Spudich et al., 2012).
- Neurocognitive disorder, memory loss and compromised intelligent quotient (IQ) (Spudich et al., 2012; Navia, 1987).

Neuropsychological effects include major changes in behavior manifested as apathy, withdrawal syndrome, irritability, depression, and personality changes. There are cases of compromised social skills, and difficulties in emotional and activity spheres (Paul et al., 2002; Rausch et al., 2001). In the neurocognitive sphere, HIV is associated with loss of memory and cognitive impairment. Studies are

currently investigating the roles different brain tissues play in the manifestation of these symptoms and their neuropathogenesis, since most symptoms are also linked with comorbid disease conditions and with aging (Paul et al., 2002; Holt et al., 2012).

Recent studies have redefined HIV-associated neurological disorders (HAND) into stages of severity of cognitive imbalance, based on the results of neurocognitive tests. These stages are: Asymptomatic Neurocognitive Impairment (ANI), which is seen at the earliest stage of infection; Mild Neurocognitive Disorder (MND), which occurs as infection progresses; and the most significant and severe case: HIV Associated Dementia (HAD) (Leon et al., 1986; Rausch et al., 2001; Spudich et al., 2012), which is characterized by loss of concentration, impaired short-term memory loss and general loss of memory (Epstein et al., 1986; Rausch et al., 2001). HAD is linked with AIDS dementia complex (ADC) or sub-acute encephalitis, a syndrome of progressive dementia associated with progressive cognitive, motor and behavioral dysfunction, which is one of the earliest manifestations of AIDS (Navia et al., 1987; Broderick et al., 1993).

1.4.3 Neurological effects of HIV infection in children.

In contrast to adults, HIV infection in children has more pronounced effects on the central nervous system (CNS) than the peripheral nervous system, and the brain is affected more than the spinal cord (George et al., 2009). At autopsy, findings in pediatric patients include impaired brain growth, reactive gliosis, myelin pallor, calcifications of the basal ganglia, cortical and cerebral atrophy with neuronal loss and ventricular enlargement, and abnormalities of the cerebral vasculature (George et al., 2009). The basal ganglia calcification observed in pediatric infection is not seen in adults (George et al., 2009; Kieck et al., 2004; Gavin et al., 1999) and is also a marker for acquired vascular injury (George et al., 2009).

Although these initial pediatric studies were based on autopsy reports (George et al., 2009; Kieck et al., 2004; Gavin et al., 1999), recent studies have shown increased use of living subjects, more cross sectional comparisons and longitudinal monitoring of cohorts, which have furthered understanding of HIV infection in children. The most common features observed in neuroimaging of pediatric patients are cerebral atrophy (68%) and ventriculomegaly (78%) (Kieck et al., 2004; Gavin et al., 1999).

In children, neuronal supporting cells (microglia, macrophages and astrocytes) are prone to HIV infection. The fetal astrocytes are most susceptible to infection and play a significant role in HIV encephalopathy among children, while high neuronal loss due to brain cell atrophy leads to microcephaly (Van Rie et al., 2007; Bank, 1999). These two conditions that adversely affect CNS development are unique to pediatric infections.

HIV encephalopathy (HE) is common in pediatric cases. It is synonymous with specific clinical features that include impaired brain growth, delay or loss of developmental milestones with consequent neurocognitive deterioration, and symmetric motor deficits (Tardieu et al., 2000; Rausch et al., 2001; George et al., 2009; Kieck et al., 2004; Mitchell, 2001: McCoig et al., 2002). The prevalence of HIV encephalopathy ranges from 20%-90% in HIV-infected subjects and is an AIDS-defining condition in child infection (George et al., 2009; Kieck et al., 2004). Before the era of HAART, cases were seen mostly in ART naïve children younger than 3 years, or in older children with advanced stage disease (Epstein et al., 1986). It is diagnosed in HIV-infected children by a combination of neurological examination, neurodevelopmental testing, and neuroimaging (George et al., 2009; Gavin et al., 1999).

It is worth noting that any of the less severe forms can at any time degenerate to the rapidly progressive form, depending on factors like HIV progression and brain viral load (Kieck et al., 2004). There are also cases of significant motor deficit in the form of tone movement disorder (Wachsler-Felder et al., 2002), learning difficulties and behavioral changes in older children (Van Rie et al., 2007; George et al., 2009; Kieck et al., 2004). Studies emphasize the need for consistent clinical examinations and tests in the management of HIV encephalopathy (George et al., 2009; Gavin et al., 1999).

Microcephaly is another significant condition in the advanced stages of pediatric HIV infection (Van Rie et al., 2007; Kozlowski et al., 1997; McCoig et al., 2002; Chriboga et al., 2005). This is due to global and tissue-specific neuronal atrophy, which leads to a decrease in brain volume, especially in gray matter regions (McCoig et al., 2002; Van Rie et al., 2007; Chriboga et al., 2005). The extent of atrophy correlates with viral load and severity of infection (Kieck et al., 2004; Gavin et al., 1999). In the basal ganglia region, calcification is also observed (Van Rie et al., 2007; Kozlowski et al., 1997).

Cerebrovascular complications are also observed among infected children. In an autopsy study, 52% of 42 children had at least one cerebrovascular complication (Gavin et al., 1999). These complications result

from viral agents and toxic cytokines produced as a result of HIV infection and are most often observed in vertically transmitted infections (Patsalides et al., 2002; George et al., 2009). The commonly-observed complications in cerebrovascular conditions include aneurysms - accumulation of blood in sac-like formations in blood vessels - or stroke (ischemic and hemorrhagic), which results from insufficient supply of oxygen and glucose to brain cells (Patsalides et al., 2002; Kieck et al., 2004, Gavin et al., 1999). There are also cases of vascular lesions and infarctions closely linked with vascular blocking of blood flow by dead cells (George et al., 2009; Gavin et al., 1999). MRI and CT imaging are useful in the management of cerebrovascular complications (George et al., 2009).

Other complications associated with pediatric HIV infection include progressive multiple leukoencephalopathy (PML), and brain tumours (Van Rie et al., 2007; Kozlowski et al., 1997; George et al., 2009; Kieck et al., 2004). These neurological complications severely impact brain development in children and have debilitating effects on executive function performance, intellectual ability, life survival skills, memory retention, and performance in both behavioral and emotional spheres (Epstein et al., 1986; Wachsler-Felder et al., 2002; Van Rie et al., 2007; George et al., 2009; Kieck et al., 2004). Scientific investigations and debates are still ongoing over which of these severe effects on the pediatric brain can be reversed in the HAART era.

1.4.4 Effects of Highly Active ART (HAART) treatment on the brain

Initially, ART with just one class of anti-retroviral (ARV) drugs (monotherapy) was used in HIV management but this was found to increase the chance of developing a drug resistant strain of HIV type 1 (HIV-1). Studies have shown that the use of at least three different classes of ARV is necessary to inhibit viral replication and to suppress viral load, thus increasing CD4+ lymphocytes (Ellis, 2010; Lindsey et al., 2007; Avison et al., 2012).

The purpose of highly active anti-retroviral therapy (HAART) is to suppress HIV replication through a combination of different classes of ARV drugs, to improve CD4 lymphocyte count and possibly reverse complications of infection (Gavin et al., 2009; Avison et al., 2002). It is not yet generally agreed that HAART reverses completely incidences of encephalopathy and other related neurodevelopmental conditions in children, although Le Doare et al (2012) found that HAART reversed encephalopathy by 50% more than non-HAART treatments (Le Doare et al., 2012; Mitchell, 2001). Some studies have reported that HAART alone can't restore HIV-infected children to "normal" neuropsychological performance and may even

contribute to neuromotor decline in the long term (Laughton et al, 2013; Von Giesen et al, 2003; Koekkoek et al, 2006).

Different ARV drugs have varying bioavailability in brain tissues; they differ in influx rate, and target different brain processes and tissues (Avison et al., 2002). HIV-infected children have higher drug clearance than their adult counterparts, therefore higher doses are needed to achieve similar systemic ARV exposure (Phelps and Rakhmanina, 2011). In the pediatric brain, a major source of concern is the ability of the ARV drug to cross the BBB into the CSF and target brain tissues, as well as to reach the concentration required to suppress viral load (Mitchell, 2001; Avison et al., 2002). To improve the management of pediatric HIV complications in the CNS, attention has been focused on ARV penetration and maintenance of the concentration needed for viral load suppression: little or no attention has been paid to the effect of this ARV concentration on brain tissues or structures.

Unlike Dideoxyinosine (ddI), which is used mostly in peripheral CD4 cell reconstitution, Zidovudine (AZT) and Stavudine (D4T), both nucleoside reverse trancriptase inhibitors (NRTI), have high BBB penetration and are effective in suppressing viral load (Gavin et al., 1999; Le Doare et al., 2012) and are thus necessary in ART combinations for managing CNS conditions. A combination of D4T and Lamivudine has also been shown to penetrate CSF and decrease viral load, proving that NRTIs other than AZT can be used in managing neurologic complications (McCoig et al., 2002). HIV protease inhibitors such as Indinavir, Nelfinavir, Ritonavir, and Efavirenz have limited penetration ability in the CNS (Gavin et al., 1999) but have high protein binding ability and low water solubility (McCoig et al., 2002) which is important for viral suppression. The use of AZT in the management of expectant mothers and treatment of infants in the first 6 weeks of life has reduced transmission from 25% to 8% or less (Violari et al., 2008; Laughton et al., 2012; Mitchell, 2001). The combination of Lamivudine (3TC) and AZT and also 3TC and D4T are effective in reducing CSF HIV RNA. A pharmacokinetic study of 3TC and D4T showed that they can reach a higher concentration in the CSF than AZT (McCoig et al., 2002). With these breakthroughs in ARV penetration through the BBB, studies need to focus on the possible effects of these ARVs' on brain structures.

There is no clear picture yet of the long-term effects of various ARV regimens in children on CNS development. Inclusion of a neuroprotective drug in the ARV regimen is being recommended, especially in children, to protect brain cells from neurotoxins and side effects of ARV drugs (Gavin et al., 1999). Some

studies have listed general toxic effects of specific ARVs (Ellis, 2010; McCoig et al., 2002), but there are few that concentrate specifically on effects in children. In Africa a study indicated that although treatment regimens containing protease inhibitors like Efavirenz and Nelfinavir improved CNS development, these were linked to cerebral events like hypoxic brain injury and cerebral hemorrhage that affected future neurodevelopment (Le Doare et al., 2012). Neuropsychometric studies have traced infants or older children initiated early into ART to investigate the effects of treatment on developmental milestones and locomotor functions (Le Doare et al., 2012), but much is unknown about long-term effects on brain development and cognitive function (Le Doare et al., 2012; Lindsey et al., 2007, Langford et al. 2006; Phelps and Rakhmanina, 2011), especially in sub-saharan Africa. Long-term effects on the brain are of increasing concern, as patients with HIV live longer and are exposed to drugs for longer periods. Patients may develop resistance to drugs, there may be cumulative neurotoxic effects compounded through long-term use, and patients might at some stage need newer, effective drugs to combat possible new neurological complications (Avison et al., 2002).

With the emergence of early ART for HIV-infected mothers, to prevent mother –to –child transmission (MTCT), new generations of children are born to HIV-infected mothers without being infected, but having been exposed to ARV *in utero*. Little is known about the effect of *in utero* exposure to ARV on children's development.

With the recent recommendation of an early ART regimen (Violari et al, 2008; Phelps et al, 2011, UNAID report, 2013), the long-term effects on the developing brain of HIV and early ARV treatment, as well as *in utero* exposure to HIV/ARV, require further investigation.

1.4.5 Neuroimaging in HIV

Neuroimaging is a powerful tool in the investigation and understanding of the pathophysiology of HIV, its effects, and the outcomes of ART (Paul et al., 2002; Holt et al., 2012; Du et al., 2012; Tucker et al., 2004; Spudich et al., 2012). Neuroimaging has been used in validation of clinical examinations and neuropsychometric tests, to conduct longitudinal and comparative studies, and to understand treatment outcomes of different ART regimens in living subjects (Hoare et al., 2012; George et al., 2009; Avison et al., 2002; Steinbrink et al., 2013; Spreer et al., 1994). It has been shown in the longitudinal monitoring of pediatric cohorts to examine development that child mortality due to vertical infection has decreased

significantly with early and *in utero* ARV treatment (Wachsler-Felder et al., 2002; UNAIDS., 2012; WHO., 2013). This shift to managing a chronic rather than an acute infection has increased the need to understand HIV treatment progression and effects of both early therapy and *in utero* exposure on brain structure, and to determine whether HIV-related volume changes, neural atrophy and white matter changes may be reversed with treatment (George et al., 2009).

1.4.6 Brain structure investigation in HIV infection

MRI is used for investigation of brain structure due to its high sensitivity to lesions and superior contrast resolution (Steinbrink et al., 2013). Global and localized white matter abnormalities as well as brain volume shrinkage are the most significant structural defects that have been detected with MRI in HIV associated dementia (HAD) and HIV encephalopathy (Steinbrink et al., 2013; Hanning et al., 2011; Dal Pan et al., 1992; Thurnher et al., 2000). Hanning et al. found that cerebral signal intensity abnormalities increase with progression of HIV infection and degeneration of immune status as measured by CD4+ measures (Hanning et al., 2011). In addition, sulcal and lateral ventricular enlargement with a diffuse patchy pattern of white matter lesions were observed (Steinbrink et al., 2013; Hanning et al., 2011; Thurnher et al., 2000).

Advanced stages of HAD are characterized by confluent, bilateral and symmetrical white matter lesions observed at periventricular regions and centrum semiovale, while sub-cortical white matter and the posterior fossa are relatively spared (Steinbrink et al., 2013). A study by Steinbrink et al. observed that severity of periventricular white matter abnormalities and changes in basal ganglia correlate with clinical progression of dementia, suggesting that HIV dementia is associated with white matter changes, rather than cortical atrophy or gray matter changes (Steinbrink et al., 2013). In contrast, another study reported that HAD was associated with cerebral atrophy and signal intensity at the splenium, with no significant difference between deep white matter abnormalities in patients with dementia and those without (Broderick et al., 1993). Both overall cerebral atrophy and prominent caudate atrophy as measured using the ventricular-brain ratio (VBR) and the bi-caudate ratio (BCR), respectively, have been shown to be consistent with HIV dementia (Dal Pan et al., 1992). Thurnher et al. (2000) reported stabilization and regression in signal intensity abnormalities on MR in patients with AIDS dementia complex (ADC) after treatment with HAART, suggesting disease regression (Thurnher et al., 2000).

There are few MRI studies in children with HIV infection and ART. The main findings include increased incidence of cerebrovascular disease (Patsalides et al., 2002), and evidence of demyelination as shown by reduced radial diffusivity in the corpus callosum and the superior longitudinal fasciculus (Hoare et al., 2012). Cerebral mitochondrial dysfunction, which is marked by diffuse hyperintensities in supra -tentorial white matter and in the tegmentum of the pons, similar to that seen in HIV symptomatic or asymptomatic children has been observed in perinatal exposed, uninfected children treated with AZT (Tardieu et al., 2005). Spreer et al. (1994) reported that neuro-radiological effects of AIDS in pediatric subjects differ from those in adults. All 21 children in their study had atrophy and delayed myelination: 7 exhibited both atrophy and multifocal nearly symmetric white matter lesions that did not affect the U-fibres; AIDS-associated vasculopathy and symmetric calcifications in basal ganglia were observed; and an intra-medullary ring-shaped structure was noticed in the cervical cord. In contrast to adults, none of the children in their study had intracranial lesions or disturbed BBB after application of intravenous contrast medium (Spreer et al., 1994).

An interesting question that can be addressed using MRI is the reversibility of brain structural changes caused by HIV-infection in patients enrolled into a HAART regimen. Though it is accepted that HAART suppresses viral load in the brain, it is still a major point of debate to what extent ART is able to reverse HIV-related structural alterations such as cortical thinning in PHE, microcephaly and sulcal enlargement. It is also not clear at what rate any such reversal would occur. Recent studies agree that these conditions can be reversed but few have mentioned the extent of the reverse. Chirboga et al., (2005) concluded that PHE is “infrequent and reversible” though it may relapse if control is lost on viral replication/load. However, there may be residual neurologic, cognitive and scholastic impairment, as evident in arrested pediatric PHE (Chirboga et al., 2005). McCoig et al., (2002) also concluded that there is improvement in neurologic status, but recommended the inclusion of agents with CNS activity in the HAART regimen (McCoig et al., 2002).

To date, most neuroimaging studies in children with HIV infection have been performed in Europe and America while the largest disease burden is in developing countries like South Africa (Thomaidis et al., 2010; Blanchette et al., 2001; 2002; Thurnher et al., 2000; Tardieu et al., 2005). The focus on eliminating HIV-related conditions in Africa and especially SA has made it important to investigate the outcome of ART/HIV infection in children. This will help in developing suitable treatment guidelines locally for pediatric cases which will consider the benefits and adverse effects of different HAART combinations. The

current study benefits from a highly homogeneous study population due to government-regulated treatment regimens, large subject numbers in a narrow age range, and a well-characterized cohort that has been followed since birth with detailed clinical and neurobehavioral assessments and follow-up. The expectation of this study is to advance our understanding of effects of HIV infection and ART on children at age 7. The primary aim was to examine the effects of HIV infection and ART on children's brain structure, to determine which brain tissues are most affected by HIV and ART in children, and also to investigate which ART treatment regimen showed better outcomes in answer to the question of when best to commence treatment of HIV-infected children.

1.4.7 Cortical thickness, gyrification and brain volume changes in HIV

Since many studies have linked neurocognitive abilities, psychomotor skills, and IQ and memory retention to cortical thickness, sulcal enlargement (a reverse of gyrification), and regional and total brain volumes, especially in HIV infection, we investigated these measures in this cohort.

Cortical thickness is closely associated with cognitive ability and is believed to have a combined effect with gyrification on fine motor control (Treble et al., 2012; Kallianpur et al., 2012). Kallianpur et al. (2012) found that cortical thinning in regions that form part of cognitive and emotional processing networks of subjects with detectable HIV DNA correlated significantly with measures of psychomotor speed (Kallianpur et al., 2012). Thompson et al. (2005) found that cortical thinning in the frontopolar and language cortices correlated with immune system deterioration, while prefrontal and parietal tissue loss was correlated with cognitive motor deficits. The authors therefore concluded that HIV selectively damages brain cortex in adults (Thompson et al., 2005).

Studies have shown that cortical thickness varies significantly between sexes, with females having greater cortical thickness than males in most regions of the brain (Kiho Im et al., 2006; Luders et al., 2006).

Closely related to cortical thinning is cortical folding, often known as gyrification – the development of folding patterns on the cerebral cortex surface to form sulci and gyri (White et al., 2010). A literature search failed to find any previous studies that have investigated gyrification in pediatric HIV/ART cases. Studies have found that gyrification is positively associated with Intelligence Quotient (IQ) and has a combined effect with cortical thickness on fine motor dexterity (Treble et al., 2012; Kallianpur et al., 2012).

Regional and global neural atrophy in pediatric HIV infection is the major cause of brain volume loss (microcephaly) (Kozlowski et al., 1997; Mitchell., 2001; Paul et al., 2002; Treble et al., 2012; Kallianpur et al., 2012). Reduction in brain volume and global atrophy is linked with high viral load with progression of infection (Kozlowski et al., 1997; Treble et al., 2012) and with adverse cognitive and motor functions (Treble et al., 2012; Kallianpur et al., 2012). Severity of pediatric infection seems to be higher in particular brain tissues (caudate nucleus, hippocampus, thalamus, putamen, lateral ventricle and corpus callosum) than others (Treble et al., 2012). Ortega et al. (2013) found that adult HIV-infected subjects had significantly smaller regional brain volumes in the thalamus, hippocampus, corpus callosum, cortical gray and white matter compared to uninfected controls, which was associated with slower processing speed and memory retention (Ortega et al., 2013). Heaps et al. (2012) confirmed that HIV-infected adults had lower total white and cortical and sub-cortical gray matter volume, as well as lower thalamus volumes**.**

2. Principles of MRI and brain morphometry

2.1 Basic physics of magnetic resonance imaging (MRI)

MRI gives high spatial resolution of soft tissues like the brain, making it the modality of choice for neuroimaging (Du .H et al., 2012; Tucker et al., 2004; Spudich et al., 2012). Different tissue properties, including relaxation time, density of nuclear particles (protons) and perfusion, temperature and diffusion rate are exploited to create images with different types of contrast. Images generated are useful in clinical research for studying connectivity, function and structure of the brain (Weishaupt et al., 2008; Plewes and Kucharczyk, 2012).

MRI takes advantage of the spin property of elements with an odd number of nuclear particles (protons and neutrons) to create a net magnetisation (Khan, 2013). One such element, hydrogen (one proton) is found in abundance in body water and is useful to generate high resolution spatial images of different tissues of the body (Horowitz, 1989).

At the particle level, each proton spins about its axis generating a relatively small magnetic dipole moment. When placed inside the strong magnetic field (B_0) of an MR scanner, protons within the magnetic field will align in the direction of B_0 and precess at a frequency known as the Larmor frequency, ω_L. This frequency of precession is dependent on the external magnetic field strength B_0 and the gyromagnetic ratio of the nucleus γ

$$\omega_L = \gamma \, . \, B_0$$

To generate the MRI signal, the bulk magnetisation arising from millions of precessing dipole moments is rotated away from its equilibrium position parallel to B_0 through the application of an alternating magnetic field, B_1, that is applied perpendicular to B_0 at the Larmor frequency (Horowitz, 1989; Weishaupt et al., 2008). The time-varying transverse component of this magnetisation can be detected by measuring the current induced in a receiver coil.

The time it takes for spins (protons) to return back their original equilibrium position that aligns to the static magnetic field, B_0, is known as relaxation time (Horowitz, 1989; Weishaupt et al., 2008; Plewes and Kucharczyk, 2012; Khan, 2013). At equilibrium, the transverse magnetisation is zero while the longitudinal magnetisation due to B_0 is at its maximum. The concept of relaxation time is important in MRI, as it provides contrast that is useful for detecting and differentiating pathologies (Weishaupt et al., 2008; Plewes and Kucharczyk, 2012). Various body tissues have unique relaxation times, for example studies

have shown that neoplastic tissue has a longer relaxation time than its corresponding normal tissue (Weishaupt et al., 2008; Plewes and Kucharczyk, 2012; Khan, 2013).

In relaxation, two concepts are important, the first is T1 – the time constant that describes how magnetisation in the Z plane returns to its equilibrium position - also known as spin lattice relaxation time. The second, T2, is the time constant that describes the rate at which magnetisation in the transverse plane returns to its equilibrium state, or the time it takes for the spins to dephase, also known as spin-spin relaxation time.

The important time factors that are manipulated to vary contrast in MRI scans are repetition time (TR) and echo time (TE). TR is the time interval between successive RF pulses applied to a particular slice. Varying the value of TR controls the T1 contrast of the MR signal. TE is the time in milliseconds between the application of the radiofrequency pulse and the peak of the echo signal (Weishaupt et al., 2008; Plewes and Kucharczyk, 2012) and determines the T2 weighting of the images.

These relaxation times and the spin density vary from one tissue type to another and between diseased and normal tissues (Horowitz, 1989; Weishaupt et al., 2008). Different image contrasts are generated depending on the nuclear spin density and by manipulating the time variables defined above. The most basic contrasts in MRI are:

1. **T1- weighted contrast**, created by using short TR and TE, maximizes contrast arising from differences in T1 between different tissues. T1 contrast is most often used for detecting structural abnormalities in soft tissues like the brain. In T1-weighted images, tissues with high fat content (like white matter) appear bright and compartments filled with water (like CSF) appear dark

2. **T2-weighted contrast**, created by using long TR and long TE, optimizes contrast due to differences in T2 relaxation time between tissues. T2 weighting is often used in structural imaging and for investigating fluid in the body. With T2-weighted contrast, compartments filled with water (CSF) appear bright and tissues with high fat content appear dark.

3. **Proton density weighted contrast** involves the use of long TR and short TE to reduce the effect of T1 and T2 contrast. Such images are dependent on the density of protons in different tissue types in the slice or volume of interest. Higher proton density in a given tissue gives a greater transverse component of magnetisation and brighter signal, while fewer protons generates darker signal.

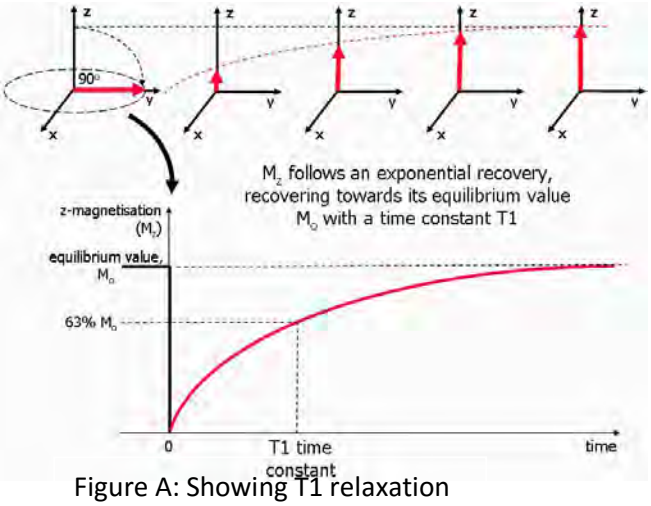

Figure A: Showing T1 relaxation

From: http://www.jcmr-online.com/content/12/1/71/figure/F3?highres=y

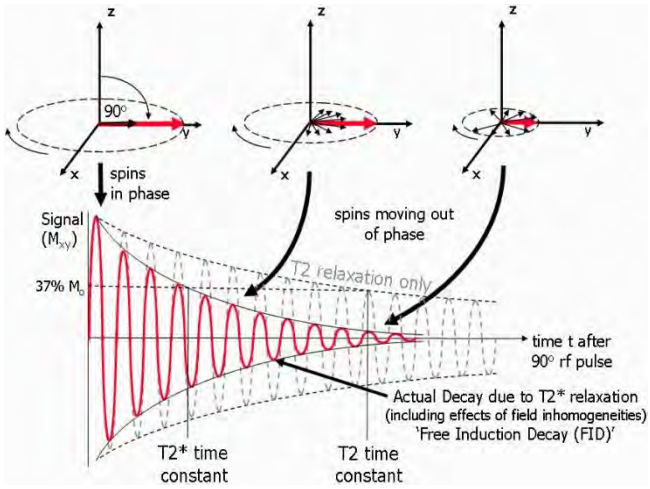

Figure B: Showing T2 relaxation

From: http://www.jcmr-online.com/content/12/1/71/figure/F4?highres=y

In this study, we used T1-weighted MRI scans because of the high contrast and resolution for structural MRI studies. In brain morphometry studies that produce multiple images and contrasts there is usually image distortion due to imperfect shimming in certain regions as a result of rapid magnetic signal changes (Van der Kouwe et al., 2008). Accurate undistorted images are important in brain morphometry. The multiecho magnetisation prepared rapid gradient echo (MEMPRAGE) sequence reduces B_0 distortion without signal-to-noise ratio (SNR) consequences. Further, the MEMPRAGE improves cortical segmentation and segmentation of boundaries of structures such as the globus pallidum and thalamus compared to the standard magnetisation prepared rapid gradient echo (MPRAGE) sequence (Van der Kouwe et al., 2008). It has been recommended for accurately estimating intracranial volume, volume of sub-cortical structures and cortical thickness and its bandwidth can be matched with other multispectral morphometry protocols so that fine edges of structures register accurately across different contrasts (Van der Kouwe et al., 2008).

2.2 MRI morphometry with FreeSurfer

FreeSurfer is widely used to study brain cortical and sub-cortical anatomy (http://freesurfer.net/fswiki/FreeSurferAnalysis PipelineOverview). It is an open source suite for processing and analysing human neuroimaging data (Fischl et al., 2000; Dale et al., 1999), developed at the Martinos Center for Biomedical Imaging by the Laboratory for Computational Neuroimaging (Fischl, 2012). It uses an array of algorithms to quantify functional, connectional and structural properties of the human brain (Fischl, 2012). It evolved from a simple package that aimed to construct a cortical surface model of the brain, into a tool that creates an automated segmentation of the macroscopic visible structure of the brain from a T1-weighted image (Fischl et al., 1999b, 2002; Fischl, 2012).

The group that developed FreeSurfer has also developed optimised imaging protocols for T1-weighted MRI scans that are required for input to FreeSurfer. There are specifications for optimised (fast low angle shot) FLASH and magnetisation prepared rapid gradient echo (MPRAGE) sequences.

What later became FreeSurfer was originally developed to create cortical surface models to be used to solve the EEG/MEG inverse problem. Some of the tools that were later brought together as FreeSurfer were initially used in research on retinotopic representation in the visual cortex, which later helped in understanding the human visual system (Fischl, 2012).

FreeSurfer extensively analyses most structural features of the adult human brain. Some of its specific functionalities include:

1. Volumetric segmentation of macroscopic visible brain structures (Fischl et al., 2002. 2004a)
2. Segmentation of the hippocampal subfields (Van Leemput et al., 2009)
3. Inter-subject alignment based on cortical folding patterns (Fischl et al., 1999b)
4. Segmentation of white matter regions using diffusion MRI (Yendiki et al. 2008)
5. Parcellation of cortical folding patterns (Desikan et al., 2006; Destrieux et al., 2010, Fischl et al., 2004b)
6. Estimation of architectonic boundaries from in-vivo data (Fischl et al., 2008, 2009; Hinds et al., 2008; Yeo et al., 2009).
7. Mapping of the thickness of cortical gray matter (Fischl and Dale, 2000).
8. Construction of surface models of the human cerebral cortex (Dale et al., 1999; Fischl et al., 1999a)

The main uses of FreeSurfer are to produce a volumetric segmentation and labelling of sub-cortical brain structures and to create a surface model of the cerebral cortex (Fischl and Dale, 2000; Fischl et al., 2004a). The cortical structure created can be overlaid with fMRI data and cortical thickness and gyrification data can also be gathered (Fischl and Dale, 2000; Fischl et al., 2004a, 2004b, 2008, 2009). From the sub-cortical structure, volumetric data of global and regional volumes can be obtained. Both cortical and sub-cortical analysis can be done for cross-sectional and longitudinal studies (Fischl et al., 2004a, 2004b).

FreeSurfer is open source and freely available, and is compatible with most hardware and software platforms (Fischl, 2012). FreeSurfer runs on Mac Os or LINUX machines and has all its processing streams controlled by a shell script (recon-all). It requires an enormous amount of CPU processing power and memory space due to the numerous algorithms that the different processing streams use in image reconstruction. At least a 2GHz or faster processor, 4GB of RAM and 3D graphics memory is required for

the processing of MRI data. FreeSurfer also requires a minimum of 8.5GB of disk space for a complete installation (binaries, support libraries, MINC toolkit and sample MRI data). A graphical tool, QDEC (Query, Design, Estimate, Contrast), can be used to perform structural comparisons of brain surface measurements and subsequently display brain regions where there are significant differences between groups (FreeSurfer wiki, 2014)

2.3 Image processing with FreeSurfer

The process of generating the cortical and sub-cortical data is achieved by a series of workflow commands linked together as pipelines, which are divided into a surface-based (Fischl et al, 1999; Dale et al, 1999) and volume-based stream (Fischl et al, 2002, 2004).

The surface-based stream, or cortical surface reconstruction, involves:

1. Registration to Talairach space
2. Intensity normalization to correct for B1 magnetic field inhomogeneities
3. Removal of extra-cerebral voxels (skull-stripping)
4. Structural segmentation of the gray-white interface, which involves separating the two brain hemispheres and disconnecting cortical structures from the sub-cortical components
5. Filling of possible interior holes in the white matter components of each hemisphere
6. Deformation to produce a smooth white/gray matter surface and gray matter/CSF (pial) surface

When the surface reconstruction process is completed, cortical thickness, local gyrification index (LGI), local curvature, surface area and surface normal data can be computed at each vertex on the reconstructed cortical surface.

The volume-based (sub-cortical) stream involves:

1. Talairach registration using a procedure which is insensitive to pathologic brain tissues
2. Initial volumetric labelling
3. Correction of varying sub-cortical tissue intensity due to B1 bias field (using a different method from that performed in the surface-based stream)
4. High dimensional, non-linear volumetric alignment to the Talairach atlas
5. Final detailed volume labelling

The cortical and sub-cortical labelling use the same basic set of algorithms which yield the final segmentation. After segmentations have been created, various analyses can be performed using both

cortical and sub-cortical data. Longitudinal analysis can also be performed using the FreeSurfer longitudinal processing stream.

2.4 Statistical analysis using QDEC

QDEC - is an acronym for Query, Design, Estimate, Contrast. It is the graphical user interface (GUI) platform in FreeSurfer for performing inter-subject averaging and group comparison, and drawing inferences on morphometry data generated from FreeSurfer's reconstruction processes.

Surface-based vertex-wise analysis involves performing the General Linear Model (GLM) at each vertex to test how surface-based measures are influenced by demographic, clinical or genetic conditions. In FreeSurfer, vertex-wise surface-based analysis may be performed with the (GUI)-based **QDEC** or the command-based **mri_glmfit**. For our study cortical thickness and Local Gyrification Index (LGI)/Gyrification comparisons were performed in QDEC.

All vertex-wise analyses performed with QDEC involve an initial analysis to locate regions where there are significant differences between groups at an uncorrected threshold significance level (α). Multiple comparison correction can then be performed on clusters (regions) at a specified level of significance.

The multiple comparison problems in neuroimaging refers to simultaneous comparisons performed on a large number of voxels, some of which will be significant by chance (false positives). The reason for performing multiple comparison correction is to minimize type-1 error (finding significant voxels that are not truly significant).

The QDEC processing stream performs cluster-size correction for multiple comparisons using Monte Carlo simulation. This works on the principle that for a certain smoothness of data and uncorrected *p* threshold, larger clusters are more likely to be truly significant while smaller ones may be false positives that appear significant by chance. Using Monte Carlo simulation the distribution of the maximum cluster size under the null hypothesis can be generated, and for each cluster in the thresholded data, the probability *p* of seeing a maximum cluster that size or larger can be determined. Only clusters with a *p* value smaller than a selected threshold are retained.

Most studies performed with FreeSurfer compare brain structure between healthy and diseased subjects, delineate the effect of particular conditions on brain structure, or aim to detect specific regions that are affected by disease conditions (Fischl and Dale, 2000; Fischl et al., 2004a, 2004b). FreeSurfer has been used in studies investigating various conditions, including semantic dementia, autism, and Alzheimer's

disease (Fischl et al. 2002; Fischl, 2012). It has also found application in research of the effect of biochemical and synthetic drugs on brain structures (Fischl and Dale, 2000; Fischl, 2012).

In this study FreeSurfer was used to investigate the effect of HIV-infection and different ART regimens on the brain structure of children at age 7 years.

2.5 Neuroimaging measures for the study

Based on the reviewed literature, the current study focused on the investigation of cortical thickness, sulcal enlargement (using local gyrification indices) and brain volume differences among our subject groups: HIV-infected (3 different treatment arms) and HIV-uninfected (consisting of HIV-exposed and unexposed).

In FreeSurfer, cortical thickness is a measure of the distance between the white matter(wm)-gray matter(gm) interface and the gm-CSF surface. Local Gyrification Index (LGI) quantifies the amount of cortex buried within the sulcal folds, as compared with the amount of cortex on the outer visible cortex (Schaer et al., 2008; FreeSurfer Tutorial, 2009; White et al., 2010). A higher degree of cortical folding gives a larger LGI value. LGI is inversely related to sulcal enlargement which is a neurological condition that has been observed in HIV-infected children.

2.6 Hypotheses

Based on the literature reviewed, we expected that:

1. There would be little or no significant difference in cortical thickness between infected and uninfected children, because HIV-infected children were initiated to early ART, causing a reduction of brain viral load and nearly normal development of brain cortex in infected children through birth until 7 years.
2. There would be little or no difference in LGI between HIV-infected children and uninfected controls, due to early ART initiation.
3. There would similarly be little difference in global gray and white matter volume, and general brain size (intracranial volume) between infected and uninfected children because of considerable reduction in brain viral load by early ART initiaition. Also we expected that volume of most ROIs would not be different between infected and uninfected children, but because of the selective effect of ART on different brain tissues, we expected that there might be certain ROIs, such as the bilateral caudate, where volume would be significantly different between infected and uninfected children.

4. In all regions that differ between infected and uninfected children, we hypothesized that infected children would have smaller volumes than uninfected children except in the lateral ventricles where HIV-associated enlargement is expected.
5. Increased neuroimaging measures (cortical thickness, LGI, global and regional brain volume) would be associated with improved clinical outcomes (higher CD4 and CD4/CD8 ratio, longer cumulative duration of ART and earlier age at ART initiation) within infected children.

Overall, we expected that cortical changes would be associated with neurocognitive impairment (Gavin et al., 1999), while sub-cortical volumetric changes have been linked to progression of HIV encephalopathy, psychomotor, emotional and behavioral disorders (Steinbrink et al., 2013).

3. Methods

3.1 Study participants

The participants for this study were children from the Cape Town arm of the Children with HIV Early Antiretroviral Therapy (CHER) follow- on study, who all received an MRI scan within 6 months of their 7th birthday. There was no inclusion or exclusion criteria, data of all children that presented for MRI were used. HIV-infected participants were randomized in infancy into three treatment arms, differing in time of initiating ART and duration of treatment before initial interruption, while the uninfected control group was divided into two groups based on the mothers' HIV status during pregnancy. The different groups were:

- ART (Lamivudine, Zidovudine, Lopinavir and Ritonavir) delayed until clinical/immunological criteria were met – **ART-Def**
- ART commenced before 12 weeks and interrupted at 40 weeks until symptomatic – **ART-40W**
- ART commenced before 12 weeks and interrupted at 96 weeks until symptomatic – **ART-96W**

Infected

- HIV-exposed in utero, but uninfected – **Exposed (HEU)**
- Born to uninfected mothers – **Unexposed (HUU)**

Uninfected

3.2 Image acquisition and analysis

T1 high-resolution structural MRI brain scans were acquired in all participants in the sagittal orientation on a 3T Allegra scanner (Siemens, Erlangen, Germany) at the Cape Universities Brain Imaging Centre (CUBIC) using a 3D EPI-navigated multiecho magnetisation prepared rapid gradient echo (MEMPRAGE) sequence (Field of View (FOV) 224 x 224 mm^2, TR 2530 ms, T1 1160 ms, TE's = 1.53/3.19/4.86/6.53 ms, 144 slices, 1.3 x 1.0 x 1.0 mm^3 spatial resolution). Scanning was performed according to protocols that had been approved by both the University Of Cape Town Faculty Of Health Sciences Human Research Ethics Committee and the Human Research Ethics committee of Stellenbosch University. Parents/guardians of participants provided written informed consent for scanning while participants gave oral assent.

MRI scans were analysed with FreeSurfer version 5.1.0 on a 64-bit Linux (Ubuntu 13.04) machine, to generate measures of cortical thickness, local gyrification and regional brain volume. The manual and automated steps involved in the process can be summarized as follows:

1. Conversion of each subject's high resolution T1 structural MRI scan from DICOM format to FreeSurfer .mgz format.
2. Execution of the recon-all process to perform the reconstruction of the subjects' brain models in three stages (recon-all autorecon1, autorecon-2, autorecon-3). The entire reconstruction process for each subject takes between 15-20 hours assuming no runtime error.
3. Manual inspection of reconstructed surfaces and segmentations. Initially TKSURFER was used to view the cortical surface while TKMEDIT was used for the sub-cortical surface but a recent innovation is the use of FREEVIEW platform for both surfaces was used subsequently.
4. Troubleshooting and manual editing of reconstructed image models. This involves:
    i. Talairach transformation edits
    ii. Skull stripping corrections
    iii. White and pial surface troubleshooting, including white matter intensity normalization and correction of improper boundary segmentation between different brain tissues (pial, gray, and white matter).

    Reconstruction is repeated after manual editing and inspection until the desired model with minimal structural error is generated.
5. Generation of structural brain measures such as cortical thickness, local gyrification indices (LGI), intracranial and regional brain volumes for analysis using QDEC (FreeSurfer) or R.

3.3 Outlier exclusion

Mean measures of cortical thickness and LGI for each hemisphere, as well as total brain volume, were examined for outliers. Subjects were excluded from all analyses if their data from any of these measures were classified as extreme outliers: greater or less than the median $\pm$ 3 x interquartile range (IQR) in the sample. In addition, in the brain volume analysis, subjects whose regional brain volumes were extreme outliers were excluded from analysis of that region only.

3.4 Analysis of cortical thickness and LGI

Mean values of surface-based measures (cortical thickness and LGI) were calculated within certain ROIs and exported to a statistical program (R, Stata) for further analysis. In addition, Data from FreeSurfer's surface based stream were analysed using vertex-wise analysis over the whole brain. Surface-based vertex-wise analysis involves performing the General Linear Model (GLM) at each vertex to test how

surface-based measures are influenced by demographic, clinical or genetic conditions. In FreeSurfer, vertex-wise surface-based analysis may be performed with the command-based **mri_glmfit** or with the graphical user interface (GUI)-based **QDEC** (http://surfer.nmr.mgh.harvard.edu/fswiki/FsTutorial/QdecGroupAnalysis_freeview)**.**

In this study, cortical thickness and LGI were analysed vertex-wise over the whole brain using QDEC. In each vertex-wise analysis, results were thresholded at an initial uncorrected threshold of $p<0.05$; cluster size correction for multiple comparisons was then performed using Monte Carlo simulation, and results are reported for a cluster size corrected threshold of $p<0.05$.

Group analyses of cortical thickness and LGI were performed to investigate:

- The effect of HIV infection on cortical thickness and LGI (HIV-infected vs. uninfected children)
- The effect of HIV exposure on cortical thickness and LGI in uninfected children (HIV-exposed uninfected children vs. unexposed uninfected children)

The effect of sex on cortical thickness and LGI measures was also investigated. If there were regions where measures were significantly different between sexes, the HIV infection/exposure analysis was repeated while controlling for sex as a confounder.

We then also tested for a sex-HIV infection interaction and, in HIV-uninfected children, a sex-HIV exposure interaction on cortical thickness and LGI.

3.5 Brain volume region of interest (ROI) comparison

Statistical analysis on brain volumes was performed with Rstudio and STATA statistical software to compare total brain, gray and white matter volumes between groups, as well as volumes of certain regions of interest (ROIs), which were selected based on the literature. Intracranial volume, generated from the FreeSurfer automated stream, was controlled for as a potential confounder. Studies on pediatric HIV have linked changes in specific brain tissues with HIV infection and ART (Mitchell, 2001; Paul et al, 2002). Based on this, the brain regions included in the volume comparison part of this study were the bilateral caudate,

thalamus, hippocampus, putamen and lateral ventricles. The corpus callosum volume, as well as the global white matter, gray matter and total intracranial volume were also investigated.

Initial exploratory, descriptive and visualization analyses were performed to understand the nature of the available data and to determine which statistical analyses were most appropriate. Data were checked for normal distribution and for correlation with possible confounders (sex and intracranial volume). If a confounder was correlated with the dependent variable at $p<0.05$ it was included as a control variable in subsequent analyses. Group analyses of regional brain volumes were performed to investigate the effect on brain volume of:

- HIV-infection - Student's *t*-test was used to compare volumes between HIV-infected and uninfected children. Confounders were controlled for using analysis of covariance (ANCOVA).

- Different ART treatment arms - analysis of variance (ANOVA) was used to compare volumes among the three treatment arms (ART-Def, ART-40W and ART-96W). Pairwise post-hoc tests for the ANOVA were performed with Bonferroni correction. Similarly, an ANCOVA test was used to control for confounding variables and Tukey's test was used for pairwise post-hoc tests for the ANCOVA analysis.

- HIV-exposure - Student's *t*-test was used to test for differences in brain volume between HIV-exposed and unexposed children. Subsequently, confounding variables were controlled for using an ANCOVA test.

All significance tests were performed at $p<0.05$.

3.6 Relationship between neuroimaging measures and clinical data in HIV-infected children.

The relationship between neuroimaging measures (cortical thickness and LGI) and clinical data at enrollment (CD4 count (cell/mm^3), CD4 percentage (cell/mm^3), CD4/CD8 ratio), age at ART initiation (weeks) and cumulative period on ART (weeks) was also investigated in 58 HIV-infected children. The nadir CD4 was not included in this study, because childrens' nadir CD4's were within a narrow range. Children

not in early treatment groups were started on ART once their CD4 percentage dropped below 25%, and for children on early treatment, CD4 dropped to similar levels after interruption. As such there was little or no variation in nadir CD4 of HIV-infected children.

Vertex-wise analyses were performed using QDEC to investigate the relationship between neuroimaging measures and these 5 clinical measures. Initial pairwise correlation was performed between each of the clinical measures and cortical thickness/LGI at a significance threshold of $p<0.05$, and cluster-size multiple comparison correction was performed at $p<0.05$. The correlation between sex and each of the neuroimaging measures was also performed at the same significance level to investigate a possible confounding effect of sex. Subsequently another correlation was performed between each clinical measure and cortical thickness/LGI while controlling for the effect of sex. All analyses were cluster-size corrected for multiple comparisons using Monte Carlo simulation at a threshold of $p<0.05$. For each subject, the mean LGI/cortical thickness value was extracted in each cluster that survived multiple comparison correction, and the Pearsons' correlation coefficient (r) between the clinical measure and mean LGI/cortical thickness is reported

The relationship between clinical data and brain volumes in the selected ROIs was also investigated using Rstudio tools. The Pearson product-moment correlation was calculated between the 5 clinical measures and the volumes of the bilateral caudate, thalamus, hippocampus, putamen and lateral ventricle, and corpus callosum, as well as the global white matter, gray matter and total intracranial volume at a level of significance of $p<0.05$. A possible confounding effect of sex and intracranial volume was also investigated by calculating their correlation with the ROI volumes. Subsequently, multiple regression analyses of brain ROI volume and clinical measures were performed while controlling for the effect of sex and intracranial volume. All analyses were performed at a significance level of $p<0.05$.

4. Results

4.1 Comparison of HIV-infected children to HIV-uninfected children

4.1.1 Sample characteristics

Of the 100 isiXhosa children (57 infected; 43 uninfected) who received MRI, data from one girl in the ART-40W treatment arm were excluded as her mean LGIs for both hemispheres were extreme outliers (> 3 IQRs below the 25th percentile). As such, we present data for 99 isiXhosa children (56 HIV-infected (25 boys); 43 uninfected children (25 boys); age 7.00 – 7.83 years). Sample characteristics are presented in Table 1. Groups did not differ in age or gender.

Table 1: Sample characteristics of HIV-infected children and uninfected controls

	HIV-infected	**Uninfected**	***t* or χ^2**	***p*-value**
Sample size (*N*)	56	43		
Age at scan (years)	7.20 (0.13)	7.23 (0.15)	-1.20	0.23
Number of males (% males)	25 (45%)	25 (58%)	1.27	0.26

Values are *N* (% of total) or mean (standard deviation)

4.1.2 Vertex-wise analysis of cortical thickness

No regions showed significant differences in cortical thickness between infected and uninfected children after cluster size correction for multiple comparisons. However, in a separate analysis including both infected and uninfected children, boys showed significantly thinner cortex than girls in several regions in both hemispheres (Table 2 and Figure 1(a)), most of which remained significant after controlling for HIV infection status (Table 2 and Figure 1(b)). Even after controlling for sex, no regions emerged where cortical thickness differed between infected and uninfected children.

Table 2: Regions where boys have thinner cortex than girls (*N*=99: 49 female, 50 male) before and after controlling for HIV infection

	Before controlling for HIV infection status		After controlling for HIV infection status	
Region label	**MNI co-ordinates at peak**	**Cluster size (mm^2)**	**MNI co-ordinates at peak**	**Cluster size (mm^2)**
Left				
Superior/ rostral middle frontal	-11.1, 7.3, 36.6	9897	-12.7, 37.9, 18.1	9443
Superior/ caudal middle frontal	-20.5, 1.5, 45.3	883	ns	ns
Pars opercularis	-51.2, 13.4, 5.6	2007	-50.9, 13.6, 5.6	1557
Isthmus cingulate	-10.9, -44.7, 29.5	1361	-11.5, -44.7, 29.5	1278
Supramarginal	-57.5, -43.3, 33.5	3549	ns	ns
Inferior temporal	-45.7, -42.8, -11.1	3130	-45.0, -43.1, -10.5	5875
Right				
Middle temporal	61.6, -44.3, 1.5	1754	ns	ns
Fusiform	34.7, -7.7, -29.9	1074	34.7, -7.7, -29.9	3160
Insula	31.3, 20.5, 0.2	3209	31.5, 20.2, 0.5	2190
Superior frontal	9.7, 28.6, 30.9	1101	ns	ns
Precentral	43.3, 3.0, 42.0	1177	43.3, 3.0, 42.0	1409
Superior temporal	64.1, -34.6, 14.3	956	64.1, -34.6, 14.3	1017

ns – Not significantly different after controlling for HIV-infection status

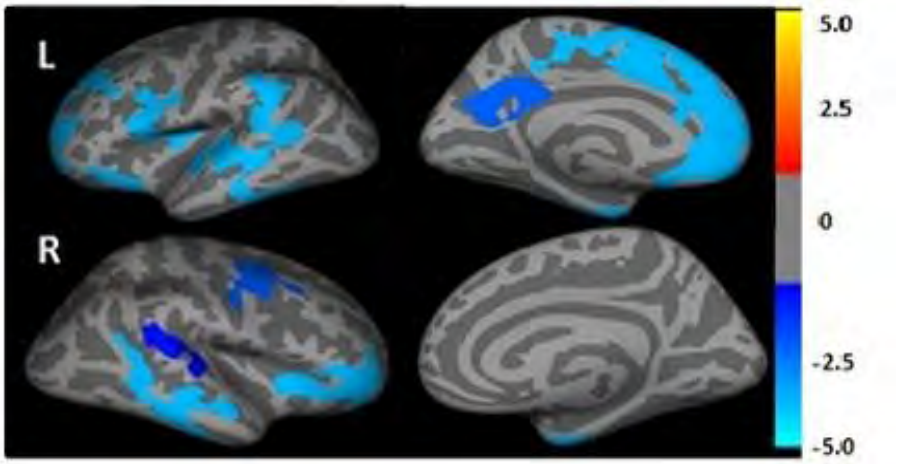

a) Before controlling for HIV infection status

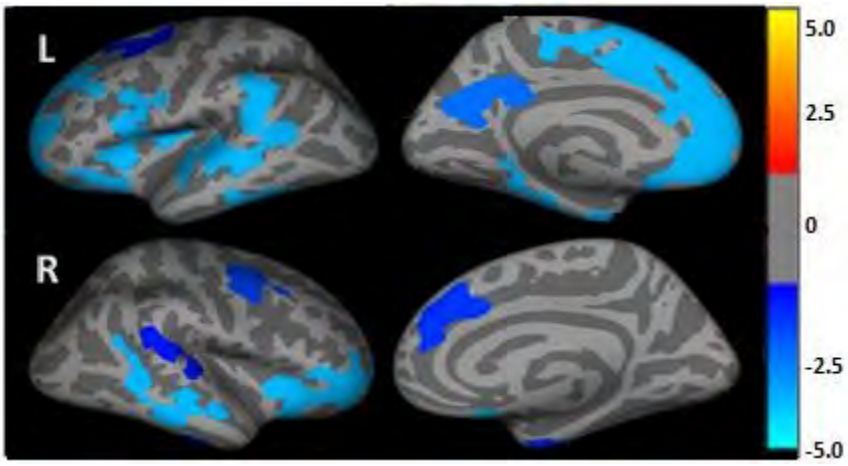

b) After controlling for HIV infection status

Figure 1: Lateral and medial views of regions in the left and right hemispheres where cortex was significantly thinner in boys than in girls (threshold at $p<0.05$, cluster size threshold $p<0.05$)

4.1.3 Vertex-wise analysis of local gyrification indices (LGIs)

Local gyrification was greater in uninfected children than HIV-infected children in a large (8223 mm^2) left medial parietal region (MNI co-ordinates -6.2, -25.5, 51.3; Figure 2(a))

Further, boys showed significantly greater LGIs than girls bilaterally in a parahippocampal/fusiform region (left: MNI co-ordinates -32.5, -26.3, 15.8, 2999mm^2; right: MNI co-ordinates 34.8, -32.8, -18.9, 6333mm^2; Figure 3). After controlling for the potential confounding influence of sex on LGIs, two left medial parietal regions were identified where LGIs were greater in uninfected children compared to infected children,

both of which overlapped with the single large medial parietal cluster previously identified (Table 2 and Figure 2(b))

Separate comparisons of the HIV-infected group with each of the exposed uninfected and unexposed uninfected subgroups, showed that exposed and unexposed children contributed to different components of the large medial parietal cluster where LGIs were greater in uninfected children. Exposed children had greater LGIs than infected children in a more lateral area of the left superior parietal region (MNI co-ordinates: -22.0, -72.9, 32.9; cluster size: 1931mm^2) as shown in Figure 4 (top) while the unexposed children had greater LGIs than infected children in two more medial regions of the same hemisphere, namely paracentral (MNI co-ordinates: -5.6, -26.5, 50.9; cluster size: 1751 mm^2) and superior parietal (MNI co-ordinates: -15.5, -70.7, 41.4; cluster size: 1554mm^2) regions as indicated in Figure 4 (bottom).

There was a significant interaction effect of sex on the relationship between HIV status and LGI bilaterally in inferior parietal regions and in a left hemispheric supramarginal region (Table 4 and Figure 5). The plots of mean LGIs in the two left parietal clusters in Figure 6 show that mean LGIs in these regions were significantly higher in uninfected boys compared to infected boys, while LGIs of infected and uninfected girls were similar. At the right hemispheric inferior parietal region, a similar result was obtained for both sexes.

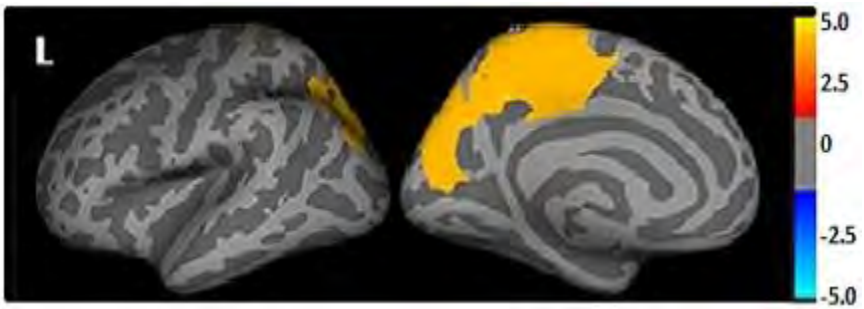

a) Before controlling for sex

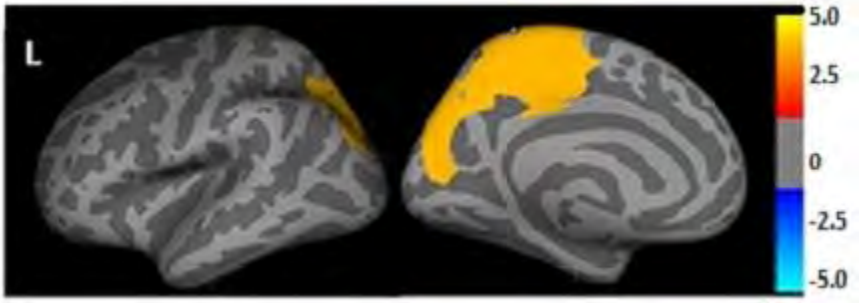

b) After controlling for sex

Figure 2: Left lateral and medial parietal region where uninfected (exposed and unexposed) children showed significantly greater LGIs than HIV infected children (threshold at *p*<0.05, cluster size threshold *p*<0.05)

Table 3: Regions where uninfected children have greater LGIs than infected children after controlling for sex (*N*=99: 56 infected, 43 uninfected)

Comparison	Hemisphere	Region label	MNI co-ordinates at peak	Cluster size (mm^2)
Uninfected > infected	Left	Paracentral	-6.2, -25.5, 51.3	1387
		Superior parietal	-15.8, -72.2, 42.9	820

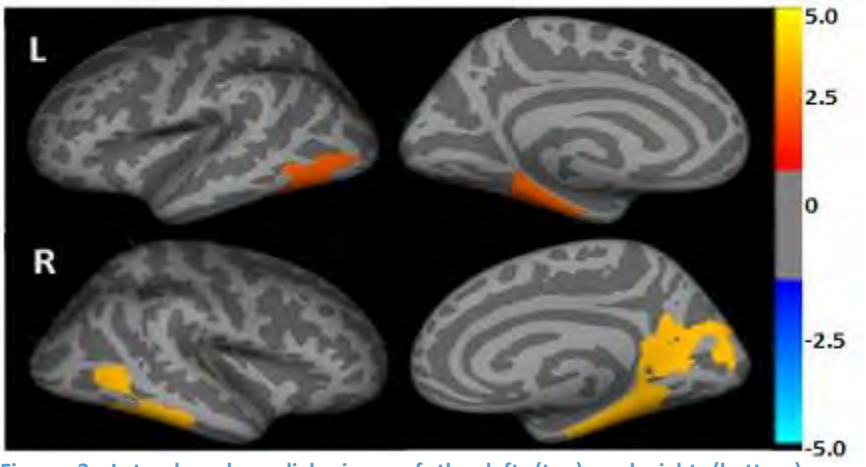

Figure 3: Lateral and medial views of the left (top) and right (bottom) fusiform/parahippocampal region where boys have greater LGIs than girls (threshold at $p<0.05$, cluster size threshold $p<0.05$)

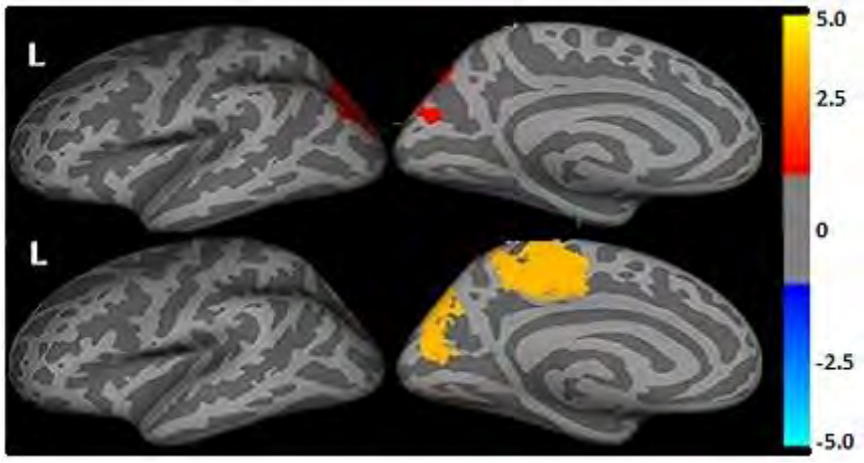

Figure 4: Lateral and medial views of left lateral parietal region where exposed children showed significantly greater LGIs than HIV infected children (top) and where unexposed children showed significantly greater LGIs than HIV infected children (bottom) (threshold at $p<0.05$, cluster size threshold $p<0.05$)

Table 4: Regions exhibiting an interaction effect of sex on the relationship of HIV status to LGIs (N=99: 56 infected, 43 uninfected)

Comparison	Hemisphere	Region label	MNI co-ordinates at peak	Cluster size (mm^2)
Gender-Diagnosis interaction	Left	Inferior parietal Supramarginal	-37.1, -54.0, 21.8 -51.9, -37.5, 44.0	1807 911
Gender-Diagnosis interaction	Right	Inferior parietal	40.8, -68.1, 19.8	4915

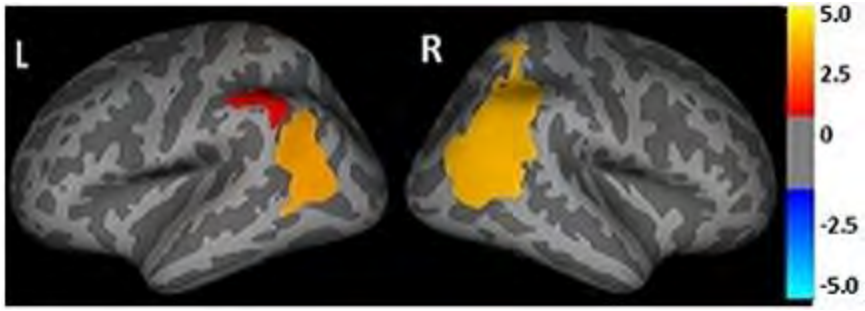

Figure 5: Left (on left) and right (on right) parietal clusters where there was a significant interaction effect of sex on the relationship between HIV infection status and LGIs (threshold at $p<0.05$, cluster size threshold $p<0.05$)

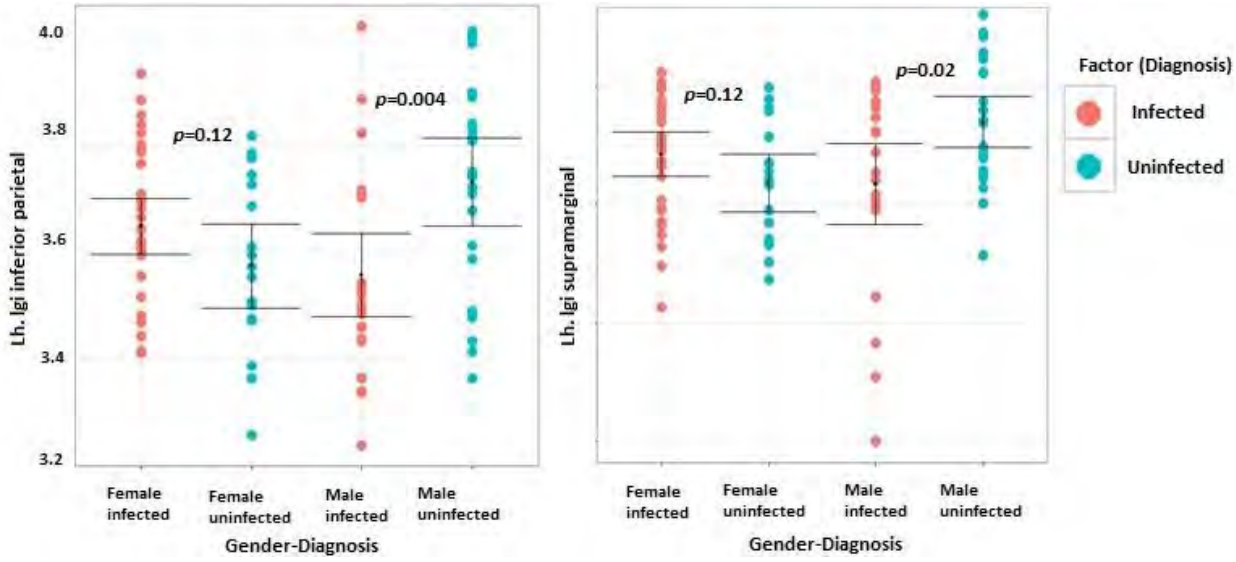

Figure 6: Plots showing how the effect of HIV infection on LGIs differs in girls and boys in left inferior parietal (left) and left supramarginal (right) clusters

4.1.4 Region of interest (ROI) volume comparison between infected and uninfected children

Since global and regional brain volumes were all strongly related to both total intracranial volume and sex (Table 5), we controlled for both intracranial volume and sex in all subsequent analyses. Global white matter volume and left and right thalamus volume showed the strongest relationship with intracranial volume (Figure 7). All global and regional volumes were larger in boys than girls.

Before controlling for confounders, uninfected children had significantly larger volumes of global white matter, as well of the right hippocampus, and putamen bilaterally (Table 6) effects that remained after controlling for sex and total intracranial volume. After controlling for sex and total intracranial volume, global gray matter volume was also larger in uninfected children compared to infected children.

Table 5: Association of regional brain volumes with total intracranial volume and sex (*N*=99: 56 infected, 43 uninfected)

Brain region	Intracranial volume		Sex	
	Correlation (*r*)[a]	*p*-value	Correlation (*r*)[a]	*p*-value
Intracranial volume			0.48	<0.001
Global gray matter	0.67	<0.001	0.25	0.01
Global white matter	0.79	<0.001	0.44	<0.001
Corpus callosum	0.42	<0.001	0.27	0.01
L caudate	0.63	<0.001	0.29	0.004
R caudate	0.63	<0.001	0.28	0.01
L hippocampus	0.34	<0.001	0.23	0.02
R hippocampus	0.45	<0.001	0.34	<0.001
L putamen	0.51	<0.001	0.35	<0.001
R putamen	0.49	<0.001	0.37	<0.001
L thalamus	0.72	<0.001	0.45	<0.001
R thalamus	0.71	<0.001	0.40	<0.001
L lateral ventricle	0.59	<0.001	0.25	0.01
R lateral ventricle	0.61	<0.001	0.22	0.03

[a] *r* is Pearson's correlation coefficient

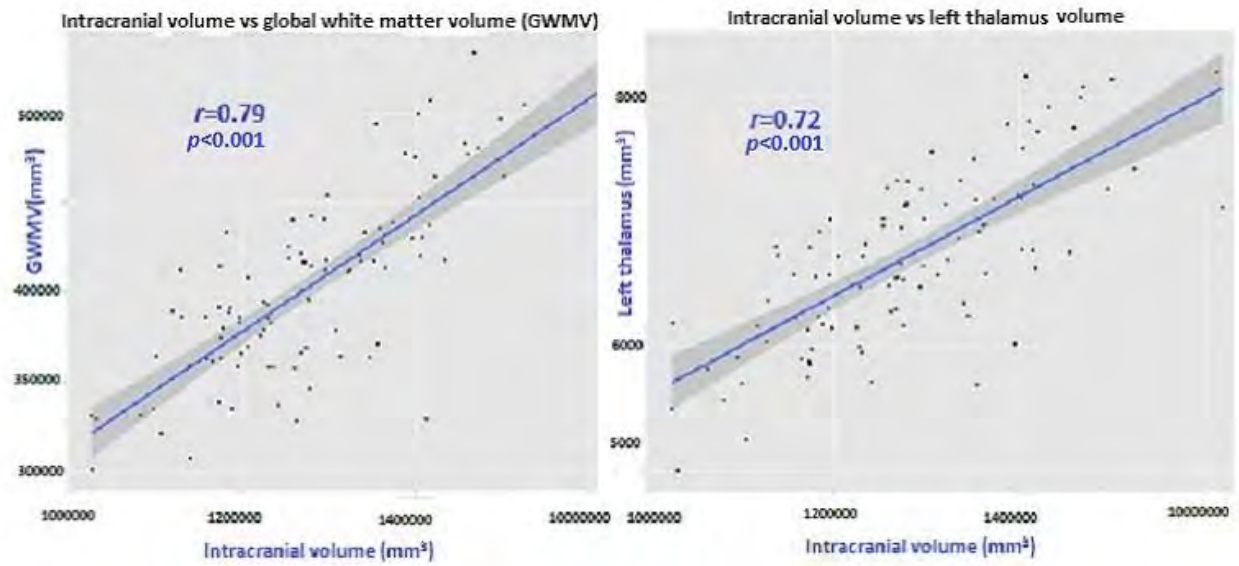

Figure 7: Scatter plots showing the association of brain size with global white matter (GWMV; left) and left thalamus (right) volumes

Table 6: Effect of HIV infection on regional brain volumes (*N* = 99: 56 infected, 43 uninfected)

Brain region	Median (IQR) volume (mm^3)		Students' t-test		ANCOVA controlling for sex		ANCOVA controlling for sex and intracranial volume	
	Infected	Uninfected	*t*-value	*p*-value	*F*-value	*p*-value	*F*-value	*p*-value
Intracranial volume	1268000 (156682)	1294000 (200975)	-1.49	0.14	2.83	0.09	2.83	0.09
Global gray matter	707500 (60460)	721600 (116210)	-1.85	0.07	3.56	0.06	5.96	0.02
Global white matter	393000 (63027)	416800 (76108)	-2.19	0.03	5.75	0.02	12.29	0.001
Corpus callosum	3044 (527)	3121 (632)	-0.96	0.34	0.99	0.32	1.10	0.29
L caudate	3862 (650)	4053 (562)	-1.23	0.22	1.62	0.21	2.43	0.12
R caudate	3972 (764)	4239 (788)	-1.43	0.16	2.17	0.14	3.24	0.08
L hippocampus[1]	3460 (499)	3633 (457)	-1.15	0.25	2.14	0.15	2.27	0.14
R hippocampus[2]	3542 (538)	3657 (648)	-2.24	0.03	6.34	0.01	7.06	0.01
L putamen	6058 (886)	6514 (1006)	-3.16	0.002	11.06	0.001	13.06	0.001
R putamen	5820 (860)	6322 (993)	-3.23	0.002	11.73	<0.001	13.48	<0.001
L thalamus	6598 (964)	6766 (813)	-0.50	0.62	0.31	0.58	0.53	0.46
R thalamus	6900 (1106)	6959 (980)	-0.90	0.37	0.95	0.33	1.61	0.21
L lateral ventricle	4852 (2981)	4622 (3957)	-3.30	0.74	0.12	0.74	0.16	0.69
R lateral ventricle	4648 (2487)	4398 (2331)	-0.17	0.87	0.03	0.86	0.05	0.83

[1, 2] Left and right hippocampus had one extreme outlier each, which was removed before comparison (*N* = 98)
Comparisons significant at p<0.1 are denoted in red.

4.2 Comparison of exposed uninfected children to unexposed uninfected children

4.2.1 Sample characteristics

The uninfected group comprised 22 HIV-exposed uninfected (HEU) and 21 HIV-unexposed uninfected (HUU) children (age range: 7.00 – 7.75 years; Table 4).

.

Table7: Sample characteristics of HIV-uninfected children

	Exposed	**Unexposed**	***t* or χ^2**	***p*-value**
Sample size (*N*)	22	21		
Age at scan (years)	7.23 (0.14)	7.24 (0.18)	-0.18	0.86
Number of males (% males)	12 (57%)	13 (59%)	0	1

Values are *N* (% of total) or means (standard deviation)

4.2.2 Vertex-wise analysis of cortical thickness

Amongst the uninfected children, HIV-exposed children had thicker cortex than unexposed children in a left frontal region centered on the pars opercularis of the inferior frontal gyrus (MNI co-ordinates 43.2, 24.8, 13.0; cluster size 838 mm^2; Figure 8). The difference in this region was no longer significant after controlling for the potential confounding influence of sex on cortical thickness.

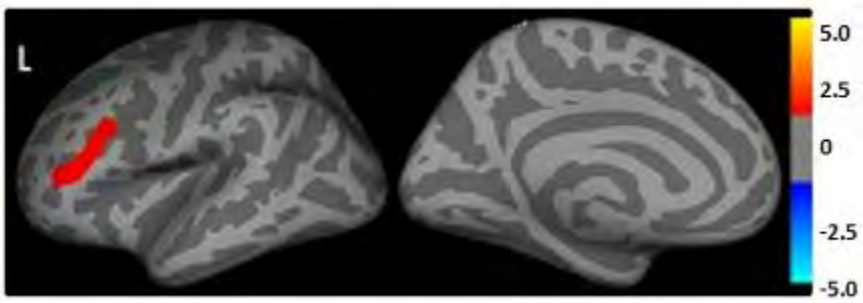

Figure 8: Region in left inferior frontal gyrus where exposed uninfected children had thicker cortex than unexposed uninfected children (threshold at *p*<0.05, cluster size threshold *p*<0.05)

4.2.3 Vertex-wise analysis of local gyrification indices (LGIs)

Amongst uninfected children, there were no regions where LGIs differed between HIV-exposed and unexposed children. However, after controlling for sex, a region emerged in the right precuneus (MNI co-ordinates 7.4, -64.0, 42.1; 2489 mm^2) where exposed children had greater LGIs than unexposed children (Figure 9).

One region emerged in the right lingual gyrus (MNI co-ordinates: 4.4, -73.8, 4.5; 1813 mm^2) where sex altered the effect of HIV exposure on LGI (Figure 10). It is evident from the plot of mean LGIs in Figure 11 that LGIs are higher in exposed girls compared to unexposed girls in this region, while LGIs in exposed and unexposed boys did not differ.

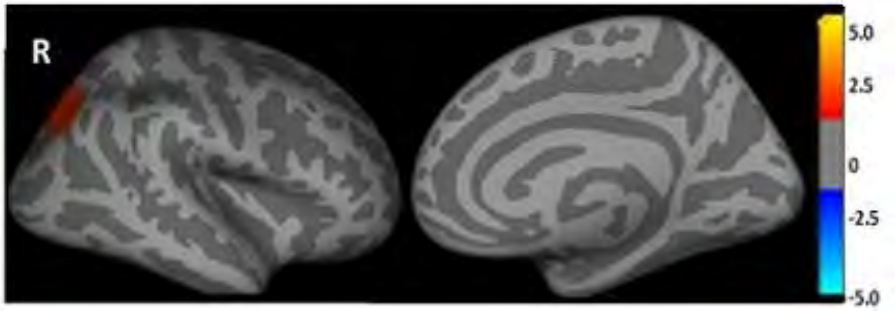

Figure 9: Right precuneus region where the LGI is greater in HIV exposed uninfected children than unexposed uninfected children after controlling for sex (threshold at p<0.05, cluster size threshold p<0.05)

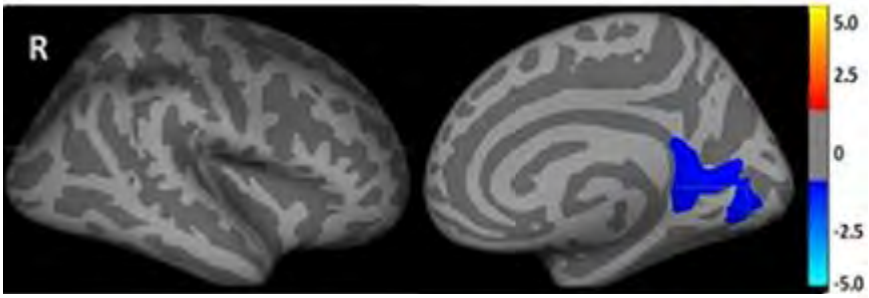

Figure 10: Lateral and medial views of the right hemisphere showing right lingual gyrus cluster where sex altered the effect of HIV exposure on LGI (threshold at p<0.05, cluster size threshold p<0.05)

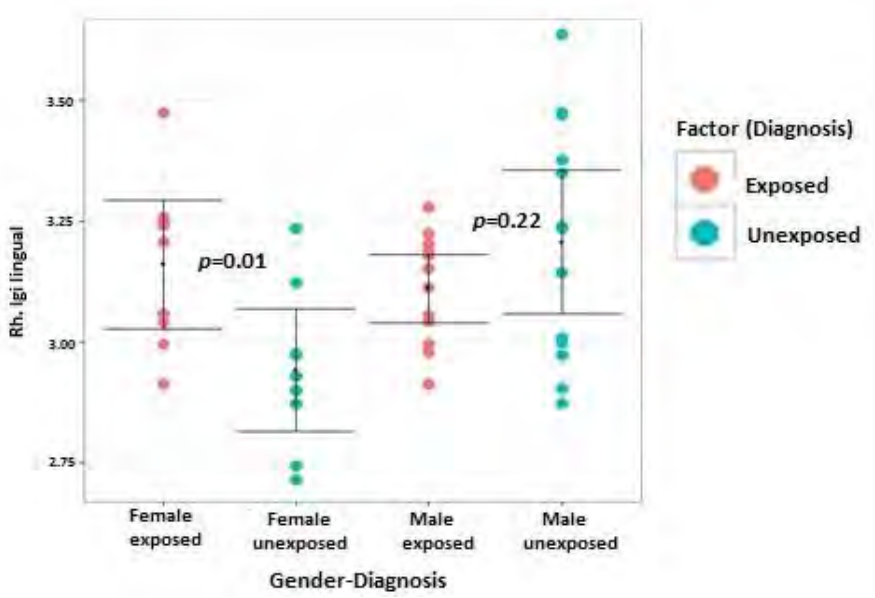

Figure 11: Plot showing how sex alters the effect of HIV exposure on LGIs in the right lingual gyrus in uninfected children

4.2.4 Effect of HIV exposure on ROI volumes in HIV-uninfected children

There were strong associations between global and regional brain volumes and total intracranial volume which were all significant. Almost all ROI brain volumes also had an association with sex which was significant except in the left caudate and the lateral ventricles bilaterally, as indicated in Table 8. Therefore the effect of global intracranial volume and sex was accounted for in subsequent comparisons.

There were no significant differences in brain volumes between HIV-exposed and unexposed uninfected children, before and after controlling for possible confounders and no significant difference in average intracranial volume between groups (Table 9).

Table 8: Association of global and regional brain volumes with total intracranial volume and sex within uninfected children (*N* = 43: 22 exposed, 21 unexposed)

Brain Region	Intracranial volume		Sex	
	Correlation (*r*)[a]	*p*-value	Correlation (*r*)[a]	*p*-value
Intracranial volume			0.52	<0.001
Global gray matter	0.65	<0.001	0.36	0.02
Global white matter	0.81	<0.001	0.54	<0.001
Corpus callosum	0.57	<0.001	0.33	0.03
L caudate	0.62	<0.001	0.24	0.12
R caudate	0.67	<0.001	0.31	0.04
L hippocampus	0.35	0.02	0.30	0.05
R hippocampus	0.58	<0.001	0.41	0.01
L putamen	0.43	0.003	0.47	0.001
R putamen	0.44	0.003	0.56	<0.001
L thalamus	0.82	<0.001	0.56	<0.001
R thalamus	0.80	<0.001	0.53	<0.001
L lateral ventricle	0.57	<0.001	0.16	0.32
R lateral ventricle	0.62	<0.001	0.23	0.15

[a] *r* is Pearson's correlation coefficient
Correlations significant at $p<0.1$ are indicated in red.

Table 9: Effect of HIV-exposure on regional brain volumes (*N* = 43: 22 exposed, 21 unexposed)

Brain region	Median (IQR) volume (mm^3)		t-test		ANCOVA controlling for sex		ANCOVA controlling for sex and intracranial volume	
	Exposed	Unexposed	*t*-value	*p*-value	*F*-value	*p*-value	*F*-value	*p*-value
Intracranial volume	1290701(143263)	1309093(209834)	-0.43	0.67	0.24	0.63	0.24	0.63
Global gray matter	737634 (114771)	718206(82414)	0.92	0.36	0.96	0.33	1.46	0.24
Global white matter	416252 (78574)	417407 (69683)	-0.07	0.95	0.01	0.94	0.01	0.91
Corpus callosum	3167 (753)	3191 (423)	-0.18	0.86	0.04	0.85	0.05	0.83
L caudate	3957(596)	3967(315)	-0.06	0.95	0.004	0.95	0.01	0.94
R caudate	4149 (811)	4107 (640)	0.28	0.78	0.08	0.77	0.14	0.71
L hippocampus	3687 (408)	3549 (500)	0.99	0.33	1.06	0.31	1.11	0.30
R hippocampus	3735 (612)	3722(665)	0.09	0.93	0.01	0.92	0.01	0.91
L putamen	6315 (1319)	6535 (687)	-0.94	0.35	1.10	0.30	1.15	0.29
R putamen	6157 (1203)	6415 (817)	-1.29	0.20	2.39	0.13	2.43	0.13
L thalamus	6751 (771)	6760 (999)	-0.04	0.97	0.003	0.96	0.01	0.94
R thalamus	6979 (830)	7013 (1076)	-0.14	0.89	0.03	0.87	0.06	0.82
L lateral ventricle	5738 (4239)	5534 (3106)	0.25	0.81	0.06	0.81	0.09	0.77
R lateral ventricle	5027 (2909)	4934 (1869)	0.13	0.90	0.02	0.90	0.03	0.88

4.3 Relation between clinical variables and neuroimaging measures in HIV-infected children

4.3.1 Sample characteristics

After excluding one (ART-Def) child for whom no CD4 data were available, the infected group comprised 16 ART-Def, 20 ART-40W and 19 ART-96W children, as well as 3 children who were excluded from previous analysis due to being very sick (CD4%<20%) at initiation. Of these 3 children, 2 were allocated into ART-40W and 1 to ART-96W. Sample characteristics are presented in Table 10. Most children's viral load was suppressed at time of scan

Table 10: Sample characteristics of HIV-infected children

	ART-Def	ART-40W	ART-96W	*F* or χ^2	*p*-value
Demographics					
Sample size (*N*)	16	22	20		
Age at scan (years)	7.19 (0.10)	7.19 (0.10)	7.21 (0.18)	0.12	0.98
Number of males (% males)	6 (35 %)	11 (46 %)	11 (55 %)	1.44	0.49
Clinical data at enrollment(6-8 weeks)					
CD4 count (cells/mm^3)	1827 (706)	1989 (973)	2107 (962)	2.43	0.06
CD4% (cells/mm^3)	34.0 (8.86)	35.9(9.16)	32.9 (8.52)	0.18	0.83
CD4/CD8	1.24 (0.71)	1.59 (0.95)	1.21 (0.56)	2.10	0.11
Clinical data at scan (7 years)					
Cumulative time on ART (weeks)	347.59 (18.04)	330.96 (42.59)	295.02 (106.52)	1.63	0.18
CD4 count (cells/mm^3)	1414.24 (476)	1113.76 (307)	1223.79 (592)	1.95	0.15
CD4% (cells/mm^3)	37.30 (7.92)	38.24 (4.94)	35.39 (6.78)	0.97	0.39
Other					
Age of ART initiation (weeks)	25.91 (16.22)	8.48 (1.66)	10.69 (9.24)	16.53	<0.001
Age at ART interruption (weeks)	Not interrupted	48.44 (1.81)[a]	107.50 (9.92)[c]	367.9	<0.001
Length of ART interruption (weeks)	0	41.76 (46.82)[a,b]	29.14 (52.34)[c,d]	0.58	0.68
Viral load at enrollment					
High (> 750, 000)	9 (56%)	10 (45%)	12 (60%)		
Low (400 – 750, 000)	7 (44%)	12 (55%)	8 (40%)		
Suppressed (< 400)	0 (0%)	0 (0%)	0 (0%)		
Viral load at scan (Age 7 years)					
High (> 750, 000)	0 (0%)	0 (0%)	0 (0%)		
Low (400 – 750, 000)	0 (0 %)	2 (9%)	2 (10%)		
Suppressed (< 400)	16 (100%)	20 (91%)	18 (90%)		

Values are *N* (% of total) or means (standard deviation)
Correlations significant at $p<0.1$ are marked in red.
[a] interruption data missing for one ART-40W child

[b] calculation included 3 ART-40W children in whom treatment was not interrupted
[c] interruption data missing for one ART-96W child
[d] calculation included 3 ART-96W children in whom treatment was not interrupted
p-values are ANOVA/Chi-square tests for significant group differences.

4.3.2 Vertex-wise analysis of the relationship between clinical measures at enrollment and cortical thickness within the HIV-infected group

There was no significant relationship between cortical thickness and the three clinical variables CD4 count, CD4 percentage and CD4/CD8 ratio at enrollment. Further, comparison within HIV-infected children showed no significant difference in cortical thickness between the three groups.

4.3.3 Vertex-wise analysis of the relationship between clinical measures and LGI within the HIV-infected group

4.3.3.1 Relationship between CD4 percentage at enrollment and LGI

In the left hemisphere, two clusters showed a significant negative relationship between CD4 percentage at enrollment and LGI, before and after accounting for sex, as indicated in Table 11 and Figure 12. In the right hemisphere, before controlling for sex, LGIs in a lateral occipital cluster were negatively related to CD4 percentage (Figure 12(a)) but after controlling for sex, LGIs in superior parietal and precuneus clusters showed, respectively, negative and positive relationships with CD4 percentage at enrollment (Figure 12 (b)).

Table 11: Regions in the right and left hemisphere where there was a significant relationship between CD4 percentage at enrollment and LGI before and after controlling for sex (*N*=58)

	Before controlling for sex				After controlling for sex			
Left hemisphere	**MNI co-ordinates at peak**	**Size (mm^2)**	***R***	***p*-value**	**MNI co-ordinates at peak**	**Size (mm^2)**	***r***	***p*-value**
Lateral occipital	-42.6, -72.6, -1.3	2738	-0.51	<0.001	-36.9, -76.2, -7.8	2220	-0.53	<0.001
Superior parietal	-16.0, -61.9, 52.3	1033	-0.38	0.004	-17.9, -60.7, 50.6	2341	-0.35	0.01
Right hemisphere								
Lateral occipital	40.4, -79.5, 6.8	542	-0.37	0.005				
Superior parietal					21.3, -58.1, 43.5	1124	-0.25	0.07
Precuneus					21.9, -62.3, 12.5	583	0.22	0.09

r is Pearson's correlation coefficient

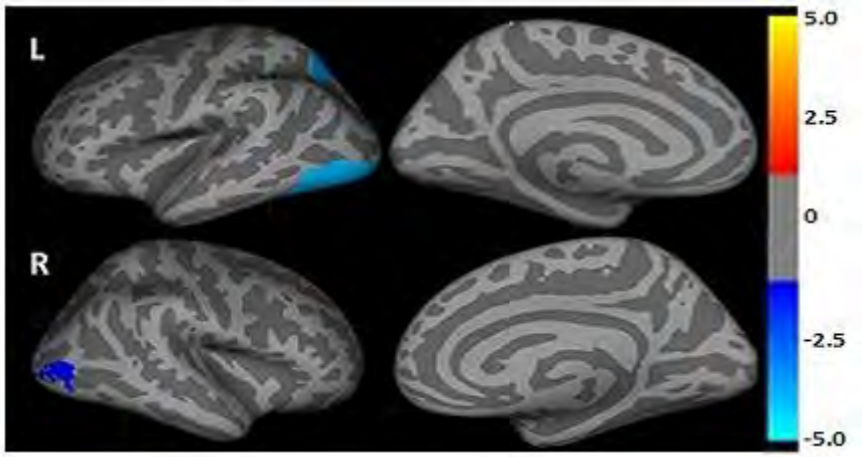

a) Before controlling for sex

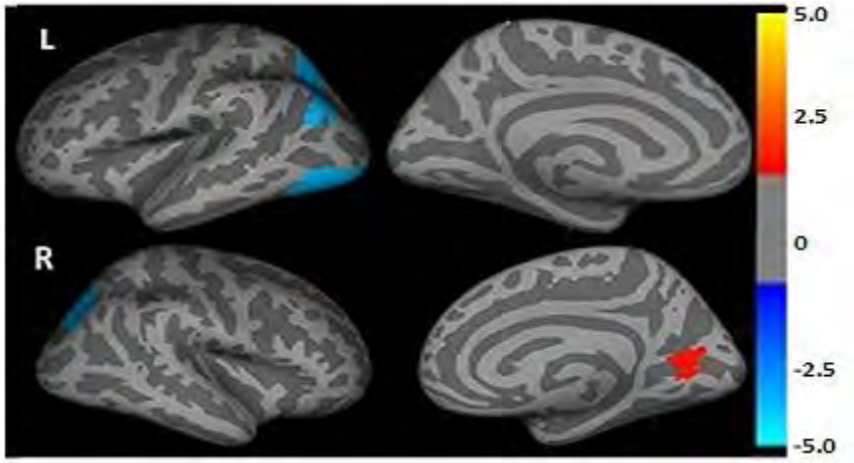

b) After controlling for sex

Figure 12: Lateral and medial views of regions with significant relationship between CD4 percentage at enrollment and LGI (*N*=58) (threshold at *p*<0.05, cluster size threshold *p*<0.05).

4.3.3.2 Relationship between CD4 count at enrollment and LGI

In the left hemisphere, there was a positive relationship between CD4 count and LGI in the pars orbitalis and a caudal middle frontal region (Figure 13 (a)); after controlling for sex, there was an additional cluster in the superior temporal region that showed a positive relationship between CD4 count at enrollment and LGI (Figure 13 (b)).

In the right hemisphere, before controlling for sex there were no significant clusters (Figure 13(a)), but after controlling for sex a lateral orbitofrontal region showed a positive relationship between CD4 count and LGI as indicated in Table 12 and Figure 13(b).

Table 12: Regions in the left and right hemispheres where there was a significant relationship between LGI and CD4 count at enrollment before and after controlling for sex (*N*=58)

Left hemisphere	**Before controlling for sex**				**After controlling for sex**			
Location	**MNI co-ordinates at peak**	**Size (mm^2)**	***r***	***p*-value**	**MNI co-ordinates at peak**	**Size (mm^2)**	***r***	***p*-value**
Parsorbitalis	-43.4, 36.3, -13.6	1218	0.43	0.001	-42.2, 34.9, -13.6	1520	0.42	0.001
Caudal middle frontal	-39.7, 12.6, 37.8	603	0.34	0.01	-39.7, 12.6, 37.8	783	0.33	0.01
Superior temporal					-39.5, 9.3, -25.4	536	0.38	0.004
Right hemisphere								
Lateral orbitofrontal					34.6, 27.5, -6.9	558	0.32	0.02

r is Pearson's correlation coefficient

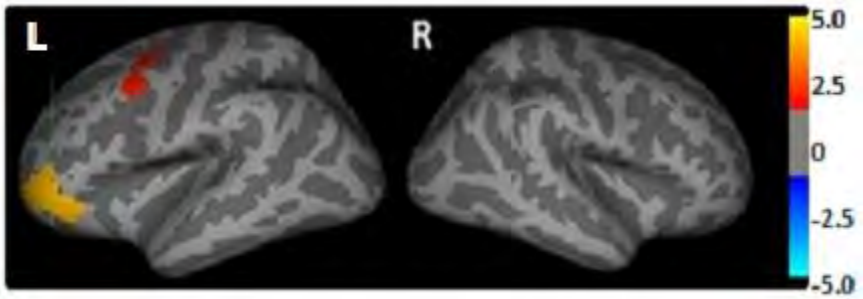

a) Before controlling for sex

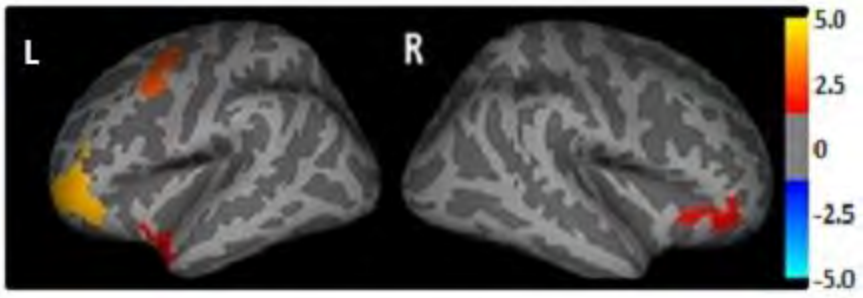

b) After controlling for sex

Figure 13: Lateral views of regions with significant relationship between CD4 count at enrollment and LGI (*N*=58) (threshold at $p<0.05$, cluster size threshold $p<0.05$).

4.3.3.3 Relationship between CD8 count at enrollment and LGI

There was a positive relationship between CD8 count at enrollment and LGI in a lateral occipital region of the left hemisphere, which became significant after controlling for sex (MNI co-ordinates: -37.1, -78.2, -8.0; cluster size: 1345mm^2, r=0.35, p=0.01) as indicated in Figure 14. There was no significant relationship between CD8 count at enrollment and LGI in the right hemisphere.

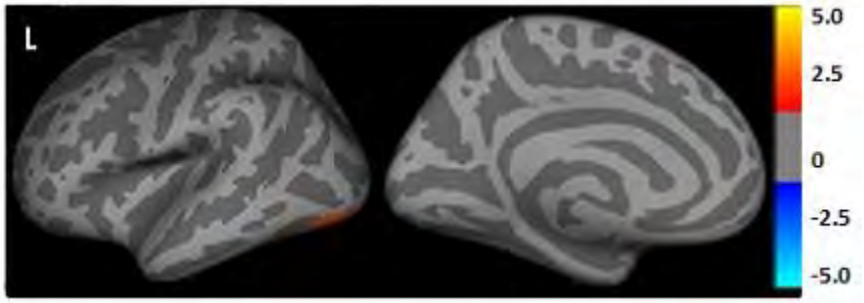

a) Before controlling for sex

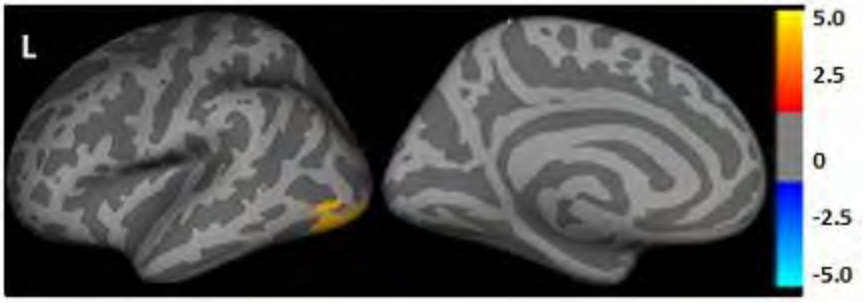

b) After controlling for sex

Figure 14: Lateral and medial views of the left hemisphere showing the lateral occipital region where there was a significant relationship between CD8 count at enrollment and LGI (*N*=58) (threshold at *p*<0.05, cluster size threshold *p*<0.05)

4.3.3.4 Relationship between CD4/CD8 ratio at enrollment and LGI

There was an inverse relationship between CD4/CD8 ratio at enrollment and LGI in a left hemispheric lateral occipital region (MNI co-ordinates at peak: -37.1, -78.2, 8.0) before (cluster size: 2056mm^2, r=-0.51, p=<0.001) and after (cluster size: 2390mm^2, r=-0.52, p<0.001) controlling for sex, as shown in Figure 15. There was no significant relationship between CD4/CD8 ratio and LGI in the right hemisphere.

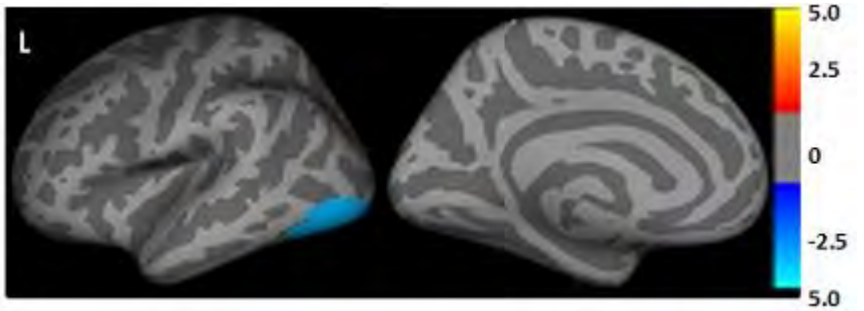

a) Before controlling for sex

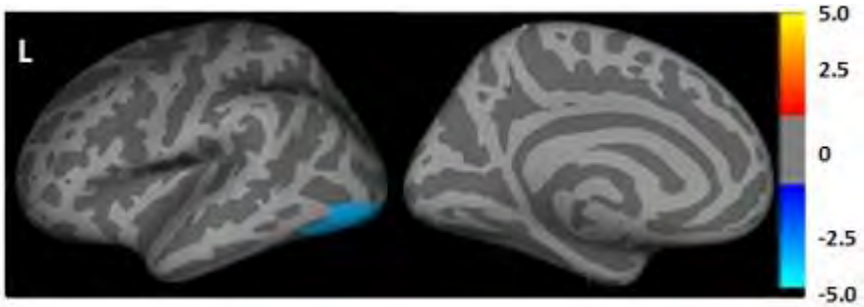

b) After controlling for sex

Figure 15: Lateral views of a region in the left hemisphere with a significant relationship between CD4/CD8 ratio at enrollment and LGI before (left) and after (right) controlling for sex (*N*=58) (threshold at *p*<0.05, cluster size) threshold *p*<0.05)

4.3.3.5 Sex-clinical measures interaction on LGI

In the LGI comparison, there were significant differences between the sexes in the relationship between CD4 count and CD4/CD8 ratio and LGI in several clusters shown in Table 13, Figures 16 – 17.

Table 13: Regions where the relationships between CD4 count, CD4/CD8 ratio at enrollment and LGI differ with sex (*N* = 58)

Location	MNI co-ordinates at peak	Size (mm^3)	Correlation (*r*)[a]		*p*-value	
Left hemisphere: CD4 count and LGI						
			Boys	**Girls**	**Boys**	**Girls**
Supramarginal	-59.4, -45.9, 20.5	4121	0.47	-0.39	0.02	0.03
Rostral middle frontal	-20.6, 56.2, 11.3	1001	0.45	-0.21	0.03	0.26
Right hemisphere: CD4 count and LGI						
Rostral middle frontal	26.3, 42.3, 25.9	1628	0.50	-0.21	0.01	0.25
Rostral middle frontal	41.1, 25.2, 18.3	655	0.35	-0.31	0.09	0.10
Supramarginal	58.6, -33.2, 36.1	5660	0.41	-0.44	0.04	0.01
Inferior temporal	45.1, -62.4, -4.2	612	0.50	-0.25	0.01	0.18
Left hemisphere: CD4/CD8 ratio and LGI						
Fusiform	-26.7, -46.2, -12.4	1036	0.38	-0.11	0.06	0.58

[a] *r* is Pearson's correlation coefficient

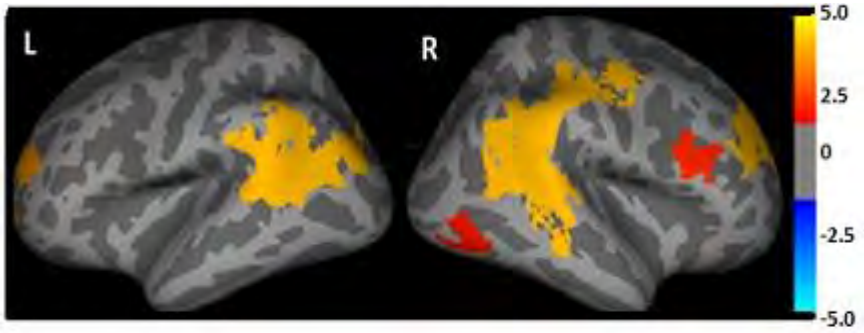

Figure 16: Lateral view of regions in the left (left) and right (right) hemispheres where the relationship between CD4 count at enrollment and LGI differs between sexes

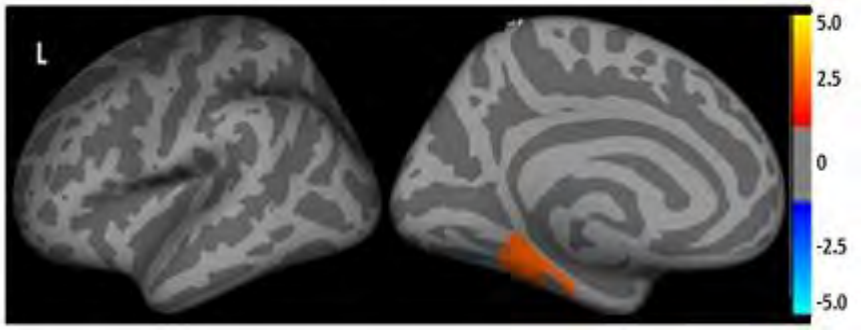

Figure 17: Lateral and medial views of the left hemisphere showing a fusiform region where the relationship between CD4/CD8 ratio and LGI differs between sexes

4.4 Relationship between ROI volumes and clinical data

A Pearson product-moment correlation performed between ROI volumes and clinical measures indicated a trend-level negative relationship between CD4 percentage at enrollment and volumes of the left and right caudate nuclei. There was a significant negative relationship between CD4/CD8 ratio and right caudate volume. There was significant positive relationship between intracranial volume and age at ART initiation, and the positive relationship between right thalamus volume and duration on ART fell just short of statistical significance (r=0.25, p=0.06). These results were before controlling for confounders as shown in Table14 and Figure 18

Subsequent comparison of brain volume between boys and girls showed that boys on average had higher brain volume than girls in all ROIs: this difference was significant for total intracranial volume, global white matter volume, right hippocampus, and bilateral caudate, thalamus and the lateral ventricles, as indicated in Table 15

Because of this, sex and intracranial volume were controlled for in regression analyses investigating the relationship between clinical measures and ROI volumes that differed by sex (Table 16). After controlling for sex and intracranial volume, the inverse relationship between CD4 percentage at enrollment and right and left caudate volume became significant. The negative relationship between CD4/CD8 ratio and right caudate volume remained significant, and there was a positive relationship between duration of ART and left and right thalamus volume. When sex and intracranial volume were controlled for, age at ART initiation was no longer associated with global white matter volume.

Table 14: Correlation of ROI volumes and clinical measures before controlling for confounders (*N*=58)

Brain region	CD4% enrollment (cells/mm^3)		CD4-Count enrollment (cells/mm^3)		CD4/CD8 ratio enrollment		Age at ART Initiation (weeks)		Duration on ART (weeks)	
	R	*p*-value	*R*	*p*-value	*r*	p-value	*R*	*p*-value	*r*	*p*-value
Intracranial volume	-0.03	0.85	0.04	0.76	-0.04	0.76	0.21	0.11	0.01	0.96
Global gray matter	-0.02	0.90	0.09	0.50	-0.01	0.93	0.22	0.09	-0.11	0.42
Global white matter	-0.12	0.38	0.07	0.58	-0.12	0.39	0.26	0.04	-0.05	0.70
Corpus callosum	-0.12	0.37	0.06	0.63	-0.10	0.45	-0.12	0.36	-0.07	0.63
L caudate	-0.22	0.09	0.07	0.61	-0.22	0.10	0.15	0.28	-0.04	0.77
R caudate	-0.25	0.06	0.03	0.85	-0.27	0.05	0.14	0.28	-0.09	0.51
L hippocampus	-0.08	0.54	-0.02	0.91	-0.03	0.85	0.11	0.42	-0.09	0.48
R hippocampus	-0.22	0.10	-0.07	0.63	-0.15	0.25	0.06	0.66	-0.03	0.81
L putamen	-0.15	0.25	-0.07	0.60	-0.08	0.54	0.22	0.10	0.003	0.98
R putamen	-0.16	0.23	-0.12	0.35	-0.15	0.28	0.20	0.13	0.05	0.71
L thalamus	-0.08	0.54	0.02	0.89	-0.12	0.36	0.25	0.06	0.22	0.10
R thalamus	-0.10	0.47	0.02	0.86	-0.15	0.26	0.23	0.09	0.25	0.06
L lateral ventricle	-0.01	0.96	0.01	0.93	0.05	0.73	-0.01	0.91	0.03	0.85
R lateral ventricle	0.03	0.86	0.12	0.38	0.09	0.51	0.0004	0.99	-0.10	0.45

[a] *r* is Pearson's correlation coefficient

Correlations significant at $p<0.1$ are indicated in red.

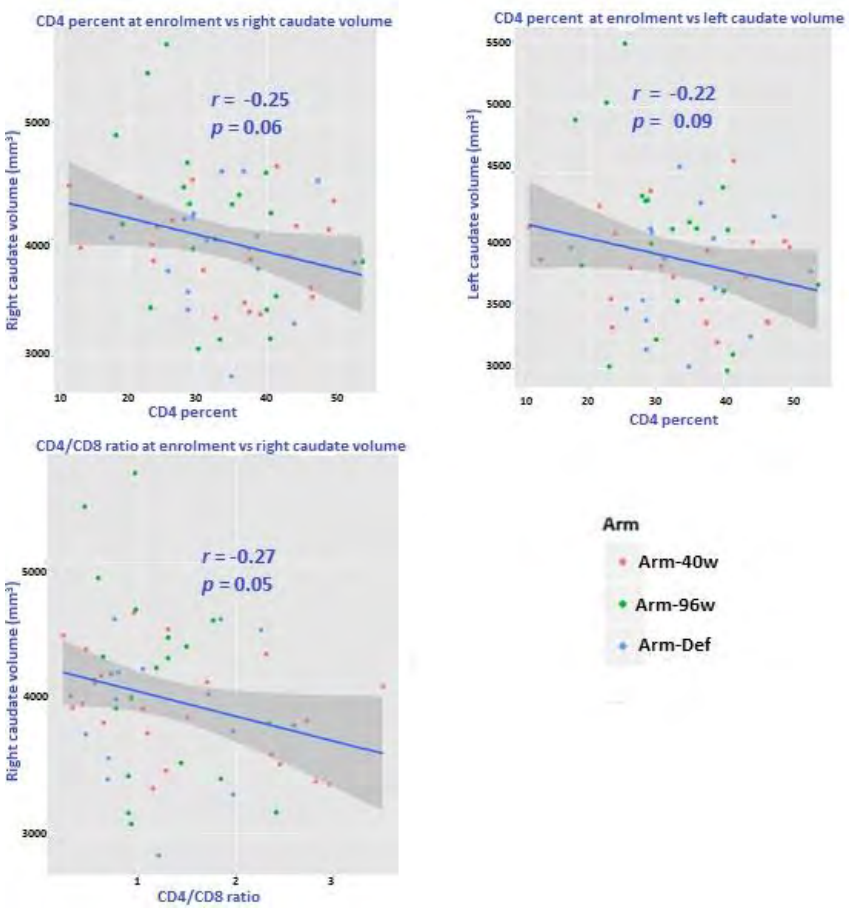

Figure 18: Plot showing relationship between CD4 percentage and right caudate volume (*r* = -0.25, *p*=0.06), CD4 percentage and left caudate volume (*r*= -0.22, *p*=0.09), and CD4/CD8 ratio and right caudate volume (*r*=-0.27, *p*=0.05), before controlling for confounders.

Table 15: Comparison of regional brain volumes between sexes (*N*=58)

Brain region	Mean (sd) in mm^3			
	Girls	Boys	*t*-value	*p*-value
Intracranial volume	1226884 (95278)	1313883 (101700)	-3.36	0.001
Global gray matter	696151 (47159)	7159712 (69134)	-1.29	0.20
Global white matter	381649 (33169)	413011 (51837)	-2.78	0.01
Corpus callosum	3009 (418)	3184 (400)	-1.62	0.11
L caudate	3694 (433)	4005 (552)	-2.40	0.02
R caudate	3865 (423)	4135 (643)	-1.91	0.06
L hippocampus	3447 (500)	3491 (406)	-0.36	0.72
R hippocampus	3393 (534)	3625 (416)	-1.83	0.07
L putamen	5894 (607)	6119 (598)	-1.42	0.16
R putamen	5811 (593)	5996 (545)	-1.23	0.22
L thalamus	6504 (520)	6915 (687)	-2.59	0.01
R thalamus	6724 (556)	7061 (654)	-2.13	0.04
L lateral ventricle	4789 (1959)	6333 (2534)	-2.61	0.01
R lateral ventricle	4799 (1960)	6342 (2534)	-2.61	0.01

Comparisons significant at $p<0.1$ are indicated in red.

Table 16: Regression of ROI volumes on clinical measures, controlling for effects of sex and intracranial volume (*N*=58)

Brain region	CD4% enrollment		CD4-Count enrollment		CD4/CD8 ratio enrollment		Age at ART Initiation (weeks)		Duration on ART (weeks)	
	B	*p*-value	*β*	*p*-value	*β*	*p*-value	*β*	*p*-value	*β*	*p*-value
Intracranial volume	0.09	0.45	0.04	0.76	0.07	0.58	0.20	0.10	-0.05	0.70
Global white matter	-0.09	0.34	0.04	0.63	-0.08	0.42	0.11	0.22	-0.06	0.49
L caudate	-0.21	0.05	0.04	0.68	-0.19	0.07	0.01	0.93	-0.05	0.63
R caudate	-0.25	0.02	0.001	0.99	-0.25	0.02	0.02	0.87	-0.09	0.39
R hippocampus	-0.19	0.15	-0.08	0.54	-0.12	0.37	-0.01	0.94	-0.05	0.70
L thalamus	-0.05	0.68	-0.006	0.98	-0.08	0.47	0.13	0.24	0.21	0.05
R thalamus	-0.08	0.49	-0.001	0.99	-0.13	0.26	0.11	0.34	0.24	0.03
L lateral ventricle	0.04	0.74	-0.11	0.92	0.10	0.36	-0.14	0.19	0.01	0.94
R lateral ventricle	0.02	0.87	0.09	0.40	0.10	0.38	-0.14	0.21	-0.09	0.38

Regressions significant at $p<0.1$ are marked in red.

β are normalized regression coefficients after controlling for potential confounding influences of sex and intracranial volume

4.5 Effect of treatment regimens on regional brain volumes

For comparisons between treatment arms, the three children who were very sick at enrollment and as such were not randomized into treatment arm, were excluded. Further, the one ART-Def child for whom clinical data were missing was included, resulting in 56 infected children (17 ART-Def, 20 ART-40W, 19 ART-96W).

There were no differences in regional brain volumes between different treatment arms at a significance level of $p<0.05$. In the left hippocampus there was a trend-level difference ($p=0.08$) before controlling for confounders. Both sex and intracranial volume were correlated with global and regional brain volumes (**Table** 17), therefore both were controlled for in subsequent analyses. When only sex was included as a confounder, left hippocampal volume was significantly different between treatment arms ($p=0.03$). *Post-hoc* tests showed significantly greater left hippocampal volumes in ART-96W children compared to the ART-40W children ($p=0.05$), while the difference between ART-Def and ART-40W fell just short of significance ($p=0.08$). When intracranial volume was included as an additional control variable, the left hippocampal differences remained essentially unchanged while the left caudate nucleus showed a trend ($p=0.09$). The results of the comparisons are shown in Table 18 and Figure 19. The significantly higher volume of ART-96W children compared to ART-40W children in the left hippocampus was lost after controlling for sex and intracranial volume, indicating that this result could be spurious.

Table 17: Association of regional brain volumes with total intracranial volume and sex within the HIV-infected group (*N*=56)

Brain region	Intracranial volume		Sex	
	Correlation (*r*)[a]	*p*-value	Correlation (*r*)[a]	*p*-value
Intracranial volume			0.43	<0.001
Global gray matter	0.67	<0.001	0.12	0.36
Global white matter	0.76	<0.001	0.32	0.02
Corpus callosum	0.26	0.04	0.21	0.12
L caudate	0.65	<0.001	0.30	0.02
R caudate	0.60	<0.001	0.24	0.08
L hippocampus	0.30	0.03	0.14	0.29
R hippocampus	0.32	0.02	0.26	0.05
L putamen	0.55	<0.001	0.19	0.16
R putamen	0.51	<0.001	0.17	0.21
L thalamus	0.61	<0.001	0.35	0.01
R thalamus	0.59	<0.001	0.27	0.04
L lateral ventricle	0.62	<0.001	0.33	0.01
R lateral ventricle	0.61	<0.001	0.21	0.12

[a] *r* is Pearson's correlation coefficient
Correlations significant at p<0.1 are indicated red.

Table 18: Effect of treatment arms on ROI volumes (*N*=56: 17 ART-Def, 20 ART-40W, 19 ART-96W)

Brain region	Median (IQR) volume (mm^3)			ANOVA		ANCOVA controlling for sex		ANCOVA controlling for sex and intracranial volume	
	ART-Def	ART-40W	ART-96W	*F*-value	*p*-value	*F*-value	*p*-value	*F*-value	*p*-value
Intracranial volume	1258000 (140041)	1246000(119157)	1277000(197236)	0.34	0.71	0.41	0.67	0.41	0.67
Global gray matter	700800 (48256)	702800 (86242)	713300 (44470)	0.14	0.87	0.14	0.87	0.27	0.77
Global white matter	388600 (46324)	393000 (61916)	412400 (67526)	0.01	0.99	0.01	0.99	0.02	0.98
Corpus callosum	3016 (413)	3054 (552)	3199 (520)	0.90	0.41	0.92	0.41	0.94	0.39
L caudate	3841(586)	3736(613.5)	4065(750)	1.49	0.23	1.59	0.21	2.49	0.09
R caudate	3990 (459)	3888 (565.75)	4221 (1043)	0.96	0.39	0.99	0.38	1.42	0.25
L hippocampus[1]	3499 (510)	3291 (223)	3626 (427)	2.65	0.08	3.60	0.03[a]	3.76	0.03[b]
R hippocampus[2]	3525 (434)	3500 (405)	3655 (638)	2.28	0.11	1.61	0.21	1.67	0.20
L putamen	6131 (1230)	6006 (731)	6012 (817)	0.19	0.83	0.19	0.83	0.26	0.77
R putamen	5791 (1018)	5784 (481)	5961 (889)	0.20	0.82	0.20	0.82	0.26	0.77
L thalamus	6747 (1035)	6560 (848)	6621 (1037)	0.45	0.64	0.50	0.61	0.69	0.50
R thalamus	7156 (952)	6510 (919)	6951 (1008)	0.97	0.39	1.02	0.37	1.42	0.25
L lateral ventricle	4856 (2394)	4478 (2652)	5002 (3964)	0.25	0.78	0.28	0.76	0.39	0.68
R lateral ventricle	4738 (1846)	3746 (2331)	4706 (2968)	0.36	0.70	0.36	0.69	0.54	0.58

[1, 2] Left and right hippocampus had one extreme outlier each which was removed before comparison (*N*=55)
Comparisons significant at p<0.1 are indicated in red.

[a]ART-Def > ART-40W (*p*=0.08), ART-96W > ART-40W (p=0.05)
[b]ART-Def > ART-40W (*p*=0.11), ART-96W > ART-40W (*p*=0.07)

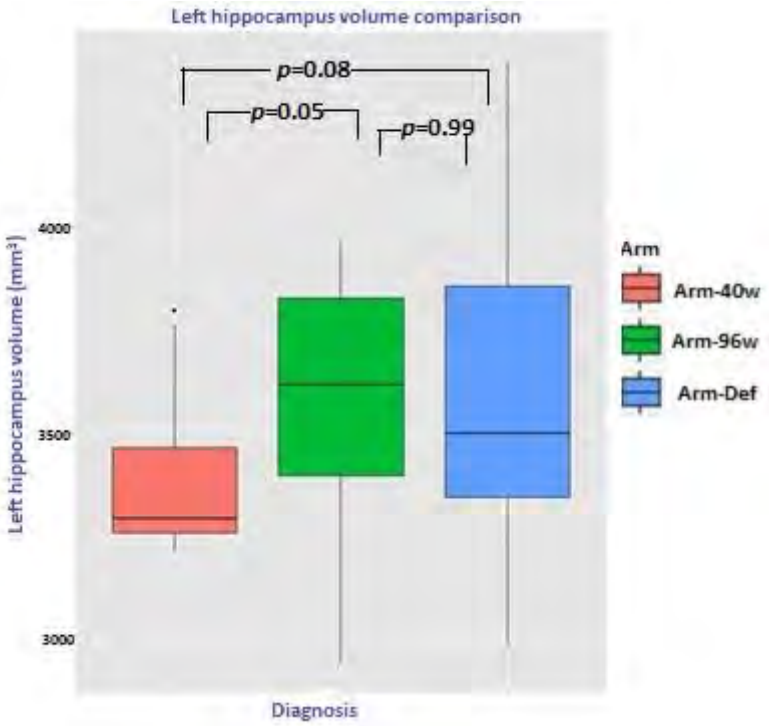

Figure 19: Boxplot showing left hippocampal volumes for ART-40W, ART-96W and ART-Def treatment arms (*p*-value for *post-hoc* test after controlling for sex)

5. Discussion

5.1 MRI morphometry in HIV-infected children

To date no study have investigated cortical thickness and sulcal enlargement changes in HIV-infected children (Hoare et al., 2015), making this one of the first automated, quantitative morphological neuroimaging studies in vertically-infected young children with HIV stable on ART and the first in Africa. To our knowledge, this is also the first study to examine quantitative measures of cortical thickness and local gyrification across the whole brain in HIV-infected children.

5.1.1 HIV infection and brain volumes

Consistent with previous studies in adults, our study showed that HIV-infected children have significantly less global white and gray matter volume than uninfected controls, a trend for smaller total intracranial volume, and significantly smaller volumes in the right hippocampus and bilateral putamen. Left hippocampal volumes were also greater in uninfected children, but this difference was not statistically significant.

HIV-infected adult subjects similarly show reduced global white and gray matter volumes, as well as enlarged lateral ventricles and volume reductions in the corpus callosum, hippocampus, thalamus and most of the basal ganglia, due to neuronal atrophy (Towgood et al., 2012; Aylward et al., 1993; Paul et al., 2008; Ortega et al., 2013[b]; Kallianpur et al., 2013; Heaps et al., 2012; Ances et al., 2012). Generally, brain volume reduction has been associated with low memory retention, slow processing speed, adverse cognitive and motor function, and in extreme conditions, different stages of HIV-associated dementia (HAD) depending on the severity and duration of infection (Heaps et al., 2012; Towgood et al., 2012; Ortega et al., 2013; Treble et al., 2012; Kallianpur et al., 2012). Although HAART has reduced the incidence of severe neurocognitive deficits (Becker et al., 2011; Ellis et al., 2007; Ellis., 2010), white matter volume loss (Hua et al., 2013) and cerebral (Cohen et al., 2010) and subcortical (Ances et al., 2012, Becker et al., 2011) atrophy is still evident, even with HAART. It has been suggested that this may be due to damage sustained before the start of treatment, or due to subclinical processes that continue despite it (Becker et al., 2011).

In HIV-infected children common structural neuroimaging findings include ventricular enlargement, cerebral and subcortical atrophy and basal ganglia calcification (Hoare et al., 2014; George et al., 2009; McCoig et al., 2002; Van Rie et al., 2007). Early and aggressive intervention with HAART is thought to protect the brain from long term effects of the virus (Becker et al., 2011; Cohen et al., 2010). Because of associations between disease severity and poorer neuropsychological outcomes, it has been suggested that ART treatment should not be delayed, in order to prevent neurological damage

(Laughton et al., 2012; Lindsey et al., 2007; Puthanakit et al., 2013). In the current study of HIV-infected children who had been started on HAART early in life, we nevertheless found volume reductions of hippocampus and putamen relative to controls, as well as reductions in total gray and white matter; however, we found no significant difference in caudate or thalamus volume, the latter in contrast to studies on HAART-naïve adults (Heaps et al., 2012 and Ortega et al., 2013).

The subcortical neuronal atrophy observed in HIV infection is thought to be due to the proximity of these regions to the ventricle – a channel for cerebrospinal fluid and a major carrier of the AIDS virion – proximity may allow for easier viral penetration by HIV-infected mononuclear cells going into the brain as well as increased HIV toxic products, such as gp120 and Tat, leading to neuronal atrophy (Ances et al., 2012; Kallianpur et al., 2013). Early HAART is expected to have both clinical and immunological benefits by suppressing HIV replication, particularly in the CNS, and boosting the immune system, thereby protecting the brain morphology and neurodevelopment of HIV-infected children (Laughton et al., 2012; Lindsey et al., 2007).

It is worth noting that the volume reductions that we observed were not merely a result of intracranial volume decrease in these children, but represent a decrease in volume even over and above reductions in total brain size. However, this was not associated with ventricular enlargement, of which there are multiple reports in the literature (van Arnhem et al., 2013; Hoare et al., 2014). Although in our study HIV-infected children tended to have higher bilateral lateral ventricular volumes than uninfected controls, the difference was not significant, possibly suggesting that ventricular enlargement is variable in this group.

Our findings showed reduced global white matter in HIV-infected children, while other studies are inconsistent on reduction in global white matter volume in HIV (Heaps et al., 2012; Hoare et al., 2014; Hoare et al., 2012). One other study measuring brain volumes in perinatally-infected youth similarly found reduced white matter volumes - these adolescents had only started HAART at approximately 4 years of age (Sarma et al., 2014). We found no significant difference in corpus callosum volume between HIV-infected children and controls. Because white matter damage in HIV-infected children is not consistently detected with structural MRI, several studies have proposed that the structure of white matter and the corpus callosum is initially affected at a microscopic scale –subtle abnormalities that can only be detected using diffusion tensor imaging (DTI) (Filippi et al., 2001; Hoare et al., 2012; 2014; Heaps et al., 2012). Within this cohort at age 5 years no group differences in corpus callosum volumes were found using FreeSurfer, however group differences were found using a manual tracing technique (Randall, 2015). This result suggests that some inaccuracies may result from FreeSurfer's automated segmentation of the corpus callosum in this dataset due to difficulties in distinguishing

cerebral blood vessels that appear bright on the T1 weighted images from white matter. Although every attempt was made to correct this manually, this possibility should be investigated in future work.

Lower nadir CD4 counts (Martin et al., 2006, Koekkoek et al., 2006), higher viral loads and the history of an AIDS-defining illness (Smith et al., 2006; Wood et al., 2009) have been associated with poorer neurodevelopmental outcomes in perinatally-infected children (Laughton et al., 2012; Lindsey et al., 2007), despite later immune system recovery with ART. Similarly, the structural integrity of the brain in HIV is likely to reflect a combination of the effects of current immune status and HIV replication, on top of effects associated with a history of immunosuppression, as reflected by lower CD4 count/percentage (Jernigan et al., 2011).

We found a negative relationship between CD4 percentage at enrollment and bilateral caudate volume. CD4/CD8 ratio at enrollment was also negatively associated with volume of the right caudate. These effects remained significant after controlling for the potential confounding influences of sex and intracranial volume. This implies that worse baseline immune status in these stable HIV-infected children leads to increased caudate nucleus volume at 7 years. In contrast, in adult subjects worse immunological status as reflected by lower nadir CD4 count has generally been associated with smaller hippocampi (Cohen et al., 2010; Gongvatana et al., 2014) and reduced subcortical gray (Cohen et al., 2010; Gongvatana et al., 2014) and white (Hua et al., 2013; Gongvatana et al., 2014) matter volumes, even in subjects on stable ART with viral suppression (Cardenas et al., 2009). However, lower CD4 at time of scan has previously been associated with increased subcortical volumes (Jernigan et al., 2011). Increased tissue volumes with worse immunological status, as observed for caudate volume in our study, may be a result of neuroinflammatory processes, perhaps because of glial activation or oedema (Jernigan et al., 2011).

An alternative explanation is that the children in our study who were sickest at enrollment, as reflected by their low CD4%, may have shown the greatest CD4 recovery between HAART initiation and scanning. A greater extent of CD4 recovery on HAART has also been associated with increased subcortical gray matter volume (Fennema-Notestine et al., 2013). Future work should examine the association of immune system recovery with brain volumes.

Comparison of the three different treatment arms (ART-Def, ART-40W, ART-96W), showed no significant differences in global and regional brain volumes between treatment arms, except in the left hippocampus, where children randomised into ART-96W had greater left hippocampal volume than those in ART-40W. Increased total duration on ART was associated with increased bilateral

thalamus volume in HIV-infected children; increased total duration on ART was not associated with volume reductions in any regions.

Although early ART initiation has been associated with improvement and preservation of neurodevelopment (IQ, memory, psychomotor, and behavioral outcomes), at least in the short term (Laughton et al., 2012), we observed no difference in brain volumes between the early and deferred treatment groups at age 7, and no association between age at ART initiation and brain volumes. Although another benefit of early ART is the possibility of longer duration of treatment interruption and less cumulative exposure to ART compared to delayed treatment (Cotton et al., 2013), in the study of Laughton et al. (2012), children in the ART-40W and ART-96W arms who had better cognitive scores than those in the ART-Def arm at 6 months also had a longer duration on ART. This may tie in with our observation of increased thalamus volume with increased ART duration at 7 years. However, it will be necessary to see whether the short term improvements in cognitive function with early ART are still observed at age 7 years.

5.1.2 HIV infection and cortical thickness

We found no significant difference in cortical thickness between HIV-infected children who are stable on ART and uninfected controls. Although no previous studies have investigated cortical thickness in HIV-infected children, cerebral atrophy on CT and MRI imaging has commonly been reported in children (Hoare et al., 2014) as well as adults (Gavin et al., 1999; Hoare et al., 2012; Kallianpur et al., 2012; Kozlowski et al., 1997).

Previous studies in adult patients have concluded that HIV-infection is associated with cortical thinning, especially in the orbitofrontal, parietal and temporal cortices, bilateral insula, right superior frontal cortex, and right anterior cingulate (Thompson et al., 2005, Kallianpur et al., 2011). Cortical thinning is an index for declining neurological and immune function in AIDS (Thompson et al., 2005), where decreased thickness in frontopolar and language cortices was associated with decreased CD4 lymphocyte count. Using CT in children, higher CD4 has been found to be correlated with less cortical atrophy (Brouwers et al., 2000*).* Based on these findings we expected that cortical thickness in infected children would have an association with CD4 parameters – a measure of immune system health - just before they commenced ART, but a vertex-wise analysis showed no significant relationship between CD4 parameters at enrollment and brain cortical thickness at age 7.

It is possible that, particularly during this childhood period of cortical growth, cortical thickness is more closely related either to current immunological status or to nadir CD4 count. Another study in adults found no relation between cortical thickness and current or nadir CD4 count (Kallianpur et al., 2011), however, thinner frontal, parietal and temporal cortices was observed in subjects with detectable

levels of HIV DNA (Kallianpur et al., 2011), where thinner temporal cortex was also associated with decreased psychomotor speed. Also in children, CSF viral load has been linked with a higher degree of cortical atrophy seen on CT (Brouwers et al., 2000*). The association of viral load with cortical thickness remains to be investigated.*

Because previous studies were done on HIV-infected adults, the differences between those results and ours may indicate that the effect of HIV on the cerebral cortex varies between adults and children. A second possible reason for the varying results between this study and previous ones is that ART may have reversed or prevented the effects of HIV on the cortex. Although some of the adult subjects in the study of Thompson et al. (2005) were on HAART, no differences in cortical thickness due to ART were found. However, our finding may be a sign of possible cortical thickening (recovery) or prevention of cortical thinning due to early initiation of ART.

Since cortical thickness has been linked to performance in cognition, memory and fine motor activities (Kozlowski et al., 1997; Gavin et al., 1999; Kallianpur et al., 2012), we suggest that if it is early ART initiation that prevents an HIV-related reduction in cortical thickness, early ART may similarly prevent the associated decline in cognitive ability and psychomotor activities (Kallianpur et al., 2011; Kuper et al., 2011; Thompson et al., 2005). The improvement of neurodevelopmental function in HIV-infected children who started treatment in infancy (Laughton et al., 2012; Lindsey et al., 2007) may be related to preserved cortical thickness.

5.1.3 HIV infection and LGI

Our results showed significantly lower LGI in HIV-infected children than in uninfected controls in a large left hemisphere medial parietal region. This may be due to sulcal enlargement - a condition that has been reported in most of the literature on HIV infection (Van Arnhem et al., 2013; Gavin et al., 1999; George et al., 2009) and that has previously been shown to be negatively related to LGI (Destrieux et al., 2010; White et al., 2010) and to intelligence quotient (IQ) (Treble et al., 2012), while increased LGI, together with cortical thickness, is associated with better cognitive and psychomotor outcomes (Treble et al., 2012; Kallianpur et al., 2012). Our results may indicate that IQ and psychomotor functions are also affected in these children; however, this remains to be investigated.

Our vertex-wise results also showed that LGIs in several brain regions, especially caudal middle frontal, pars orbitalis, lateral occipital and superior parietal regions, were correlated with measures of immune system function at enrollment, as reflected by CD4 count, CD4 percentage, and CD4/CD8 ratio. Of interest is the relationship in the left lateral occipital region, where CD4 percentage and CD4/CD8 ratio at enrollment showed a negative relationship with LGI – indicating lower LGIs with better immunological status. Further investigation revealed that increased CD8 count at enrollment was also

associated with greater LGI in the same region. Since CD8 count can be associated with inflammation due to microglial/macrophage activation in the brain (Suidan et al., 2010; Anthony et al., 2005), we suspect a possible HIV/ART-associated inflammatory reaction may disrupt normal cortical development in the left lateral occipital region. HIV infection has been shown to be linked with neuroinflammation, of subcortical brain regions particularly, even with HAART (Castelo et al., 2007; Anthony et al., 2005).

5.1.4 Effect of sex and HIV infection on brain morphometry

Although we found no significant interaction between sex and HIV infection status on cortical thickness, there was a significant interaction of HIV infection status with sex on LGI in bilateral inferior parietal and left supramarginal regions. A similar interaction effect was observed in the right supramarginal region but it was not significant. The larger LGI observed in uninfected children was shown to be largely attributable to higher LGI's in uninfected boys. The relationship of CD4 count and CD4/CD8 with LGI also differed between boys and girls bilaterally in supramarginal and rostral middle frontal regions, as well as a right inferior temporal and left fusiform region. In all except the fusiform region, lower CD4 count at enrollment was associated with *reduced* LGI in boys only, while in girls lower CD4 count at enrollment was associated with *increased* LGI bilaterally in the supramarginal gyrus only. These results show that sex, as well as ART, is an important factor to consider in subsequent investigations of LGI and sulcal enlargement. This study and other previous studies have shown differences in cortical thickness between genders (Kiho Im et al., 2006; Luders et al., 2006), but no such differences have been reported with gyrification. Therefore the effect of sex on all brain morphometric (cortical thickness, LGI and brain volume, etc.) measures should be considered in HIV infection studies. Again, since the effect of HIV/ART on LGI differs between sexes, the effect of HIV on IQ and motor control may also differ between sexes.

5.2 Effects of HIV exposure on brain morphometrics

5.2.1 Effects of HIV exposure on brain volumes

We found no significant difference between HIV/ART-exposed uninfected (HEU) children and HIV-unexposed uninfected (HUU) children in global white and gray matter, and intracranial volume. In addition, none of the brain regions investigated: caudate, hippocampus, thalamus, putamen, lateral ventricle and corpus callosum differed between these groups. It appears that exposure to HIV/ART without infection has no effect on global or regional brain volumes, including regions that show reduced volumes in HIV-infected children.

The lack of difference we observe is consistent with several studies that have shown little effect of HIV/ART exposure on neurodevelopment and little difference in neurocognitive functioning and

language development between HEU and HUU children (Ngoma et al., 2014; Springer et al., 2012) once environmental factors have been properly controlled for (Alimenti et al., 2006, Williams et al., 2010).

There are, however, several concerns associated with prenatal exposure to HIV/ART. Evidence suggests that protease inhibitor-containing HAARTs may lead to premature delivery and low birth weight in children exposed to HIV/ART *in utero*; however, this low weight is corrected within the first 6 months of life (Powis et al., 2011; Van der Merwe et al., 2011). Cases of severe infant anemia (Scott Dryden-Peterson et al., 2011), blood mitochondrial DNA mutation (Jitratkosol et al., 2012; Hernandez et al., 2012) and cardiac growth complications (Lipshultz et al., 2011; 2012) have also been reported in infants exposed to HAART *in utero*. Further investigation of these abnormal conditions has been recommended to understand the long term effects on HEU children (Zareba et al., 2004; Lipshultz et al., 2011). Also, one recent study did find small deficits in areas of neurocognitive function among HEU children (Kerr et al., 2014) motivating the need for further research into the effects of HIV/ART exposure on neurodevelopment.

5.2.2 Effects of HIV exposure on cortical thickness and LGI

Although our results showed that HEU children had significantly thicker cortex than HUU children in the inferior frontal gyrus, this difference was lost after controlling for sex. This follows the hypothesis of sexual dimorphism that holds that on average global and regional cortical thickness differs between male and female brains, where females tend to have thicker cortex than males at the same age (Kiho Im et al., 2006; Luders et al., 2006), a result found in our data too. Although we found no evidence of an interaction effect of sex and *in -utero* HIV/ART exposure on cortical thickness, the effect of sex is an important consideration for future work investigating effects of *in -utero* HIV/ART exposure on brain morphometry in children.

As evidence of this sex effect on morphometry, across all the children in our study boys had higher LG indices than girls in the bilateral fusiform/parahippocampal area. The effect of sex was also evident within the uninfected group: there was no significant difference in LGI between HEU and HUU children until sex was controlled for, when a region in the right precuneus was revealed where HEU children had significantly higher LGIs than HUU children.

Thus although brain volume and cortical thickness are not affected by *in -utero* exposure to HIV/ART, it appears that gyrification is affected by one or both of these factors. This may be because there are major changes in fetal gyrification that occur during the third trimester of gestation in humans (White et al, 2010; Keslera et al., 2006), while cortical thickness changes start in the first few months of life after birth (Li et al., 2014; Epstein, 1986).

Abnormal increases in gyrification relative to healthy controls have previously been observed in disorders such as autism (Wallace et al., 2013), Williams syndrome (Schmitt et al., 2002; Gaser et al., 2006) and schizophrenia (Schultz et al., 2010), as well as with preterm birth (Kesler et al., 2006). Because inclusion of protease-inhibitors in HAART combination therapy during pregnancy has been shown to increase the risk of premature delivery (Powis et al., 2011; Townsend et al., 2007; Cotter et al., 2006), future work should investigate whether birth weight or gestational age at delivery is associated with LGI in HEU children.

The mechanism behind the development of cortical gyrification is not known: one model holds that gyri form as a result of tension within areas of strong neural connections (Van Essen, 1997). This means that if distant axonal connections were malformed, there would be an increase in regional gyrification, as we observed in the precuneus of HEU children. A second model proposes that the decrease in gyral width associated with increased gyrification results in a restriction of contact with underlying white matter (Prothero et al., 1984). Inflammation of the gyri in the precuneus due to HIV/ART exposure may therefore also affect the underlying white matter in our HEU cohort. The implication of this altered gyrification on the neurodevelopment of our HEU cohort needs to be investigated further.

5.3 Limitations

Some limitations of this study are: first, the study is cross-sectional at a single time point at age 7 years, therefore we cannot draw any conclusions about longitudinal brain development. Secondly, we only controlled for sex and brain volume while there are many environmental variables associated with HIV that may have a profound effect on neurodevelopment. For example, HIV-infected children may come from disadvantaged socioeconomic backgrounds and are more likely to have had to cope with stressors such as poor health or the loss of a parent. Thirdly, the use of FreeSurfer in pediatric populations should be validated through manual segmentation of the same MRI data. While it would have been valuable to examine differences in cognitive impairment between the groups using neuropsychological performance data, this data were unfortunately not available at this time. As such, we could not investigate here associations between morphological variations and cognitive function, but this will form the basis of planned future work.

6. Summary and conclusions

This is the first automated, quantitative morphological neuroimaging study in vertically-infected young children with HIV stable on ART in Africa.

HIV-infected children show similar patterns of white and gray matter volume reductions as HIV-infected adults, as well as similar subcortical reductions in the putamen and right hippocampus, but not the caudate or thalamus. Caudate and thalamus volume, as well as cortical thickness may be spared from the effects of HIV by the suppression of HIV replication in the CNS through early ART.

The lack of difference in cortical thickness between HIV-infected children and uninfected controls may reflect the preserved neurocognitive function in HIV-infected children who started treatment in infancy (Laughton et al., 2012; Lindsey et al., 2007). However, there is nonetheless a reduction in the volume of gray matter, and the reduced left hemispheric parietal LGI in HIV-infected children may indicate the presence of sulcal enlargement despite early treatment.

Worse baseline immune status (lower CD4/CD8 ratio) is associated with increased caudate nucleus volume and greater left lateral occipital LGI in stable HIV-infected children, possibly as a consequence of neuroinflammation resulting in glial activation/oedema and disruption of cortical development.

There are no differences in brain volume or cortical thickness between HIV-exposed uninfected and HIV unexposed uninfected children, in agreement with several studies that have found little effect of HIV/ART exposure on neurocognitive functioning and language development. However, the increased gyrification in the precuneus that HIV/ART-exposed children showed relative to unexposed children may result from inflammation during fetal development. The association of this altered gyrification with neurocognitive development in HEU children should be investigated.

Environmental variables associated with HIV may affect neurodevelopment and should be considered in future studies on brain morphometry in HIV-affected children. Morphometric measures in children are also sex-dependent.

References

1. Ances, B. M., Ortega, M., Vaida, F., Heaps, J., & Paul, R. (2012). Independent effects of HIV, aging, and HAART on brain volumetric measures. *Journal of acquired immune deficiency syndromes (1999)*, *59*(5), 469.

2. Anthony, I. C., Ramage, S. N., Carnie, F. W., Simmonds, P., & Bell, J. E. (2005). Influence of HAART on HIV-related CNS disease and neuroinflammation. *Journal of Neuropathology & Experimental Neurology*, *64*(6), 529-536.

3. Avison, M. J., Nath, A., & Berger, J. R. (2002). Understanding pathogenesis and treatment of HIV dementia: A role for magnetic resonance? *Trends in Neurosciences, 25*(9), 468-473.

4. Aylward, E. H., Henderer, J. D., McArthur, J. C., Brettschneider, P. D., Harris, G. J., Barta, P. E., & Pearlson, G. D. (1993). Reduced basal ganglia volume in HIV-1-associated dementia Results from quantitative neuroimaging. *Neurology*,*43*(10), 2099-2099.

5. Banks, W. A. (1999). Physiology and pathology of the blood-brain barrier: Implications for microbial pathogenesis, drug delivery and neurodegenerative disorders. *Journal of Neurovirology, 5*(6), 538-555.

6. Becker, J. T., Sanders, J., Madsen, S. K., Ragin, A., Kingsley, L., Maruca, V., & Thompson, P. M. (2011). Subcortical brain atrophy persists even in HAART-regulated HIV disease. *Brain imaging and behavior*, *5*(2), 77-85.

7. Blanchette, N., Fernandes-Penney, A., King, S., & Read, S. (2001). Cognitive and motor development in children with vertically transmitted HIV infection. *Brain and Cognition, 46*(1), 50-53.

8. Blanchette, N., Smith, M. L., King, S., Fernandes-Penney, A., & Read, S. (2002). Cognitive development in school-age children with vertically transmitted HIV infection. *Developmental Neuropsychology, 21*(3), 223-241

9. Broderick, D. F., Wippold II, F. J., Clifford, D. B., Kido, D., & Wilson, B. S. (1993). White matter lesions and cerebral atrophy on MR images in patients with and without AIDS dementia complex. *American Journal of Roentgenology, 161*(1), 177-181.

10. Brouwers, P., DeCarli, C., Tudor-Williams, G., Civitello, L., Moss, H., & Pizzo, P. (1994). Interrelations among patterns of change in neurocognitive, CT brain imaging and CD4

measures associated with anti-retroviral therapy in children with symptomatic HIV infection. *Advances in neuroimmunology*, *4*(3), 223-231.

11. Castelo, J. M. B., Courtney, M. G., Melrose, R. J., & Stern, C. E. (2007). Putamen hypertrophy in nondemented patients with human immunodeficiency virus infection and cognitive compromise. *Archives of neurology*, *64*(9), 1275-1280.

12. Cardenas, V. A., Meyerhoff, D. J., Studholme, C., Kornak, J., Rothlind, J., Lampiris, H., & Weiner, M. W. (2009). Evidence for ongoing brain injury in human immunodeficiency virus-positive patients treated with antiretroviral therapy. *Journal of neurovirology*, *15*(4), 324-333.

13. Chang, L., Ernst, T., Witt, M. D., Ames, N., Gaiefsky, M., & Miller, E. (2002). Relationships among brain metabolites, cognitive function, and viral loads in antiretroviral-naïve HIV patients.*Neuroimage, 17*(3), 1638-1648.

14. Chen, Y., An, H., Zhu, H., Stone, T., Smith, J. K., Hall, C., Lin, W. (2009). White matter abnormalities revealed by diffusion tensor imaging in non-demented and demented HIV+ patients.*Neuroimage,47*(4),1154-1162. doi:http://dx.doi.org/10.1016/j.neuroimage.2009.04.030

15. Chriboga.C.A, Fleishman.S, Champion.S, Gaye-Robinson.L, Abrams.E.J (2005). Incidence and prevalence of HIV encephalopathy in children with HIV infection receiving highly active anti-retroviral therapy (HAART). The Journal of Pediatrics pp. 401-407

16. Cohen, R. A., Harezlak, J., Schifitto, G., Hana, G., Clark, U., Gongvatana, A., & Navia, B. (2010). Effects of nadir CD4 count and duration of human immunodeficiency virus infection on brain volumes in the highly active antiretroviral therapy era. *Journal of neurovirology*, *16*(1), 25-32.

17. Cotter, A. M., Garcia, A. G., Duthely, M. L., Luke, B., & O'Sullivan, M. J. (2006). Is antiretroviral therapy during pregnancy associated with an increased risk of preterm delivery, low birth weight, or stillbirth?. *Journal of Infectious Diseases*, *193*(9), 1195-1201.

18. Cotton, M. F., Violari, A., Otwombe, K., Panchia, R., Dobbels, E., Rabie, H., Josipovic,D., Liberty, A., Lazarus, E., Innes, S., Janse van Rensburg, A., Pelser, W., Truter, H., Madhi, S.A., Handelsman, E., Jean-Philippe, P., McIntyre, J.A., Gibb, D.M., Babiker, A.G., & CHER Study Team. (2013). Early time-limited antiretroviral therapy versus deferred therapy in South African infants infected with HIV: results from the children with HIV early antiretroviral (CHER) randomised trial. The Lancet,382(9904), 1555-1563.

19. Dale A.M, Fischl.B, Sereno.M.I. (1999) Cortical Surface-Based Analysis. I. Segmentation and surface reconstruction. Neuroimage 9 (79-194).

20. Dal Pan .G.J., McArthur, J. H., Aylward, E., Selnes, O. A., Nance-Sproson, T., Kumar, A. J., McArthur, J. C. (1992). Patterns of cerebral atrophy in HIV-1-infected individuals: Results of a quantitative MRI analysis. *Neurology, 42*(11), 2125-2130.

21. Desikan R.S, Segonne F, Fischl B, Quinn B.T, Dickerson B.C, Blacker D, Buckner R.L, Dale A.M, Maguire R.P, Hyman B.T, Albert M.S, Killiany R.J. (2006). An automated labeling system for subdividing the human cerebral cortex on MRI scans into gyral based regions of interest. Neuroimage; 31:968–980. [PubMed: 16530430]

22. Destrieux C, Fischl B, Dale A, Halgren E. (2010). Automatic parcellation of human cortical gyri and sulci using standard anatomical nomenclature. Neuroimage; 53:1–15. [PubMed: 20547229]

23. Donald, K. A., Hoare, J., Eley, B., & Wilmshurst, J. M. (2014). Neurologic complications of pediatric human immunodeficiency virus: Implications for clinical practice and management challenges in the African setting. In *Seminars in pediatric neurology* (Vol. 21, No. 1, pp. 3-11). WB Saunders.

24. Dryden-Peterson, S., Shapiro, R. L., Hughes, M. D., Powis, K., Ogwu, A., Moffat, C., Moyo, S., Makhema, J., Essex, M., Lockman, S. (2011). Increased risk of severe infant anemia following exposure to maternal HAART, Botswana. *Journal of acquired immune deficiency syndromes (1999)*, *56*(5), 428.

25. Du, H., Wu, Y., Ochs, R., Edelman, R. R., Epstein, L. G., McArthur, J., &Ragin, A. B. (2012). A comparative evaluation of quantitative neuroimaging measurements of brain status in HIV infection. *Psychiatry Research, 203*(1), 95-99. doi:10.1016/j.pscychresns.2011.08.014

26. Ellis, R., Langford, D., & Masliah, E. (2007). HIV and antiretroviral therapy in the brain: neuronal injury and repair. *Nature Reviews Neuroscience*, *8*(1), 33-44.

27. Ellis, R (2010). HIV and antiretroviral therapy: Impact on the central nervous system. Progress in Neurobiology, 91. pp. 185 – 187

28. Elovaara, I., Poutiainen, E., Raininko, R., Valanne, L., Virta, A., Valle, S. L., ... & Iivanainen, M. (1990). Mild brain atrophy in early HIV infection: the lack of association with cognitive deficits and HIV-specific intrathecal immune response. *Journal of the neurological sciences*, *99*(2), 121-136.

29. Epstein, H. T. (1986). Stages in human brain development. *Developmental Brain Research*, *30*(1), 114-119.

30. Epstein, L. G., Sharer, L. R., Oleske, J. M., Connor, E. M., Goudsmit, J., Bagdon, L., Koenigsberger, M. R. (1986). Neurologic manifestations of human immunodeficiency virus infection in children. *Pediatrics, 78*(4), 678-687.

31. Fennema-Notestine, C., Ellis, R. J., Archibald, S. L., Jernigan, T. L., Letendre, S. L., Notestine, R. J., Taylor, M.J., Theilmann, R.J., Julaton, M.D., Croteau, D.J., Wolfson, T., Heaton, R.K., Gamst, A.C., Franklin, D.R Jr. Clifford, D.B., Collier, A.C., Gelman, B.B., Marra, C., McArthur, J.C., McCutchan, J.A., Morgello, S., Simpson, D.M., Grant, I., & CHARTER Group. (2013). Increases in brain white matter abnormalities and subcortical gray matter are linked to CD4 recovery in HIV infection. *Journal of neurovirology*, *19*(4), 393-401.

32. Filippi, C. G., Uluğ, A. M., Ryan, E., Ferrando, S. J., & van Gorp, W. (2001). Diffusion tensor imaging of patients with HIV and normal-appearing white matter on MR images of the brain. *American Journal of Neuroradiology*, *22*(2), 277-283.

33. Fischl, B.R., Sereno, M.I., Dale, A. M (1999). Cortical Surface-Based Analysis II: Inflation, Flattening, and Surface-Based Coordinate System. NeuroImage, 9, 195-207.

34. Fischl B, Sereno M.I, Tootell R.B, Dale A.M. (1999a) High-resolution intersubject averaging and a coordinate system for the cortical surface. Hum. Brain Mapp.; 8:272–284. [PubMed: 10619420].

35. Fischl B, Sereno M.I, Tootell R.B, Dale A.M.(1999b) High-resolution intersubject averaging and a coordinate system for the cortical surface. Hum. Brain Mapp.; 8:272–284. [PubMed: 10619420]

36. Fischl, B, Salat D.H., Busa E, Albert M, Dieterich M, Haselgrove C, van der Kouwe A, Killiany R, Kennedy D, Klaveness S, Montillo A, Makris N, Rosen B, Dale A.M. (2002). Whole brain segmentation: automated labeling of neuroanatomical structures in the human brain. Neuron. 33:341–355.[PubMed: 11832223]

37. Fischl B, Salat D.H, van der Kouwe A.J, Makris N, Segonne F, Quinn B.T, Dale A.M. (2004a) Sequence independent segmentation of magnetic resonance images. Neuroimage; 23(Suppl. 1):S69–S84. [PubMed: 15501102].

38. Fischl B, van der Kouwe A, Destrieux C, Halgren E, Segonne F, Salat D.H, Busa E, Seidman L.J, Goldstein J, Kennedy D, Caviness V, Makris N, Rosen B, Dale A.M. (2004b). Automatically parcellating the human cerebral cortex. Cereb. Cortex.; 14:11–22. [PubMed: 14654453].

39. Fischl B, Rajendran N, Busa E, Augustinack J, Hinds O, Yeo B.T.T, Mohlberg H, Amunts K, Zilles K. (2008). Cortical folding patterns and predicting cytoarchitecture. Cereb. Cortex.; 18:1973–1980. [PubMed: 18079129]

40. Fischl B, Stevens A.A, Rajendran N, Yeo B.T.T, Greve D.N, Van Leemput K, Polimeni J.R, Kakunoori S, Buckner R.L, Pacheco J, Salat D.H, Melcher J, Frosch M.P, Hyman B.T, Grant P.E, Rosen B.R, van der Kouwe A.J.W, Wiggins G.C, Wald L.L, Augustinack J.C. (2009). Predicting the location of entorhinal cortex from MRI. Neuroimage; 47:8–17. [PubMed: 19376238].

41. Fischl, B., & Dale, A. M. (2000). Measuring the thickness of the human cerebral cortex from magnetic resonance images. *Proceedings of the National Academy of Sciences, 97*(20), 11050-11055.

42. Fischl,B.(2012).Freesurfer.*Neuroimage,62*(2),774-781.doi:10.1016/j.neuroimage.2012.01.021.

43. Gaser, C., Luders, E., Thompson, P. M., Lee, A. D., Dutton, R. A., Geaga, J. A., Hayashi, K.M., Bellugi, U., Galaburda, A.M., Korenberg, J.R., Mills, D.L., Toga, A.W., Reiss, A. L. (2006). Increased local gyrification mapped in Williams syndrome. *Neuroimage*, *33*(1), 46-54.

44. Gavin, P., & Yogev, R. (1999). Central nervous system abnormalities in pediatric human immunodeficiency virus infection. *Pediatric Neurosurgery, 31*(3), 115-123.

45. George, R., Andronikou, S., du Plessis, J., du Plessis, A., Van Toorn, R., &Maydell, A. (2009). Central nervous system manifestations of HIV infection in children. *Pediatric Radiology, 39*(6), 575-585.

46. Gongvatana, A., Correia, S., Dunsiger, S., Gauthier, L., Devlin, K. N., Ross, S., Navia, B., Tashima, K.T., DeLaMonte, S., Cohen, R. A. (2014). Plasma Cytokine Levels are Related to Brain Volumes in HIV-infected Individuals. *Journal of Neuroimmune Pharmacology*,*9*(5), 740-750.

47. Hanning, U., Husstedt, I. W., Niederstadt, T., Evers, S., Heindel, W., &Kloska, S. P. (2011). Cerebral signal intensity abnormalities on T2-weighted MR images in HIV patients with highly active antiretroviral therapy: Relationship with clinical parameters and interval changes. *Academic Radiology, 18*(9), 1144-1150. doi:10.1016/j.acra.2011.04.013

48. Hawkins, C. P., McLaughlin, J. E., Kendall, B. E., & McDonald, W. I. (1993). Pathological findings correlated with MRI in HIV infection. *Neuroradiology, 35*(4), 264-268.

49. Heaps, J.M., Joska .J., Hoare .J., Ortega .M., Agrawal .A., Seedat .S., Ances .B.M., Stein .D.J, Paul .R. (2012). Neuroimaging markers of human immunodeficiency virus infection in South Africa. Journal of Neurovirology, 18:151-156. DOI 10.1007/s13365-012-0090-5

50. Hernandez, S., Moren, C., Lopez, M., Coll, O., Cardellach, F., Gratacos, E., Miro, O., Garrabou, G. (2012). Perinatal outcomes, mitochondrial toxicity and apoptosis in HIV-treated pregnant women and in utero-exposed newborn. *AIDS*,*26*(4), 419-428.

51. Hinds O.P, Rajendran N, Polimeni J.R, Augustinack J.C, Wiggins G, Wald L.L, Diana Rosas H, Potthast A, Schwartz E.L, Fischl B. (2008). Accurate prediction of V1 location from cortical folds in a surface coordinate system. Neuroimage; 39:1585–1599. [PubMed: 18055222]

52. Hoare, J., Fouche, J., Spottiswoode, B., Donald, K., Philipps, N., Bezuidenhout, H., Schrieff, L. (2012). A diffusion tensor imaging and neurocognitive study of HIV-positive children who are HAART-naïve "slow progressors". *Journal of Neurovirology, 18*(3), 205-212.

53. Hoare, J., Fouche, J. P., Spottiswoode, B., Sorsdahl, K., Combrinck, M., Stein, D. J., Robert, H.P., & Joska, J. A. (2014). White-matter damage in clade C HIV-positive subjects: a diffusion tensor imaging study.

54. Hogstrom, L. J., Westlye, L. T., Walhovd, K. B., & Fjell, A. M. (2012). The structure of the cerebral cortex across adult life: age-related patterns of surface area, thickness, and gyrification. *Cerebral Cortex*, bhs231.

55. Holt, J. L., Kraft-Terry, S., & Chang, L. (2012). Neuroimaging studies of the aging HIV-1-infected brain. *Journal of Neurovirology, 18*(4), 291-302. doi:10.1007/s13365-012-0114-1.

56. Horowitz, A. L. (1989). Overview. In *MRI Physics for Physicians* (pp. 1). Springer US.

57. Hua, X., Boyle, C. P., Harezlak, J., Tate, D. F., Yiannoutsos, C. T., Cohen, R., HIV Neuroimaging Consortium. (2013). Disrupted cerebral metabolite levels and lower nadir CD4+ counts are linked to brain volume deficits in 210 HIV-infected patients on stable treatmentpatients on stable treatment.*NeuroImage: Clinical*, *3*, 132-142.

58. Jernigan, T. L., Archibald, S. L., Fennema-Notestine, C., Taylor, M. J., Theilmann, R. J., Julaton, M. D., Notestine, R.J., Wolfson, T., Letendre, S.L., Ellis, R.J., Heaton, R.K., Gamst, A.C., Franklin Jr, D.R., Clifford, D.B., Collier, A.C., Gelman, B.B., Marra, C., McArthur, J.C., McCutchan, J.A., Morgello, S., Simpson, D.M., Grant, I. and the CHARTER Group. (2011). Clinical factors related to brain structure in HIV: the CHARTER study. *Journal of neurovirology*, *17*(3), 248-257.

59. Jitratkosol, M. H., Sattha, B., Maan, E. J., Gadawski, I., Harrigan, P. R., Forbes, J. C., Alimenti, A.,Van Schalkwyk, J., Money, D.M., & Côté, H. C. (2012). Blood mitochondrial DNA mutations

in HIV-infected women and their infants exposed to HAART during pregnancy.*Aids*, *26*(6), 675-683.

60. Kallianpur.K.J, Kirk.G.R, Sailasuta.N, Valcour.V, Shiramizu.B, Nakamoto.B.K, Shikuma.C (2012). Regional Cortical Thinning Associated with Detectable Levels of HIV DNA. Cerebral Cortex 22:2065-2075. doi:10.1093/cercor/bhr285.

61. Kallianpur, K. J., Shikuma, C., Kirk, G. R., Shiramizu, B., Valcour, V., Chow, D., & Sailasuta, N. (2013). Peripheral blood HIV DNA is associated with atrophy of cerebellar and subcortical gray matter. *Neurology*, *80*(19), 1792-1799.

62. Kesler, S. R., Vohr, B., Schneider, K. C., Katz, K. H., Makuch, R. W., Reiss, A. L., Ment, L. R. (2006). Increased temporal lobe gyrification in preterm children. *Neuropsychologia*, *44*(3), 445-453.

63. Khan, A. M. (2013). Physics of MRI. *Principles and Practice of Urology*, 92.

64. Kieck, J., Andronikou, S. (2008). Usefulness of neuro-imaging for the diagnosis of HIV encephalopathy in children. *South African Medical Journal, 94*(8), 628.

65. Kiho Im, Jong-Min Lee, Junki Lee, Yong-Wook Shin, In Young Kim, Jun Soo Kwon, Sun I. Kim (2006). Gender difference analysis of cortical thickness in healthy young adults with surface-based methods. NeuroImage 31: 31 – 38.

66. Koekkoek, S., Eggermont, L., De Sonneville, L., Jupimai, T., Wicharuk, S., Apateerapong, W., chuenyam, T., Lange, J., Wit, F., Pancharoen, C., Phanuphak, P., Ananworanich, J. (2006). Effects of highly active antiretroviral therapy (HAART) on psychomotor performance in children with HIV disease. *Journal of neurology*, *253*(12), 1615-1624.

67. Kozlowski, P. B., Brudkowska, J., Kraszpulski, M., Sersen, E. A., Wrzolek, M. A., Anzil, A. P., Wisniewski, H. M. (1997). Microencephaly in children congenitally infected with human immunodeficiency virus--a gross-anatomical morphometric study.*ActaNeuropathologica, 93*(2), 136-145.

68. Küper, M., Rabe, K., Esser, S., Gizewski, E. R., Husstedt, I. W., Maschke, M., & Obermann, M. (2011). Structural gray and white matter changes in patients with HIV. *Journal of neurology*, *258*(6), 1066-1075.

69. Langford.D, Marquie-Beck.J, de Almeida.S, Lazzaretto.D, Letendre. S, Grant. I, McCutchan.J.A, Masliah. E, Ellis.R.J, and the HIV Neurobehavioral Research Center (HNRC) group (2006). Relationship of antiretroviral treatment to postmortem brain tissue viral load in human immunodeficiency virus–infected patients. Journal of NeuroVirology, 12: 100–107. DOI: 10.1080/13550280600713932.

70. Laughton, B., Cornell, M., Grove, D., Kidd, M., Springer, P. E., Dobbels, E., Janse van Rensburg, A., Violari, A., Babiker, A.,Madhi, S.A., Jean-Philippe, P., Gibb, D.M., Cotton, M. F. (2012). Early antiretroviral therapy improves neurodevelopmental outcomes in infants. *AIDS (London, England)*, *26*(13), 1685

71. Laughton, B., Cornell, M., Boivin, M., & Van Rie, A. (2013). Neurodevelopment in perinatally HIV-infected children: a concern for adolescence. *Journal of the International AIDS Society*, *16*(1).

72. Le Doaré, K., Bland, R., & Newell, M. (2012).Neurodevelopment in children born to HIV-infected mothers by infection and treatment status.*Pediatrics, 130*(5), e1326-e1344. doi:10.1542/peds.2012-0405.

73. Li, G., Nie, J., Wang, L., Shi, F., Gilmore, J. H., Lin, W., & Shen, D. (2014). Measuring the dynamic longitudinal cortex development in infants by reconstruction of temporally consistent cortical surfaces. *Neuroimage*, *90*, 266-279.

74. Lindsey.J.C, Malee.K.M, Brouwers.P, Hughes.M.D (2007). Neurodevelopmental functioning in HIV-infected infants and young children before and after the introduction of protease inhibitor-based highly active antiretroviral therapy. PEDIATRICS. DOI: 10.1542/peds.2006-1145.

75. Lipshultz, S. E., Shearer, W. T., Thompson, B., Rich, K. C., Cheng, I., Orav, E. J., Kumar, S., Pignatelli, R.H., Bezold, L.I., LaRussa, P., Starc, T.J., Glickstein, J.S., O'Brien, S., Cooper, E.R., Wilkinson, J.D., Miller, T.L., Colan, S. D. (2011). Cardiac effects of antiretroviral therapy in HIV-negative infants born to HIV-positive mothers: NHLBI CHAART-1 (National Heart, Lung, and Blood Institute Cardiovascular Status of HAART Therapy in HIV-Exposed Infants and Children cohort study). *Journal of the American College of Cardiology*, *57*(1), 76-85.

76. Lipshultz, S. E., Mas, C. M., Henkel, J. M., Franco, V. I., Fisher, S. D., & Miller, T. L. (2012). HAART to heart: highly active antiretroviral therapy and the risk of cardiovascular disease in HIV-infected or exposed children and adults.

77. Luders.E, Narr.K.L, Thompson.P.M, Rex.D.E, Woods.R.P, DeLuca.H, Jancke.L, Toga.A.W (2006). Gender Effects on Cortical Thickness and the Influence of Scaling. Human Brain Mapping (HBM) 27:314 –324.

78. Martin, S. C., Wolters, P. L., Toledo-Tamula, M. A., Zeichner, S. L., Hazra, R., & Civitello, L. (2006). Cognitive functioning in school-aged children with vertically acquired HIV infection being treated with highly active antiretroviral therapy (HAART). *Developmental neuropsychology*, *30*(2), 633-657.

79. Martinos Centre for Biomedical Imaging,Massachusetts General Hospital, Boston, MA USA. (2009). FreeSurfer tutorial. *Martinos Centre for Biomedical Imaging,MGH, Boston, MA USA;,*

80. McCoig.C, Castrejon.M.M, Castano.E, Onix de Suman, Baez.C, Redondo.W, McClernon.D, Danebower.S, Lanier Randall.E, Richardson.C, Keller.A, Hetherington.S, Saez-Llorens.X, Ramilo.O (2002). Effect of combination antiretroviral therapy on cerebrospinal fluid HIV RNA, HIV resistance, and clinical manifestations of encephalopathy. The Journal of Pediatrics. Vol. 141, Number1. pp.36-44.

81. Mitchell, W. (2001). Neurological and developmental effects of HIV and AIDS in children and adolescents. *Mental Retardation and Developmental Disabilities Research Reviews, 7*(3), 211-216.

82. Navia, B. A., & Price, R. W. (1987). The acquired immunodeficiency syndrome dementia complex as the presenting or sole manifestation of human immunodeficiency virus infection.*Archives of Neurology, 44*(1), 65.

83. Ngoma, M. S., Hunter, J. A., Harper, J. A., Church, P. T., Mumba, S., Chandwe, M., Cote, H.C., Albert, A.Y., Smith, M.L., Selemani, C., Sandstrom, P.A., Bandenduck, L., Ndlovu, U., Khan, S., Roa, L., Silverman, M. S. (2014). Cognitive and language outcomes in HIV-uninfected infants

exposed to combined antiretroviral therapy in utero and through extended breast-feeding. *AIDS*, *28*, S323-S330.

84. Ortega .M., Heaps .J.M., Joska .J., Vaida .F., Seedat .S., Stein .D.J., Paul .R., Ances .B.M. (2013). HIV clades B and C are associated with reduced brain volumetrics. Journal of Neurovirology, 19: 479-487. DOI 10.1007/s13365-013-0202-x

85. Ortega, M., Joska, J., Heaps, J., Vaida, F., Paul, R., & Ances, B. (2013). Effects of HIV Clade B and C on Brain Volumetric Measurements (P06. 177).*Neurology*, *80*(Meeting Abstracts 1), P06-177.

86. Patsalides, A. D., Wood, L. V., Atac, G. K., Sandifer, E., Butman, J. A., &Patronas, N. J. (2002). Cerebrovascular disease in HIV-infected pediatric patients: Neuroimaging findings.*American Journal of Roentgenology, 179*(4), 999-1003.

87. Patel, S.D, Larson, E, Mbengashe, T, O'Bra, H, Brown, J.W, Golman, T.M, Klausner, J.D. (2012). Increases in Pediatric Antiretroviral Treatment, South Africa 2005-2010.PLoS ONE 7(9):e44914. doi: 10.1371/journal.pone.0044914

88. Paul, R., Cohen, R., Navia, B., &Tashima, K. (2002). Relationships between cognition and structural neuroimaging findings in adults with human immunodeficiency virus type-1. *Neuroscience &Biobehavioral Reviews, 26*(3), 353-359. doi:http://dx.doi.org/10.1016/S0149-7634(02)00006-4.

89. Paul, R. H., Ernst, T., Brickman, A. M., Yiannoutsos, C. T., Tate, D. F., Cohen, R. A., & Navia, B. A. (2008). Relative sensitivity of magnetic resonance spectroscopy and quantitative magnetic resonance imaging to cognitive function among nondemented individuals infected with HIV. *Journal of the International Neuropsychological Society*, *14*(05), 725-733.

90. Phelps .R. B, Rakhmanina.N (2011). Antiretroviral Drugs in Pediatric HIV-Infected Patients Pharmacokinetic and Practical Challenges. Pediatric drugs 13(3): 175 -192.

91. Persidsky, Y., Ghorpade, A., Rasmussen, J., Limoges, J., Liu, X. J., Stins, M., Witte, M. H. (1999). Microglial and astrocyte chemokines regulate monocyte migration through the blood-brain

barrier in human immunodeficiency virus-1 encephalitis. *The American Journal of Pathology, 155*(5), 1599-1611.

92. Persidsky, Y., Ramirez, S. H., Haorah, J., &Kanmogne, G. D. (2006). Blood–brain barrier: Structural components and function under physiologic and pathologic conditions. *Journal of Neuroimmune Pharmacology, 1*(3), 223-236.

93. Plewes, D. B., & Kucharczyk, W. (2012). Physics of MRI: a primer. *Journal of Magnetic Resonance Imaging*, *35*(5), 1038-1054.

94. Powis, K. M., Smeaton, L., Ogwu, A., Lockman, S., Dryden-Peterson, S., van Widenfelt, E., Leidner, J., Makhema, J., Essex, M., Shapiro, R. L. (2011). Effects of in utero antiretroviral exposure on longitudinal growth of HIV-exposed uninfected infants in Botswana. *Journal of acquired immune deficiency syndromes (1999)*, *56*(2), 131.

95. Prendergast, A., Tudor-Williams, G., Jeena, P., Burchett, S., &Goulder, P. (2007). International perspectives, progress, and future challenges of pediatric HIV infection. *Lancet, 370*(9581), 68-80.

96. Prothero, J. W., & Sundsten, J. W. (1984). Folding of the cerebral cortex in mammals. *Brain, Behavior and Evolution*, *24*(2-3), 152-167

97. Puthanakit, T., Ananworanich, J., Vonthanak, S., Kosalaraksa, P., Hansudewechakul, R., van der Lugt, J., Kerr, S.J., PhD, Kanjanavanit, S., Ngampiyaskul, C., Wongsawat, J., Luesomboon, W., Vibol, U., Pruksakaew, K., Suwarnlerk, T., Apornpong, T., Ratanadilok, K., Paul, R., Mofenson, L.M., Fox, L., Valcour, V., Brouwers, P., Ruxrungtham,K.,& PREDICT Study Group. (2013). Cognitive function and neurodevelopmental outcomes in HIV-infected children older than 1 year of age randomized to early versus deferred antiretroviral therapy: the PREDICT neurodevelopmental study. *The Pediatric infectious disease journal*, *32*(5), 501.

98. Randall, S. (2015). The effects of HIV-1 infection on subcortical brain structures in children receiving ART: A structural MRI study (Master's thesis, University of Cape Town, South Africa.)

99. Rausch, D. M., & Stover, E. S. (2001). Neuroscience research in AIDS. *Progress in Neuro-Psychopharmacology and Biological Psychiatry, 25*(1), 231-257.

100. Safriel, Y. I., Haller, J. O., Lefton, D. R., &Obedian, R. (2000). Imaging of the brain in the HIV-positive child. *Pediatric Radiology, 30*(11), 725-732.

101. Sarma, M. K., Nagarajan, R., Keller, M. A., Kumar, R., Nielsen-Saines, K., Michalik, D. E., Deville, J., Church, J.A., Thomas, M. A. (2014). Regional brain gray and white matter changes in perinatally HIV-infected adolescents. *NeuroImage: Clinical*,*4*, 29-34.

102. Schaer, M., Cuadra, M. B., Tamarit, L., Lazeyras, F., Eliez, S., & Thiran, J. (2008). A surface-based approach to quantify local cortical gyrification. *Medical Imaging, IEEE Transactions on*, *27*(2), 161-170.

103. Schaer, M., Schmitt, J. E., Glaser, B., Lazeyras, F., Delavelle, J., & Eliez, S. (2006). Abnormal patterns of cortical gyrification in velo-cardio-facial syndrome (deletion 22q11. 2): an MRI study. *Psychiatry Research: Neuroimaging*, *146*(1), 1-11.

104. Sharland, M., &Handforth, J. (2005). Pediatric HIV infection. *Medicine, 33*(6), 28-29. doi: http://dx.doi.org/10.1383/medc.33.6.28.66013.

105. Schultz, C. C., Koch, K., Wagner, G., Roebel, M., Nenadic, I., Gaser, C., Schachtzabel, C., Reichenbach, J.R., Heinrich, S., & Schlösser, R. G. (2010). Increased parahippocampal and lingual gyrification in first-episode schizophrenia. *Schizophrenia research*, *123*(2), 137-144.

106. Shisana, O., Rehle, T., Simbayi, L., Parker, W., Zuma, K., Bhana, A., Pillay, V. (2005). South african national HIV prevalence, HIV incidence, behavior and communication survey, 2005. *Cape Town, South Africa: Human Sciences Research Council Publishers.*

107. Spreer, J., Enenkel-Stoodt, S., Funk, M., Fiedler, A., de Simone, A., & Hacker, H. (1994). [Neuroradiological findings in perinatally HIV-infected children].*Röfo: Fortschritte Auf Dem Gebiete Der Röntgenstrahlen Und Der Nuklearmedizin, 161*(2), 106-112.

108. Spudich, S. S., &Ances, B. M. (2012). Neurologic complications of HIV infection. *TopAntiviral Med, 20*, 41-47.

109. Smith, R., Malee, K., Leighty, R., Brouwers, P., Mellins, C., Hittelman, J., Chase, C., Blasini, I. and Women and Infants Transmission Study Group. (2006). Effects of perinatal HIV infection and associated risk factors on cognitive development among young children. Pediatrics, 117(3), 851-862

110. Steinbrink, F., Evers, S., Buerke, B., Young, P., Arendt, G., Koutsilieri, E.,Husstedt, I. (2013). Cognitive impairment in HIV infection is associated with MRI and CSF pattern of neurodegeneration. *European Journal of Neurology: The Official Journal of the European Federation of Neurological Societies, 20*(3), 420-428. doi:10.1111/ene.12006.

111. Suidan, G. L., Dickerson, J. W., Chen, Y., McDole, J. R., Tripathi, P., Pirko, I.,& Johnson, A. J. (2010). CD8 T cell-initiated vascular endothelial growth factor expression promotes central nervous system vascular permeability under neuroinflammatory conditions. *The journal of immunology*, *184*(2), 1031-1040.

112. Tardieu, M., Le Chenadec, J., Persoz, A., Meyer, L., Blanche, S., &Mayaux, M. J. (2000). HIV-1-related encephalopathy in infants compared with children and adults. french pediatric HIV infection study and the SEROCO group. *Neurology, 54*(5), 1089-1095.

113. Tardieu, M., Brunelle, F., Raybaud, C., Ball, W., Barret, B., Pautard, B., Blanche, S. (2005). Cerebral MR imaging in uninfected children born to HIV-seropositive mothers and perinatally exposed to zidovudine. *AJNR.American Journal of Neuroradiology, 26*(4), 695-701.

114. Thomaidis, L., Bertou, G., Critselis, E., Spoulou, V., Kafetzis, D. A., &Theodoridou, M. (2010). Cognitive and psychosocial development of HIV pediatric patients receiving highly active anti-retroviral therapy: A case-control study.*BMC Pediatrics, 10*, 99-99.doi:10.1186/1471-2431-10-99

115. Thompson .P.M., Dutton .R.A., Hayashi .K.M., Toga .A.W., Lopez .O.L., Aizenstein .H.J., Becker .J.T. (2005). Thinning of the cerebral cortex visualized in HIV/AIDS reflects CD4+ T lymphocyte decline. Proceedings of the National Academy of Sciences of the United States of America, vol. 102 no. 43, 15647–15652, doi: 10.1073/pnas.0502548102

116. Thurnher, M. M., Schindler, E. G., Thurnher, S. A., Pernerstorfer-Schön, H., Kleibl-Popov, C., &Rieger, A. (2000). Highly active antiretroviral therapy for patients with AIDS dementia complex: Effect on MR imaging findings and clinical course. *American Journal of Neuroradiology, 21*(4), 670-678.

117. Towgood, K. J., Pitkanen, M., Kulasegaram, R., Fradera, A., Kumar, A., Soni, S., & Kopelman, M. D. (2012). Mapping the brain in younger and older asymptomatic HIV-1 men: Frontal volume changes in the absence of other cortical or diffusion tensor abnormalities. *Cortex*, *48*(2), 230-241.

118. Townsend, C. L., Cortina-Borja, M., Peckham, C. S., & Tookey, P. A. (2007). Antiretroviral therapy and premature delivery in diagnosed HIV-infected women in the United Kingdom and Ireland. *Aids*, *21*(8), 1019-1026.

119. Tozzi, V, Balestra, P, Salvatori, M.F, Vlassi, C, Liuzzi, G, Giancola, M.L, Giulianelli, M, Narciso, P, Antinori, A.(2009). Changes in Cognition During Antiretroviral Therapy: Comparison of 2 Different Ranking Systems to Measure Antiretroviral Drug Efficacy on HIV-Associated Neurocognitive Disorders. Journal of Acquired Immune Deficiency Syndromes(JAIDS). Vol. 52, pp. 56-63.doi: 10.1097/QAI.0b013e3181af83d6.Clinical Science. www.jaids.com.

120. Treble. A, Juranek.J, Stuebing.K.K, Dennis.M, Fletcher.J.M (2012). Functional Significance of A typical Cortical Organization in Spina Bifida Myelomeningocele: Relations of Cortical Thickness and Gyrification with IQ and Fine Motor Dexterity. Cerebral Cortex Vol. 23 No. 10 pp.2357–2369.

121. Tucker, K. A., Robertson, K. R., Lin, W., Smith, J. K., An, H., Chen, Y., Hall, C. D. (2004). Neuroimaging in human immunodeficiency virus infection. *Journal of Neuroimmunology, 157*(1–2), 153-162. Doi : http://dx.doi.org/10.1016/j.jneuroim.2004.08.036.

122. Tudor-Williams, G. (2000). Current issues in tropical pediatric infectious diseases. HIV infection in children in developing countries.Transaction of the Royal Society of Tropical Medicine and Hygiene. 94, 3-4.

123. UNAIDS. (2013). *Global report 2012: UNAIDS report on the global AIDS epidemic* bookpartnership. com.

124. Van Arnhem, L. A., Bunders, M. J., Scherpbier, H. J., Majoie, C. B., Reneman, L., Frinking, O., Poll-The, B.T., Kuijpers, T.W., Pajkrt, D. (2013). Neurologic abnormalities in HIV-1 infected children in the era of combination antiretroviral therapy. *PloS one*, *8*(5), e64398.

125. Van der Kouwe, A. J., Benner, T., Salat, D. H., & Fischl, B. (2008). Brain morphometry with multiecho MPRAGE. *Neuroimage*, *40*(2), 559-569.

126. Van der Merwe, K., Hoffman, R., Black, V., Chersich, M., Coovadia, A., & Rees, H. (2011). Birth outcomes in South African women receiving highly active antiretroviral therapy: a retrospective observational study. *Journal of the International AIDS Society*, *14*(1), 42.

127. Van Essen, D. C. (1997). A tension-based theory of morphogenesis and compact wiring in the central nervous system. *NATURE-LONDON-*, 313-318.

128. Van Leemput K, Bakkour A, Benner T, Wiggins G, Wald L.L, Augustinack J, Dickerson B.C, Golland P, Fischl B.(2009). Automated segmentation of hippocampal subfields from ultra-high resolution in vivo MRI. Hippocampus; 19:549–557. [PubMed: 19405131]

129. Van Rie, A., Harrington, P. R., Dow, A., & Robertson, K. (2007). Neurologic and neurodevelopmental manifestations of pediatric HIV/AIDS: A global perspective. *European Journal of Pediatric Neurology, 11*(1), 1-9. doi: http://dx.doi.org/10.1016/j.ejpn.2006.10.006.

130. Violari, A, Cotton, M.F, McIntyre, J,Jean-Philippe, P. (2010). A phase III, randomised, open-label trial to evaluate strategies for providing antiretroviral therapy to infants shortly after primary infection in a resource poor setting. *Comprehensive International Program of Research on AIDS (CIPRA) South Africa, Version 3.0*.

131. Violari, A., Cotton, M. F., Gibb, D. M., Babiker, A. G., Steyn, J., Madhi, S. A., McIntyre, J. A. (2008). Early antiretroviral therapy and mortality among HIV-infected infants. *New England Journal of Medicine, 359*(21), 2233-2244.

132. Von Giesen, H. J., Niehues, T., Reumel, J., Haslinger, B. A., Ndagijimana, J., Arendt, G. (2003). Delayed motor learning and psychomotor slowing in HIV-infected children. *Neuropediatrics*, *34*(4), 177-181.

133. Wachsler-Felder, J., & Golden, C. J. (2002). Neuropsychological consequences of HIV in children: A review of current literature. *Clinical Psychology Review, 22*(3), 443-464.

134. Wallace, G. L., Robustelli, B., Dankner, N., Kenworthy, L., Giedd, J. N., & Martin, A. (2013). Increased gyrification, but comparable surface area in adolescents with autism spectrum disorders. *Brain*, awt106.

135. Weishaupt, D., Froehlich, J. M., Nanz, D., Köchli, V. D., Pruessmann, K. P., & Marincek, B. (2008). *How does MRI work?: an introduction to the physics and function of magnetic resonance imaging*. Springer.

136. White, T., Su, S., Schmidt, M., Kao, C. Y., & Sapiro, G. (2010). The development of gyrification in childhood and adolescence. *Brain and cognition*, *72*(1), 36-45.

137. Wood, S. M., Shah, S. S., Steenhoff, A. P., & Rutstein, R. M. (2009). The impact of AIDS diagnoses on long-term neurocognitive and psychiatric outcomes of surviving adolescents with perinatally acquired HIV. *Aids*, *23*(14), 1859-1865.

138. World Health Organization. (2013). consolidated guidelines on general HIV care and the use of antiretroviral drugs for treating and preventing HIV infection: Recommendations for a public health approach.

139. Yendiki A, Stevens A, Jbabdi S, Augustinack J, Salat D, Zöllei L, Behrens T, Fischl B. (2008) Probabilistic diffusion tractography with spatial priors. MICCAI Workshop on Computational Diffusion MRI: 54–61.

140. Yeo B.T.T, Sabuncu M, Golland P, Fischl B. (2009). Task-optimal registration cost functions. Med Image Comput Comput Assist Interv Int Conf Med Image Comput Assist Interv.; 12:598–606.

141. Zareba, K. M., Lavigne, J. E., & Lipshultz, S. E. (2004). Cardiovascular effects of HAART in infants and children of HIV-infected mothers. *Cardiovascular toxicology*, *4*(3), 271-279.

Turnitin Originality Report

emmnwo001:M.Sc-Thesis_Emmanuel_Nwosu.docx by Emmanuel Nwosu

From For TurnItIn Submission - 2014 - 2015 (4f4f916e-b6ff-441b-bc4c-d486cb3882ed)

Similarity Index	Similarity by Source	
10%	Internet Sources:	5%
	Publications:	9%
	Student Papers:	2%

Processed on 20-Jul-2015 13:32 SAST
ID: 556679318
Word Count: 23583

sources:

E. Meintjes

1 < 1% match (publications)
Robertson, F. C., K. L. Narr, C. D. Molteno, J. L. Jacobson, S. W. Jacobson, and E. M. Meintjes. "Prenatal Alcohol Exposure is Associated with Regionally Thinner Cortex During the Preadolescent Period", Cerebral Cortex, 2015.

2 < 1% match (publications)
Bassar, Ronald D., Thomas Heatherly, Michael C. Marshall, Steven A. Thomas, Alexander S. Flecker, and David N. Reznick. "Population size structure dependent fitness and ecosystem consequences in trinidadian guppies", Journal of Animal Ecology, 2015.

3 < 1% match (Internet from 21-May-2014)
http://surfer.nmr.mgh.harvard.edu/ftp/articles/2012/2012_-_Fischl_-_NeuroImage.pdf

4 < 1% match (publications)
Alexander Hammers. "Three-dimensional maximum probability atlas of the human brain, with particular reference to the temporal lobe", Human Brain Mapping, 08/2003

5 < 1% match (student papers from 20-Jul-2015)
Submitted to University of Cape Town on 2015-07-20

6 < 1% match (Internet from 22-Sep-2013)
http://www.medicinabih.info/wp-content/uploads/2012/11/16-1352051544.pdf

7 < 1% match (publications)
Kesler, S.R., "Increased temporal lobe gyrification in preterm children", Neuropsychologia, 2006

8 < 1% match (student papers from 17-Jul-2015)
Submitted to University of Cape Town on 2015-07-17

9 < 1% match (publications)
"Final Program Forty First Annual Meeting International Neuropsychological Society February 6–9, 2013 Waikoloa, Hawaii, USA", Journal of the International Neuropsychological Society, 2013.

10 < 1% match (publications)
Wallace, G. L., B. Robustelli, N. Dankner, L. Kenworthy, J. N. Giedd, and A. Martin. "Increased gyrification, but comparable surface area in adolescents with autism spectrum disorders", Brain, 2013.

11 < 1% match (publications)